Nanobiotechnology with S-Layer Proteins as Building Blocks

Uwe B. Sleytr, Bernhard Schuster, Eva M. Egelseer, Dietmar Pum, Christine M. Horejs, Rupert Tscheliessnig, and Nicola Ilk

Department of NanoBiotechnology, University of Natural Resources and Life Sciences, Vienna, Austria

One of the key challenges in nanobiotechnology is the utilization of self-assembly systems, wherein molecules spontaneously associate into reproducible aggregates and supramolecular structures. In this contribution, we describe the basic principles of crystalline bacterial surface layers (S-layers) and their use as patterning elements. The broad application potential of S-layers in nanobiotechnology is based on the specific intrinsic features of the monomolecular arrays composed of identical protein or glycoprotein subunits. Most important, physicochemical properties and functional groups on the protein lattice are arranged in well-defined positions and orientations. Many applications of S-layers depend on the capability of isolated subunits to recrystallize into monomolecular arrays in suspension or on suitable surfaces (e.g., polymers, metals, silicon wafers) or interfaces (e.g., lipid films, liposomes, emulsomes).

Progress in Molecular Biology and Translational Science, Vol. 103
DOI: 10.1016/B978-0-12-415906-8.00003-0

1877-1173/11 $35.00

S-layers also represent a unique structural basis and patterning element for generating more complex supramolecular structures involving all major classes of biological molecules (e.g., proteins, lipids, glycans, nucleic acids, or combinations of these). Thus, S-layers fulfill key requirements as building blocks for the production of new supramolecular materials and nanoscale devices as required in molecular nanotechnology, nanobiotechnology, biomimetics, and synthetic biology.

I. Introduction

An important area in nanobiotechnology concerns "bottom-up" routes to fabricate supramolecular structures at subnanometer precision.[1] Presently, the most complex functional nanoscale structures are efficiently built from biomolecules that self-assemble into nanoscale three-dimensional (3D) shapes or two-dimensional (2D) crystals on surfaces and interfaces. So far, a variety of biomolecules optimized through evolution, including proteins, nucleic acids, and lipids, are used as molecular building blocks in nanobiotechnology. Owing to their unique morphogenetic potential, crystalline bacterial cell surface layer (S-layer) proteins or glycoproteins represent prime candidates as patterning elements for nanobiotechnological applications.[2]

S-layers represent an almost universal feature in archaeal cell envelopes and have been identified in hundreds of different species of bacteria. Moreover, since the biomass of prokaryotic organisms by far prevail eukaryotic biomass and S-layers represent 10% of cell proteins, the crystalline protein arrays can be considered as one of the most abundant biopolymers on earth.

As outermost envelope layer in prokaryotic organisms, S-layers also represent an evolutionary adaption of the organisms to a broad spectrum of selection criteria. Most of the presently known S-layers are composed of single protein or glycoprotein species endowed with the intrinsic ability to assemble into monomolecular arrays. Thus, S-layers can be regarded as the simplest protein membrane developed during evolution. Since archaea that dwell under most extreme environmental conditions (e.g., up to 120 °C, pH 0, concentrated salt solutions, high hydrostatic pressure) possess S-layers, these protein meshworks can also exhibit remarkable chemical stability.

Studies on the structure, chemistry, genetics, morphogenesis, and function have led to a broad spectrum of applications (for reviews, see Refs. 2–20). Up to now, most applications developed for using S-layer lattices depend on the *in vitro* self-assembly capabilities of native or recombinant S-layer proteins on the surface of solids and interfaces (e.g., silicon wafers, polymers and metals, lipid films, liposomes, and nanoparticles). Most importantly, because S-layers are periodic structures composed of a single (glyco)protein species and possess

pores of identical size and morphology, they exhibit identical physicochemical properties on each molecular unit, down to the subnanometer scale. This unique feature enables very precise chemical and/or genetic modifications. Particularly, the possibility of modifying and changing the natural properties of S-layer proteins and glycoproteins by genetic engineering techniques and to incorporate specific functional domains has led to a broad spectrum of applications including ultrafiltration membranes, affinity structures, enzyme membranes, microcarriers, biosensors, diagnostic devices, biocompatible surfaces, as a matrix for biomineralization, and vaccines, as well as targeting, delivery, and encapsulating systems. It is now evident that S-layers can be used as structural basis for a versatile biomolecular construction kit involving all major species of biological molecules (proteins, lipids, glycans, nucleic acids, and combinations of these).

In this contribution, we provide a survey of the general principles of S-layers and their broad application potential in nanobiotechnology.

II. General Principles

A. Occurrence, Location, and Structure of S-Layers

Almost 60 years ago, Houwink and Le Poole described the presence of a "macromolecular monolayer" in the cell wall of *Spirillum* sp.,[21] but it took 15 more years until regular arrays of macromolecules were identified as common cell surface layers on living *Bacillus* and *Clostridium* cells.[22,23]

Crystalline cell surface layers now referred to as S-layers[24,25] have so far been identified in hundreds of different strains belonging to all major phylogenetic groups of the domain bacteria and represent an almost universal feature in archaea.[20,26–29] The location and ultrastructure of S-layers were investigated by different electron microscopy procedures, including thin sectioning, freeze-etching, and freeze-drying in combination with heavy metal shadowing and negative staining.[30–38]

Nevertheless, the most suitable procedure for identifying the presence of S-layer lattices on intact cells is still electron microscopy of freeze-etched preparations.[24,34,37,39] High-resolution studies on the mass distribution of the lattice are generally performed on negatively stained S-layer fragments or thin frozen foils.[31,40,41] High-resolution images of S-layer lattices can also be obtained by scanning force microscopy under aqueous conditions.[34,42,43]

Freeze-etching preparations (Fig. 1) of a great variety of bacteria and archaea have clearly demonstrated that S-layer lattices completely cover the cell surfaces at all stages of cell growth and cell division. Although considerable variation exists in the supramolecular structure and chemistry of cell envelopes

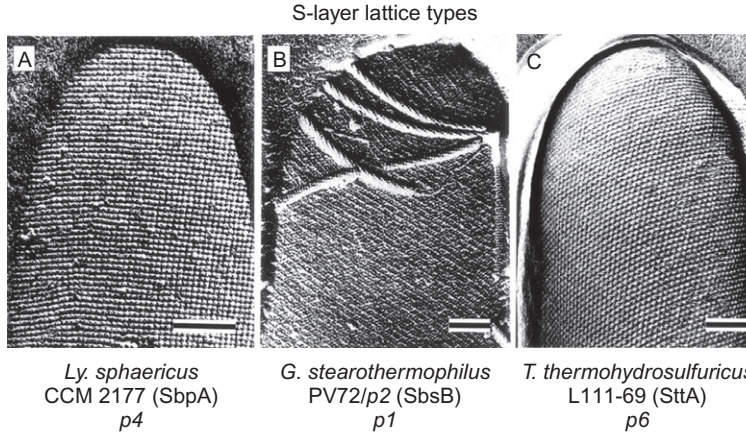

FIG. 1. Electron micrographs of freeze-etched preparations of intact cells from (A) *Lysinibacillus sphaericus* CCM 2177 showing square lattice symmetry (bar, 150 nm), (B) *Geobacillus stearothermophilus* PV72/*p2* exhibiting an oblique lattice type (bar, 50 nm), and (C) *Thermoanaerobacter thermohydrosulfuricus* L111-69 showing a hexagonal S-layer lattice (bar, 100 nm).

of prokaryotic organisms, S-layers must have coevolved with these diverse structures.[34] In most archaea, the S-layer (glyco)protein lattices are, as the only wall component, closely associated or integrated into the plasma membrane (Fig. 2). In Gram-positive bacteria and in certain archaea, S-layers assemble on the surface of the rigid wall matrix, which is composed mainly of peptidoglycan and covalently attached secondary cell wall polymers (SCWPs) or pseudomurein, respectively. In Gram-negative bacteria, the lattice is attached to the lipopolysaccharide component of the outer membrane.

Most remarkably, some Gram-positive and Gram-negative bacteria assemble two or even more superimposed S-layers which generally are composed of a different subunit species.[24,27] S-layer subunits can be aligned with oblique (*p1*, *p2*), square (*p4*), or hexagonal (*p3*, *p6*) symmetry (Fig. 3), with center-to-center spacings of the morphological units (composed of one, two, three, four, or six identical monomers) of approximately 3.5–35 nm. Hexagonal symmetry is predominant among archaea.[20] Most S-layer lattices are 5–25 nm thick and reveal a rather smooth outer and a more corrugated inner surface. As S-layers are monomolecular assemblies of identical subunits, they exhibit pores of identical size and morphology. In many S-layers, two or even more distinct classes of pores could be observed. Pore sizes were determined to be in the range of approximately 2–8 nm, and pores can occupy approximately 30–70% of the surface area.[31,38,40] Most S-layers of archaea exhibit pillar-like structures on the inner surface, which are involved in anchoring the arrays in the

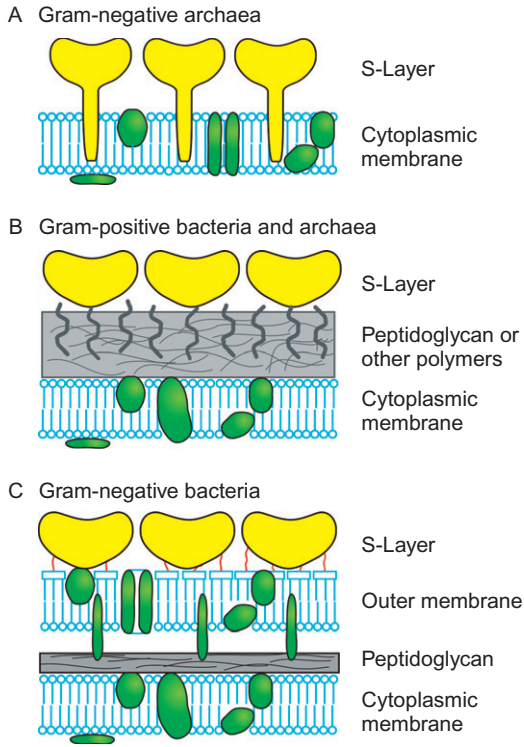

FIG. 2. Schematic illustration of the major classes of prokaryotic cell envelopes with crystalline bacterial cell surface layers (S-layers). (A) Cell envelope structure of Gram-negative archaea with S-layers as the only cell wall component external to the cytoplasmic membrane. (B) Cell envelope as observed in Gram-positive archaea and bacteria. (C) Cell envelope profile of Gram-negative bacteria composed of a thin peptidoglycan layer and an outer membrane. If present, the S-layer is closely associated with the lipopolysaccharide of the outer membrane.

underlying plasma membrane.[14,34,44,45] In many species of bacteria, the S-layers of individual strains exhibit great diversity with respect to lattice symmetry and center-to-center spacing of the morphological units.

B. Isolation, Chemical Characterization, Molecular Biology, and Function

S-layers constitute the outermost cell wall component facing the environment and are part of quite different supramolecular prokaryotic envelope structures. The latter can be classified into three main groups on the basis of the biological origin (bacteria or archaea) and their response to the so-called

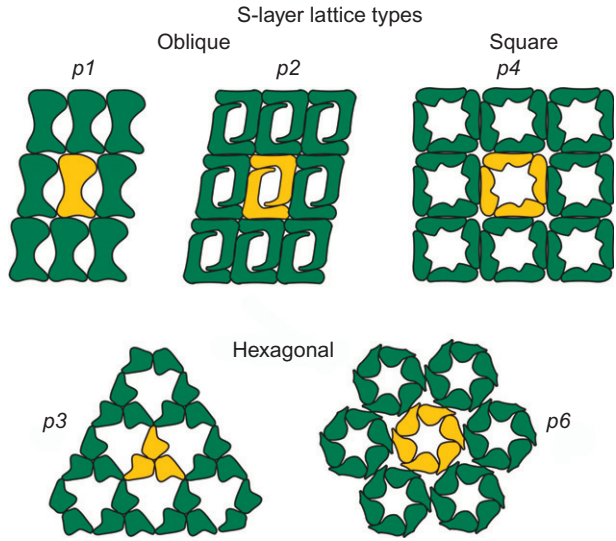

FIG. 3. Schematic drawing of different S-layer lattice types. The regular S-layer arrays show either oblique (*p1*, *p2*), square (*p4*), or hexagonal lattice symmetry (*p3*, *p6*). The morphological units are composed of one, two, three, four, or six identical subunits. Modified after Ref. 17; Copyright (1999) with permission from Wiley–VCH.

Gram-staining.[46,47] This bacteriological laboratory technique is frequently used to differentiate bacterial species into two large groups based on the physical properties of their cell walls. Gram-positive bacteria have a thick mesh-like cell wall made of peptidoglycan or pseudomurein (50–90% of cell wall), which stains purple, and the S-layer proteins assemble on the surface of this rigid wall matrix. In contrast, Gram-negative bacteria have a thinner polymer layer (10% of cell wall), which stains pink.[48] Gram-negative bacteria also have an additional outer membrane comprising lipids and lipopolysaccharides, and is separated from the cell wall by the periplasmic space.[44] In these more complex cell envelopes, the S-layers are linked to specific lipopolysaccharide fractions.[17,19,34,49–51] Gram-staining is not used to classify archaea, as these microorganisms yield widely varying responses that do not follow their phylogenetic groups.[48] In many archaea, S-layers represent the only cell wall component and can be closely associated with the plasma membrane so that it is partially integrated in the lipid layer.[44,52]

Owing to the diversity in the supramolecular structures of prokaryotic cell envelopes, S-layer proteins differ considerably in their susceptibility to disruption into constituent subunits. S-layers are usually not covalently attached to

the cell surface[50]; hence, these proteins can be isolated in the presence of dissociating agents such as lithium chloride[53] or metal-chelating agents such as ethylenediaminetetraacetic acid (EDTA) and ethyleneglycoltetraacetic acid (EGTA).[54] Further, chaotropic denaturants such as guanidine hydrochloride and urea[55,56] or detergents at a pH-value lower than 4 can be applied to isolate S-layer subunits. In certain cases, even washing cells with deionized water can lead to dissociation of the S-layer lattice.[57–59] Extraction and disintegration experiments revealed that the inter-subunit bonds in the S-layer are stronger than those binding the crystalline array to the supporting envelope layer.[39] However, in the halophilic archaea *Halobacterium halobium* and *Haloferax volcanii*, the S-layer protomers are anchored by C-terminally located membrane-spanning domains to the cytoplasmic membrane.[60,61]

Chemical and genetic analyses on many bacterial and archaeal S-layers have shown that they are generally composed of a single protein or glycoprotein species with molecular masses ranging from 40 to 170 kDa.[15,17,20,27,62,63] Amino acid analysis of S-layer proteins of organisms from all phylogenetic branches revealed a rather similar overall composition.[40,64,65] Sequencing of genes encoding the S-layer proteins and isoelectric focusing provide evidence that, with a few exceptions (e.g., *Lactobacillus* and *Methanothermus*), S-layers are composed of an acidic protein or glycoprotein species with an isoelectric point between 3 and 6. Accordingly, S-layer proteins have a high amount of glutamic and aspartic acids (approximately 15 mol%) and the lysine content of S-layer proteins is in the range of 10 mol%. Thus, approximately one-quarter of the amino acids is charged, indicating that ionic bonds play an important role in inter-subunit bonding and/or in attaching the S-layer subunits to the underlying cell envelope layer. S-layer proteins have no or only a low content of sulfur-containing amino acids and a high proportion of hydrophobic amino acids (between 40 and 60 mol%). Interestingly, hydrophilic and hydrophobic amino acids do not form extended clusters but, instead, the hydrophobic and hydrophilic segments alternate with a more hydrophilic region at the very N-terminal end.[66] Information regarding the secondary structure of S-layer proteins is either derived from the amino-acid sequence or from circular dichroism measurements. In most S-layer proteins, 40% of the amino acids are organized as β-sheet, 10–20% occur as α-helix, whereas aperiodic foldings and β-turn content may vary between 5% and 45%.

Few posttranslational modification including cleavage of amino- or carboxy-terminal fragments, phosphorylation, and glycosylation of amino-acid residues are known to occur in S-layer proteins. The latter is a remarkable characteristic of many archaeal and some bacterial S-layer proteins. The glycan chains and types of linkage differ significantly from those of eukaryotes.[27,63,67,68]

During the past two decades, numerous S-layer genes from bacteria and archaea of quite different taxonomical positions have been sequenced and cloned.[17,20,49,69,70] Recently, these informations were summarized including a complete coverage of GenBank accession numbers of S-layer structural genes and presently known data on surface-layer glycosylation (*slg*) gene clusters.[27] The S-layer gene sequence itself provides valuable information especially for pathogenic organisms such as *Bacillus anthracis*, *Clostridium difficile*, and *Campylobacter fetus*, for which specific identification and discrimination is vital for the accurate treatment of afflicted persons.[71–75]

The accumulation of S-layer gene sequences made it possible to screen for putative sequence identities and to elucidate the structure–function relationship of distinct segments of S-layer proteins by the production of N- and/or C-terminally truncated forms.[76–78] Moreover, the assembly-negative, water-soluble, N- or C-terminally truncated forms of the S-layer protein SbsC of *Geobacillus stearothermophilus* ATCC 12980 turned out to be well suited for 3D crystallization studies.[79,80] Based on the C-terminally truncated form $rSbsC_{31\text{-}844}$, the first high-resolution structure of the bacterial S-layer protein SbsC could be obtained[80] (see also the chapter: "The structure of bacterial S-layer proteins").

In the case of the S-layer protein SbsB of *G. stearothermophilus* PV72/*p2*, the tertiary structure was predicted by using molecular dynamic simulations based on the amino-acid sequence using the mean force (MF) method.[81] This approach has led to a thermodynamically favorable atomic model of the tertiary structure of the S-layer protein, which could be verified by both the MF method and the lattice model[81] (see also Section III.B.4).

Kinns and coworkers pursued the approach of using epitope insertion mutagenesis to identify surface-located mutations of the S-layer protein SbsB that block assembly without affecting the protein's overall tertiary structure.[82] SbsB was chosen because previous studies using cysteine scanning mutagenesis and targeted chemical modification had identified 23 amino-acid positions that are surface accessible in the monomer.[83,84] The insertion mutagenesis screen yielded several assembly-compromised mutants that represent an important step toward structure elucidation of an S-layer protein by NMR or X-ray crystallography.[82] Cysteine-scanning mutagenesis and targeted chemical modification were also applied for SlpA, the S-layer protein of the potentially probiotic bacterium *Lactobacillus brevis* ATCC 8287, in order to distinguish amino-acid residues located in the outer and inner surfaces of the lattice, protein interior, and interface/pore regions.[85]

Common structural organization principles have been identified at least for S-layer proteins of Gram-positive bacteria. A cell wall targeting domain was found either at the N-terminal or C-terminal region of these S-layer proteins. The existence of an N-terminal cell wall targeting domain was sustained by the

identification of the so-called S-layer homology (SLH) motifs, consisting of 50–60 amino acids each, which are mostly found in triplicate at the N-terminus of S-layer proteins.[86] If present, SLH motifs are involved in cell wall anchoring of S-layer proteins by recognizing a distinct type of SCWP, which carry pyruvic acid residues and belong to group I SCWPs.[76,87–95] Results obtained by May and coworkers indicated that a highly conserved motif termed TRAE based on the sequence of the four amino-acids threonine, arginine, alanine, and glutamic acid is necessary in all three SLH motifs forming the functional SLH domain, and at least one (preferentially positively) charged amino acid in the TRAE motif is required for the activity.[96] For SLH-mediated binding, the construction of knock-out mutants in *B. anthracis* and *Thermus thermophilus* in which the gene encoding a putative pyruvyl transferase was deleted demonstrated that the addition of pyruvic acid residues to the peptidoglycan-associated cell wall polymer was a necessary modification.[87,92] The need for pyruvylation was also confirmed by surface plasmon resonance (SPR) spectroscopy measurements using the S-layer protein rSbsB of *G. stearothermophilus* PV72/*p2* and the corresponding SCWP[97] for interaction studies.[91] The interaction proved to be highly specific for the carbohydrate component, and the exclusive and complete responsibility of a functional domain formed by the three SLH motifs for SCWP recognition was clearly confirmed.[91] In addition, by using optical spectroscopic methods and electron microscopy, rSbsB could be characterized by its two functionally and structurally separated parts, namely, the SLH domain which is responsible for "cell wall targeting" by recognizing the SCWP, and the larger C-terminal part which corresponds to the self-assembly domain.[95] Interestingly, the C-terminal part of SbsB was highly sensitive against deletions, and the removal of even less than 15 amino acids led to water-soluble S-layer protein forms.[83,98] In contrast to SbsB, in SbpA, the S-layer protein of *Lysinibacillus sphaericus* CCM 2177, an additional 58-amino-acid long SLH-like motif located behind the third SLH-motif is required.[76] In the C-terminal part of this S-layer protein, up to 237 amino acids could be deleted without interfering with the formation of the square lattice structure.

A further main type of binding mechanism between S-layer proteins and SCWPs has been described for the *G. stearothermophilus* wild-type strains PV72/*p6*, NRS 2004/3a, and ATCC 12980[78,99–102] as well as for a temperature-derived variant of the latter.[103] The N-terminal part of these S-layer proteins contains a surplus of arginine and tyrosine, which typically occur in carbohydrate-binding proteins such as lectins.[104] In this binding mechanism, nonpyruvylated group II SCWPs interact with a highly conserved N-terminal region of the S-layer proteins without SLH motifs.[78,99,100,103] First affinity studies using different N- or C-terminally truncated forms of the S-layer protein SbsC from *G. stearothermophilus* ATCC 12980 indicated that the N-terminal

part comprising amino acids 31–257 is exclusively responsible for cell wall binding.[78] This result was also corroborated by SPR studies using the S-layer protein SbsC and the corresponding nonpyruvylated SCWP of *G. stearothermophilus* ATCC 12980 as the model system.[105]

A cell wall targeting domain is not necessarily located in the N-terminal region of S-layer proteins. In the S-layer proteins SlpA of *Lactobacillus acidophilus* ATCC 4356 and CbsA of *Lactobacillus crispatus* JCM 5810, a cell wall binding domain has been identified in the C-terminal one-third of these S-layer proteins, and sequence alignment studies revealed a putative carbohydrate-binding repeat comprising approximately the last 130 C-terminal amino acids which were suggested to be involved in cell wall binding.[106,107] Although SLH motifs have not been found in *Lactobacillus* S-layer proteins, their attachment to the cell wall seems to involve SCWPs in several lactobacilli, too.[70] The S-layer proteins from *L. brevis* and *L. buchneri* are reported to bind to a neutral polysaccharide moiety of the cell wall,[70,108,109] but the location of the cell wall binding domain of these proteins is currently unknown.

In contrast to Gram-positive bacteria, no general S-layer anchoring motifs have been identified in Gram-negative organisms. Available evidence in each case so far implicates the involvement of the N-terminus of S-layer proteins. Concerning the S-layer of *Aeromonas salmonicida*, the majority of the trypsin-inaccessible residues were identified in the N-terminal 301 amino acids of the A-protein, suggesting cell surface anchoring via the N-terminus of the S-layer subunits.[110] Similarly, the *C. fetus* S-layer SapA is cell surface-anchored via its conserved N-terminal region comprising at least 189 amino acids, as N-terminal deletions disrupt SapA anchoring,[111] while C-terminal truncations do not.[112] The S-layer protein RsaA of the Gram-negative bacterium *Caulobacter crescentus* also follows this general pattern since mutations[113] and truncations[114] in the extreme N-terminus of RsaA lead to an S-layer shedding phenotype. By using reattachment assays, it became evident that the anchoring region of the *C. crescentus* S-layer protein lies within the first $\sim$225 amino acids and that RsaA anchoring requires a smooth lipopolysaccharide species found in the outer membrane.[115]

The observation of phenotypic S-layer variation was not surprising, as cell surface components can generally be considered as nonconservative structures that have to respond to changing environmental conditions in the course of evolution. S-layer variation leads to the synthesis of alternate S-layer proteins, either by the expression of different S-layer genes or by recombination of partial coding sequences, and has been described to occur in pathogens as well as in nonpathogens.[116–126] In pathogens, altered cell surface properties most probably protect the cells from the lytic activity of the immune system,[120] whereas in nonpathogens, the S-layer variation is frequently induced in response to altered environmental conditions, such as increased oxygen

supply.[70,124,125,127] In *G. stearothermophilus* strain variants, expression of a completely new type of S-layer protein is accompanied by synthesis of a different type of SCWP, and S-layer variation may also lead to a change in the lattice type.[124,125] These results indicated that, in the course of variant formation, changes in S-layer protein and SCWP synthesis were strictly coordinated and that the type of SCWP must have been changed prior to or simultaneously with the expression of a different type of S-layer gene. Genetic studies revealed that variant formation was caused by recombinational events between a naturally occurring megaplasmid and the chromosome.[128] Regarding the development of S-layer-deficient strain variants, the importance of insertion sequence elements has been demonstrated for various organisms.[129,130]

In a nutshell, multiple mechanisms leading to S-layer protein variation, modification, or complete loss of the S-layer indicate the importance of diversification of the surface properties even of closely related organisms for their survival in a competitive habitat.

Synthesis of a coherent S-layer lattice on a cell surface requires a considerable biosynthetic effort. When bacteria are no longer subject to the natural environmental selection pressure, S-layers can be lost. This was often observed during continuous culture under optimal growth conditions, and, usually, the S-layer-deficient variant outgrows the S-layered parent.[34,49] So far, a general, all-encompassing natural function for S-layers has not been found and many of the functions assigned to S-layers still remain hypothetical and not based on firm experimental data (see Table I modified after Refs. 20,27).

However, for assignment of functions, S-layers must be considered as part of complex supramolecular structures of diverse prokaryotic cell envelopes rather than an isolated monomolecular (glyco)protein lattice. The fact that no structural models at atomic resolution of S-layer proteins are available until now makes detailed interpretations of functional aspects even more difficult (for reviews, see Refs. 2,20,27,34,49,51).

III. Assembly and Morphogenesis of S-Layers

A. Self-Assembly *In Vivo*

Owing to the fact that S-layers possess a high degree of structural regularity and are composed in most cases of a single protein or glycoprotein species, they represent ideal model systems for studying the morphogenesis of a supramolecular layer during cell growth.[33,39] It can be calculated that approximately 5×10^5 S-layer protein monomers are needed to cover an average-sized rod-shaped prokaryotic cell. Consequently, at a generation time of about 20 min, at least 500 copies of a single polypeptide species with a molecular

TABLE I
GENERAL AND SPECIFIC FUNCTIONS OF S-LAYERS (MODIFIED AFTER REFS. 20,28)

General function	Specific function
Determination and maintenance of cell shape	Determination of cell shape and cell division in archaea that possess S-layers as exclusive wall component
Isoporous molecular sieves	Molecular sieves in the ultrafiltration range
Adhesion zones for exoenzymes	High molecular weight amylase of *Geobacillus stearothermophilus* wild-type strains
	Pullulanase and glycosyl hydrolases of *Thermoanaerobacter thermosulfurigenes*
Protective coats	Prevention of predation by *Bdellovibrio bacteriovorus* in Gram-negative bacteria
	Phage resistance by S-layer variation
	Prevention or promotion of phagocytosis
	Adaption of *Bacillus pseudofirmus* to alkaline environment
Templates for fine grain mineralization	Induction of precipitation of gypsum and calcite in *Synechococcus* and shedding of mineralized S-layer
Pathogenicity and cell adhesion	Virulence factor in pathogenic organisms
	Important role in invasion and survival within the host
	Specific binding of host molecules
	Protective coat against complement killing
	Ability to associate with macrophages and to resist the effect of proteases
	Production of immunologically non-cross-reactive S-layers (S-layer variation)
Surface recognition and cell adhesion to substrates	Physicochemically and morphologically well-defined matrices
	Masking the net negative charge of peptidoglycan-containing layer in Bacillacea
Antifouling layer	Prevention of nonspecific adsorption of macromolecules
	Maintaining the permeability properties through the S-layer pores
Delineating a periplasmic space	Entrapping molecules between the cytoplasmic membrane and the S-layer lattice

mass of approximately 100,000 have to be synthesized, translocated to the cell surface, and incorporated into the preexisting S-layer lattice per second in order to maintain a closed protein meshwork.[34,131]

The rate of synthesis of S-layer proteins appears to be strictly controlled, as only small amounts are detectable in the growth medium at optimal growth conditions. Nevertheless, a few species shed considerable amounts of S-layers.[132,133]

It was also demonstrated in different Bacillaceae that a pool of S-layer subunits is accumulated in the peptidoglycan-containing layer in an amount at least sufficient for generating one coherent lattice on the cell surface.[134]

Determination of the half-lives of S-layer protein mRNAs from *C. crescentus* (10–15 min), *A. salmonicida* (22 min), and *L. acidophilus* (15 min) revealed exceptionally stable transcripts compared to typical half-lives of prokaryotic mRNAs.[135–137] Secondary-structure formation in the long, untranslated leader sequences found for many S-layer protein mRNAs might contribute to such unusually long half-lives.[138] As they mediate the synthesis of a major structural component of the cell, the high stability of S-layer mRNAs is not unexpected.

Most S-layer proteins contain an N-terminal signal peptide that allows for their secretion by the Sec-dependent general secretion pathway. These signal sequences, with a length ranging from 21 to 34 amino acids for *A. salmonicida* and *H. volcanii*, respectively, are generally processed by signal peptidases, resulting in the mature S-layer proteins.[138] In some cases, such as the S-layers from *Deinococcus radiodurans*[139] and *T. thermophilus* HB8,[140] the N-terminus of the protein seems to be chemically modified. Further processing also occurs in the S-layer protein of *Rickettsia prowazekii.*[141] The best studied models of signal peptide-containing S-layer proteins are *A. salmonicida* and *Aeromonas hydrophila*. In the case of *A. salmonicida*, secretion of the S-layer protein (VapA) through its outer membrane implicates a substrate-specific main terminal branch of the general secretion pathway.[142] Interestingly, S-layer proteins from other Gram-negative bacteria do not contain an N-terminal signal peptide. Examples of signal peptide-less S-layer proteins are those from *C. crescentus*,[143] *Serratia marcescens*,[144] and *C. fetus.*[54] Secretion of these S-layer proteins involves specific type I secretion systems.[145,146]

Once secreted, the subunits interact with each other and with the supporting envelope layer through noncovalent forces. Different physicochemical surface properties at the inner and outer surface of the S-layer lattice have been shown to be responsible for the proper orientation of the S-layer subunits and their insertion in the course of lattice growth.[24,37,39,147] Depending on the supramolecular cell envelope design, S-layer subunits may interact with different components (e.g., the plasma membrane in most archaea, the rigid wall component in Gram-positive bacteria, or the lipopolysaccharide layer of the outer membrane in Gram-negative bacteria). Electron microscopy of negatively stained, thin sectioned or freeze-etched preparations and labeling experiments using fluorescent antibodies or immunogold have demonstrated that different patterns of S-layer lattice extension exist for Gram-positive and Gram-negative bacteria. In Gram-positive bacteria, lattice growth occurs primarily by insertion at multiple bands on the cylindrical part of the cell.[148] By contrast, in Gram-negative bacteria, the insertion of new subunits occurs at random.[149]

As predicted by Harris and coworkers,[150] in "closed surface crystals" dislocations and disclinations could serve as sites for incorporation of new subunits in closed lattices that grow by "intussusceptions."[2] As both types of lattice faults can be observed on high-resolution freeze-etching images of intact

cells, it can be assumed that the rate of growth of S-layer lattices by the mechanism of nonconservative climb of dislocations depends on the number of dislocations present and the rate of incorporation of new subunits at these sites.[2,19,37]

Different to organisms with S-layers attached to rigid wall components (Fig. 2), in archaea with S-layers as exclusive wall component it can be expected that the protein meshwork has the intrinsic potential to fulfill cell shape determining functions and to be involved in cell fission.[151,152] Cell division in these organisms appears to be determined by the ratio of the increase in protoplast volume and S-layer surface area extension.[152]

These observations and *in vitro* self-assembly studies (see below) have led to the speculation that S-layer-like membranes could have fulfilled barrier and support functions for self-reproducing systems at the origin of life.[34,147]

B. Self-Assembly *In Vitro*

The attractiveness of S-layer proteins for a broad range of applications in nanobiotechnology lies in their capability to form 2D arrays in suspension and at interfaces without the bacterial cell envelope from which they have been removed (Fig. 4).[20,33] Most techniques for isolation and purification of S-layer proteins involve a mechanical disruption of the bacterial cells and subsequent differential centrifugation in order to isolate the cell wall fragments.[24,37] A complete solubilization of S-layers into their constituent protein monomers and their release from the supporting cell envelope layers can be achieved with high concentrations of chaotropic agents (e.g., guanidine hydrochloride, urea), by lowering or raising the pH, or by applying metal-chelating agents (e.g., EDTA, EGTA) or cation substitution.[37] The reassembly of isolated S-layer proteins into extended self-assembly products or, alternatively, the preparation of solubilized S-layer protein monomers occurs upon dialysis of the disintegrating agent.[37] The dialysis protocol (presence of divalent cations, pH, or dialysis time) determines the final product. It has to be noted that the formation of S-layer lattices is determined only by the amino-acid sequence of the polypeptide chains where a specific part is responsible for the reassembly property.[33,76] As S-layer proteins have a high proportion of nonpolar amino acids, most likely hydrophobic interactions are involved in the assembly process. Studies on the distribution of functional groups on the surface have shown that free carboxylic acid groups and amino groups are arranged in close proximity and thus contribute to the cohesion of the proteins by electrostatic interactions.[20] Further, some S-layer proteins require divalent cations in order to form stable lattices.[153–156]

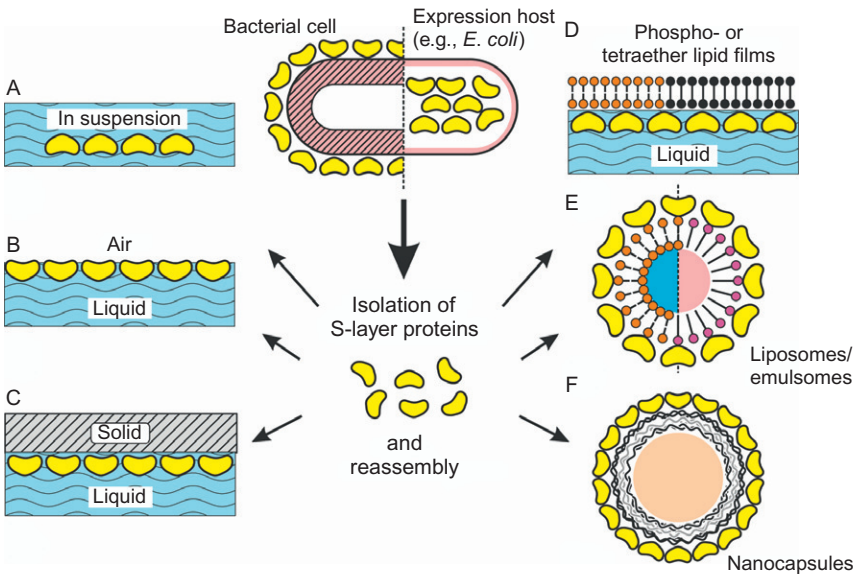

FIG. 4. Schematic drawing of the reassembly of native or recombinantly generated S-layer proteins in (A) suspension, (B) at the air–water interface, (C) on solid supports, (D) at lipid films, and (E, F) on spherical surfaces, such as liposomes, emulsomes, and nanocapsules.

1. SELF-ASSEMBLY IN SUSPENSION

Depending on the specific bonding properties and the tertiary structure of the S-layer proteins, flat sheets, open-ended cylinders, or vesicles are formed (Fig. 5).[24,37,147,157,158] Both protein concentration and temperature determine the extent and rate of association. The assembly starts with a rapid initial phase and continues with a slow consecutive rearrangement step leading to extended lattices.[159] Further, depending on the S-layer proteins used and the environmental conditions (e.g., ionic content and strength in the buffer solution), the self-assembly products consist either of monolayers or double layers. In a systematic study with the S-layer protein SgsE from *G. stearothermophilus* NRS 2004/3a, it was shown that two types of monolayered and five types of double-layered assembly products with back-to-back orientation of the constituent monolayers were formed.[2,157] The double layers differed in the angular displacement of their constituent S-layer sheets. As the monolayers had an inherent inclination to curve along two axes, cylindrical or flat double-layer assembly products were formed depending on the degree of neutralization of the inherent "internal bending strain."[157]

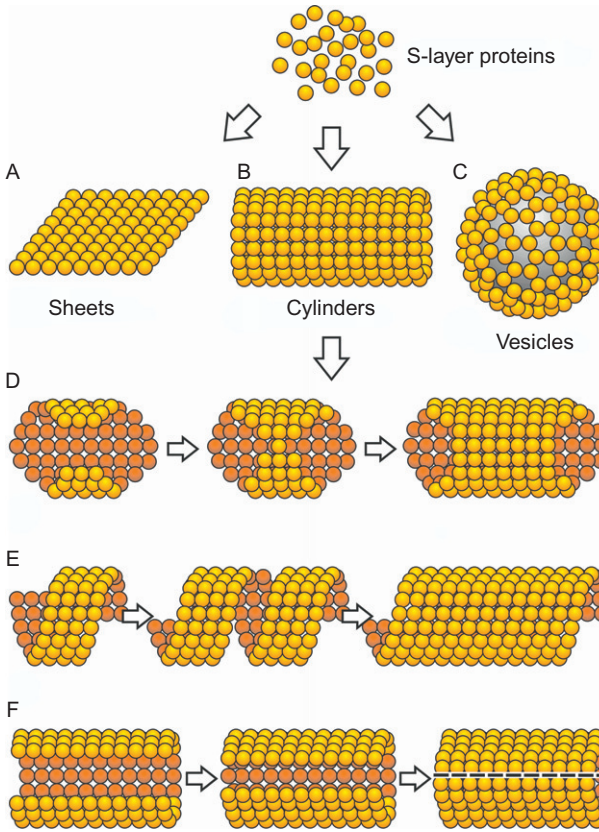

FIG. 5. Schematic drawing of the different assembly routes of S-layer proteins into (A) flat sheets, (B, D–F) cylinders, and (C) vesicles.

2. SELF-ASSEMBLY ON SURFACES AND AT INTERFACES

Crystal growth on surfaces and at interfaces is initiated simultaneously at many randomly distributed nucleation points and proceeds in plane until the crystalline domains meet, thus leading to a closed seamless mosaic of individual S-layer domains of several micrometers long.[153,156,160] S-layer protein monolayer formation at the liquid–air interface was studied by transmission electron microscopy (TEM) (Fig. 6).[160] In this work, electron microscopy grids were deposited on and removed from the water surface by a Langmuir–Schäfer transfer at regular time intervals. After staining with uranyl acetate, the samples were inspected in the transmission electron microscope. In a recent study, it was demonstrated that atomic force microscopy (AFM) is most suitable to

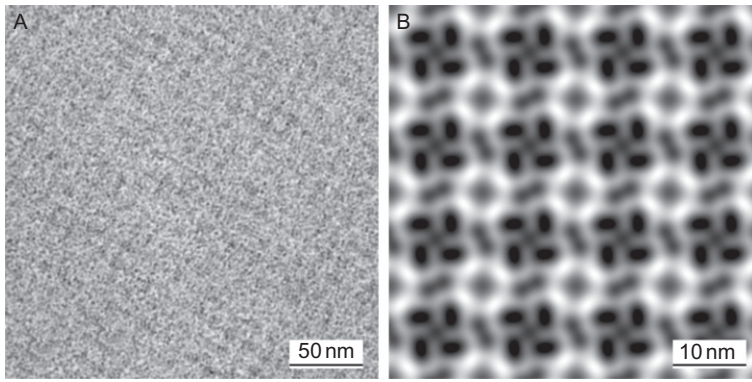

FIG. 6. Low-dose transmission electron microscopical image of a negatively stained preparation of S-layer proteins from *Lysinibacillus sphaericus* CCM 2177. (A) shows the original micrograph and (B) an image-processed zoom region.

image the lattice formation in real time.[161,162] Approximately 10 min after injection of the protein solution into the fluid cell, the first small crystalline patches became visible, and about 30 min later, the silicon surface was completely covered and only small holes remained free which were closed in due course. Extremely low loading forces of the AFM tip were necessary in order to minimize the influence of the scanning tip on the reassembly of the proteins. Nevertheless, the formed S-layer lattices showed a perfect long-range order and a resolution of the molecular details down to approximately 1 nm (as determined from the digital diffraction pattern).

The importance of controlling the hydrophobicity of the surface had been demonstrated by adsorbing disulfides on gold substrates prior to reassembling S-layer proteins.[163] Disulfides are OH- and CH_3-terminated thiolates in an inclined position.[164] By changing the length stepwise by one CH_2 unit, the hydrophobicity could be adjusted very precisely. It was shown that the length of the alkyl chains determined the lattice parameters and the domain sizes of the reassembled S-layer. An increase in hydrophobicity led to a transition from bilayer to monolayer formation.

In summary, the formation of coherent crystalline S-layer arrays depends strongly on the particular S-layer protein species, the environmental conditions of the bulk phase (e.g., temperature, pH, ion composition, and ionic strength), and, most importantly, on the surface properties of the substrate (hydrophobicity, surface charge).[153] For example, on hydrophobic silicon supports the S-layer protein SbpA form *Ly. sphaericus* CCM 2177 forms monolayers exposing the outer face of the S-layer lattices, while on silicon surfaces rendered hydrophilic the S-layer proteins form double layers facing each other with their

inner faces and thus exposing the outer face as well. At incomplete double layers where the lower S-layer is larger than the upper one, the inner S-layer face becomes visible. Binding experiments with negatively charged gold nanoparticles demonstrated that only the inner positively charged S-layer faces could be labeled, confirming the AFM results.[165]

In addition, all these parameters have a direct effect on the mobility of the S-layer proteins on the surface and their probability to be trapped at the front lines of growing domains. This continuous rearrangement of subunits leads to a stable configuration which is characteristic of crystal growth in equilibrium where large and perfectly regular arrays are formed. By changing one of these critical parameters, such as the concentration of calcium ions in the reassembly of the S-layer protein SbpA from *Ly. sphaericus* CCM 2177 (see above), crystal growth is no longer in equilibrium and a broad spectrum of crystal morphologies ranging from tenuous, fractal-like structures to large monocrystalline patches is obtained.[155] The observed patterns indicate that diffusion-limited processes are dominating. For example, the borderline may advance so rapidly that the stable phase does not have time to reach its lowest energy state on the microscopic level, and a metastable microstructure with "extended fingers" results. The structures are tenuous and open because holes are formed and not filled up. From these data, it was concluded that S-layer crystal formation at interfaces is determined by a fast nucleation and assembly process involving subunits associated with the interface, and a slow incorporation of subunits from the subphase.

The possibility for recrystallizing isolated S-layer proteins at the air/water interface or on lipid films on the air/water interface and for handling such layers by standard Langmuir–Blodgett (LB) techniques opened a broad spectrum of applications in basic and applied membrane research (for review, see Refs. 165–167). Further, the reassembly of S-layer proteins on spherical lipid structures such as liposomes and nanocapsules has great technological and, in particular, medicinal importance (drug targeting and delivery, diagnostics, etc.).[168–171] A detailed summary on the S-layer protein–lipid interaction, the biophysical and electrochemical characterization of S-layer-supported planar and spherical lipid membranes, and the application potential of these biomimetic supramolecular architectures in nanobiotechnology and synthetic biology is given in Section VIII.

3. Patterning of S-layers on Solid Supports

For many technical applications of S-layers, spatial control over the reassembly is mandatory. For example, when using S-layers as affinity matrices in the development of biochips, or as templates in the fabrication of nanoelectronic devices, the S-layer must not cover the entire device area. Several approaches including optical lithography were used to pattern S-layer lattices

on silicon wafers. Nevertheless, the soft lithographical method called *micromolding in capillaries* has proven to be most suitable for patterning S-layer lattices, as it allowed restricting the reassembly of the S-layer proteins to certain areas on a solid support.[161] For this purpose, the S-layer protein solution was dropped onto the substrate in front of the channel openings of the attached mold. The solution was sucked in and the S-layer protein started to recrystallize. After removal of the mold, a patterned S-layer remained on the support, as demonstrated by AFM. Micromolding in capillaries offers the advantage that all preparation steps may be performed under ambient conditions. In contrast, patterning S-layers by optical lithography requires drying of the protein layer prior to exposure to (deep ultraviolet) radiation.[172] This is a critical step, as denaturation of the protein and consequently loss of its structural and functional integrity cannot be excluded.

4. Molecular Modeling and Computer Simulations

Over the past decades, a large number of studies addressed the 3D structure determination of S-layer proteins, which led to a considerable knowledge about the distribution of amino acids on S-layer lattices, the structure–function relationship, molecular mechanisms of the self-assembly process, and even structural details of some S-layer species.[80,82,83,173–177] However, experimental structure determination techniques, for example, NMR and X-ray crystallography, pose problems due to the size and crystallization characteristics of S-layer proteins, as in solution they form crystallized monomolecular layers rather than isotropic 3D crystals. The dissolved proteins immediately interact to form small oligomers, which provide the nucleation seed for the formation of large layers.[178] Additionally, some S-layer proteins do not fold into their native tertiary structure as monomers in solution, but rather condense into amorphous clusters in an extended conformation. Only when assembled into the lattice structure, do they restructure into their native conformation.[173,179] Thus, 3D reconstructions were limited to truncated or mutated forms of the proteins.

The combination of molecular simulations and low-resolution experimental techniques, for example, small angle X-ray scattering (SAXS) and TEM, offers an alternative to determine the atomistic structure of unmodified native S-layer proteins and self-assembled lattices.

The folding of small protein domains and of entire proteins can be monitored by reverse and steered molecular dynamics simulations. However, in order to facilitate the equilibration process, secondary structure elements taken from homologous protein models have to be implemented first. The calculated 3D model of the entire protein can be consequently verified by a systematic exploration of the free energy, by a reverse Monte Carlo simulation based on scattering contrast data obtained by SAXS, or by 3D density

distribution data as calculated by TEM. Following this approach, the structural models of the S-layer proteins SbsB from *G. stearothermophilus* pV72/*p2* (*p1* lattice symmetry)[81,178] and of the unit cell of SbpA from *Ly. sphaericus* CCM 2177 (*p4* lattice symmetry)[179] could be calculated. Additionally, based on the model of the S-layer protein SbsB, the molecular mechanisms guiding the self-assembly into monomolecular sheets exhibiting a *p1* lattice symmetry could be analyzed using Monte Carlo simulations.[180]

The structure prediction of the S-layer protein SbsB is shown in Fig. 7. The protein is split into structurally meaningful domains based on homology searches, secondary structure, and domain predictions. To obtain 3D coordinates, a premodeling by fold recognition is performed. Molecular dynamics simulations were processed with each part, and consequently, the domains were joined and the whole structure was equilibrated in vacuum (Fig. 7A–D). The resulting structure was analyzed by pulling parts of the protein along a chosen reaction coordinate, and the protein was deformed to quantify the stability, which is expressed as the potential of MF (Fig. 7F). The final structural model of SbsB is shown in detail in Fig. 7E. The structure could be verified and additionally refined by SAXS studies, where the monomeric structure and self-assemblies were investigated. The analysis is based on a fractal mean potential, which describes best the behavior of S-layers in solution.[178]

The reconstruction of the 3D structure of an SbpA unit cell is based on a similar approach. An intermediate structural model was calculated by fold recognition and molecular dynamics simulations. The resulting 3D model of an SbpA tetramer is shown in Fig. 8A–C. In this case, 3D density data facilitated the modeling process, which were obtained by tilting studies and inverse Fourier transform using TEM. Regions of high and low electron density contrast were identified by SAXS studies (Fig. 8D), where those with high contrast were classified as noninteracting and those with low contrast as interacting with the other monomers in the tetramer. The resulting 3D model of an SbpA tetramer is shown in Fig. 8.

The structural model of the S-layer protein SbsB in combination with Monte Carlo simulations was used to study the functional protein self-assembly into S-layers.[180] Using a coarse-grained model, the specific interactions between two protein monomers in solution were investigated to determine the ground-state conformations, which led to a *p1* lattice symmetry. Consequently, the calculated energies of the interactions between two proteins were used to study the large-scale self-assembly by means of lattice Monte Carlo simulations, as schematically shown in Fig. 9. Only very few and mainly hydrophobic amino acids, located on the surface of the monomer, are responsible for the formation of the highly anisotropic protein lattice, which is in excellent agreement with known experimental results.

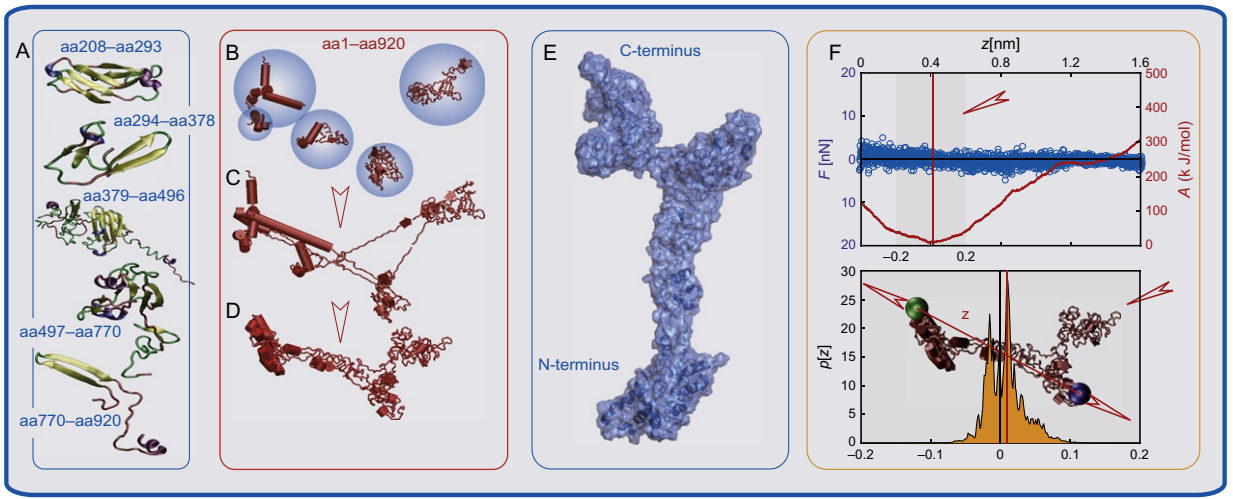

FIG. 7. (A) Three-dimensional models of the single domains of the S-layer protein SbsB created by fold recognition. Yellow arrows, beta-sheets; violet strands, alpha-helices; green line, turns; and red line, coils. Modeling method: (B) the individual domains were equilibrated in water spheres at 310 K, (C) joined in vacuum, and (D) the final structure was obtained by molecular dynamics simulations. (E) Structural model of SbsB. The protein is L-shaped, where the L is formed by the C-terminal domains. The N-terminus contains the SLH domains and is mainly made up of alpha-helices. (F) Structural analysis of the monomer structure by a calculation of the global free energy. The protein was deformed along the reaction coordinate z. Mean force values F are indicated by open blue circles. The red full line gives the potential of mean force A, which has a clear minimum at $z = 0$. Orange body gives the local density probability distribution $p[z]$. The model of the protein is given as an insert, the reaction coordinate is indicated, and the green and blue spheres indicate fixed regions. Figure modified after Ref. 81 with friendly permission of the American Institute of Physics.

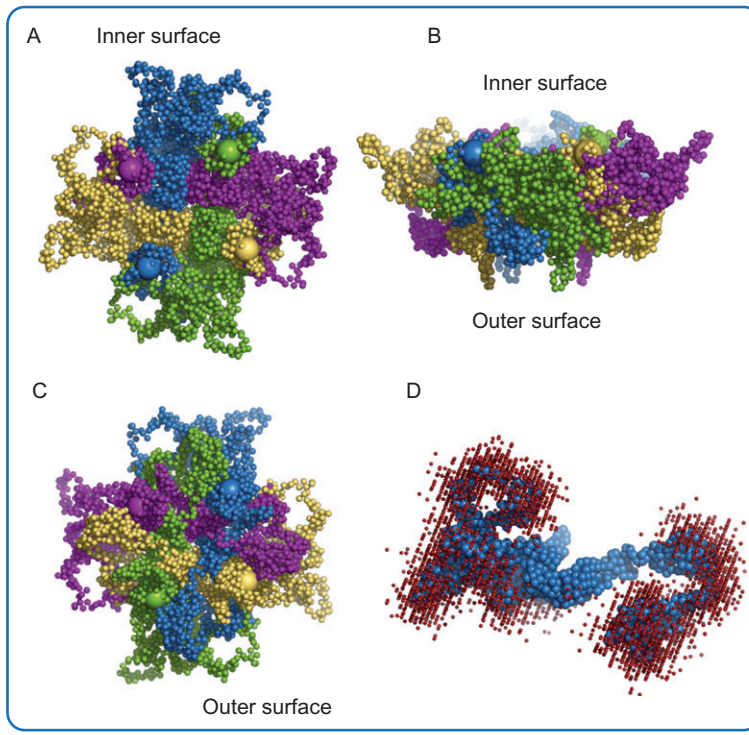

FIG. 8. Three-dimensional structure of the SbpA unit cell. Every monomer in the tetramer is illustrated in a different color. The proteins are interlocked into each other. (A) Inner surface of the tetramer, which anchors the protein on the cell surface. The N-termini are represented by magnified beads and are accessible on the surface. (B) Side view of the unit cell. (C) Outer surface of the tetramer, which is exposed to the surroundings of the cell. The C-termini are also accessible and marked as magnified beads. (D) Scattering clusters (red beads) of one SbpA monomer as determined by SAXS and a Monte Carlo algorithm. The scattering clusters represent regions of high electron density contrast, where those domains in the protein that do not show high contrast are related to interacting or overlapping parts in the tetramer. Figure modified after Ref. 179 with friendly permission of the American Institute of Physics.

IV. S-Layers for the Production of Ultrafiltration Membranes

As S-layers are composed of identical subunits, they possess pores of identical size and morphology. Depending on the mass distribution of the constituent subunits, more than one type of pore may generate the protein meshwork. High-resolution electron microscopy in combination with digital image processing methods have indicated that pore diameters can range from 2 to 8 nm and thus function in the ultrafiltration range (Fig. 10).[64,181] More

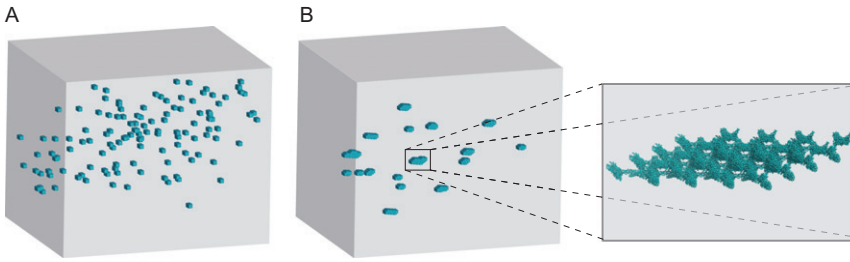

FIG. 9. Representation of the lattice Monte Carlo simulations of the large-scale self-assembly of the S-layer protein SbsB. Energy values were taken from Monte Carlo simulations of the interaction of two monomers. Proteins are represented as cubes. (A) Initial configuration: cubes are randomly distributed in the simulation box. (B) Competitive growth study. Multiple sheets start to grow during initial period. Magnified view of the corresponding S-layer sheet using a coarse-grained model. Figure modified after Ref. 180 with friendly permission of the American Institute of Physics.

precise data on the pore size could be derived from permeability studies on S-layer vesicles using the space technique[182,183] and S-layers that had been deposited on porous supports.[184] S-layers from thermophilic Bacillaceae (e.g., *G. stearothermophilus*) revealed sharp exclusion limits between molecular weights of 30,000 and 40,000 suggesting a limiting pore diameter of 3.5–5 nm. Carbonic anhydrase with a molecular weight of 30,000 and a molecular size of $4.1 \times 4.1 \times 4.7$ nm could still pass through the pores, whereas ovalbumin with a molecular weight of 43,000 was rejected to more than 90%. No significant difference in the rejection characteristics could be observed between native S-layers and S-layer protein lattices cross-linked with glutaraldehyde.[185,186]

For the production of S-layer ultrafiltration membranes (SUMs), cell wall fragments or isolated S-layers were deposited on microfiltration membranes (MFMs) using a pressure-dependent procedure and the S-layer protein was cross-linked with glutaraldehyde.

To increase the chemical stability of such cross-linked S-layer lattices, Schiff bases formed by the reaction of glutaraldehyde with ε-amino groups from lysine were reduced with sodium borohydride.[185–188] In these composite membranes, the active filtration layer consists of a coherent layer of superimposed S-layer material, whereas the MFM provides the mechanical support. Generally, SUMs were made of S-layer material from different *G. stearothermophilus* strains and *Ly. sphaericus* CCM 2120 (see Table II).

Even though S-layers of different crystallographic types were used, all molecular cut-off values resembled those determined for S-layer vesicles applying the space technique.[183]

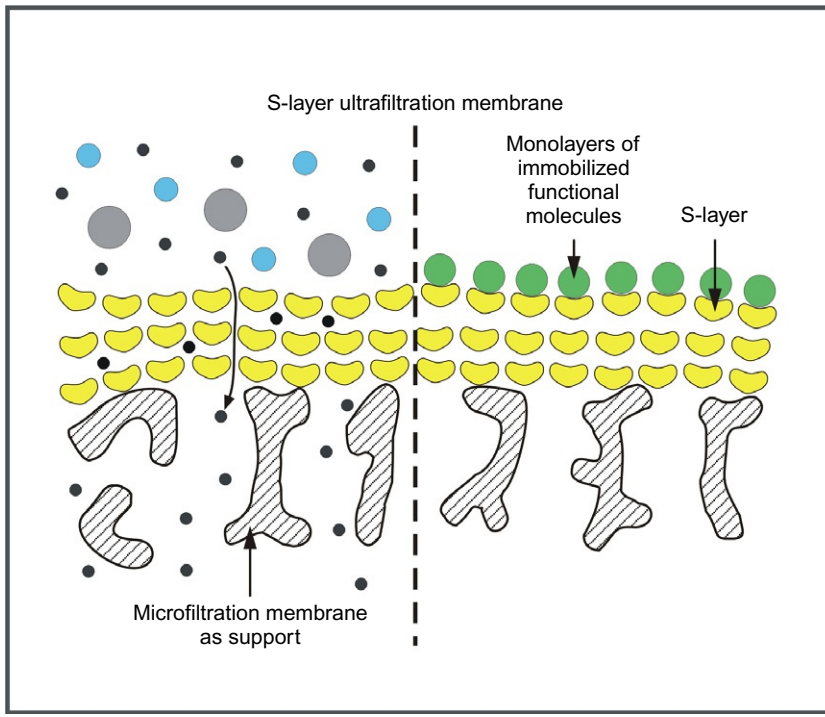

FIG. 10. Schematic drawing of the fine structure of S-layer ultrafiltration membranes (SUMs): (left) the active ultrafiltration layer consists of coherent S-layers deposited on open-celled foam-like microfiltration membranes. (right) SUMs can also be used for covalent attachment of functional molecules.

TABLE II
REJECTION CHARACTERISTICS OF SUMS PREPARED OF S-LAYER CARRYING CELL WALL FRAGMENTS FROM *LYSINIBACILLUS SPHAERICUS* CCM 2120 (MODIFIED AFTER REF. 19)

Protein	M_r	Molecular size (nm)	p*I*	%*R*	pH value of the protein solution
Ferritin	440,000	12	4.3	100	7.2
Bovine serum albumin (BSA)	67,000	4.0 × 4.0 × 14.0	4.7	100	7.2
Ovalbumin (OVA)	43,000	4.5	4.6	95	4.6
Carbonic anhydrase (CA)	30,000	4.1 × 4.1 × 4.7	5.3	80	5.3
Myglobin (MYO)	17,000	4.4 × 4.4 × 2.5	6.8	0	6.8

Cross-linking the S-layer protein with glutaraldehyde during the production of SUMs leads to net negatively charged membranes due to the reaction of a considerable proportion of free amino groups. As under physiological conditions most proteins in solution are negatively charged, it is advantageous for many ultrafiltration processes to use membranes that have a negative charge, too. Repulsive forces between the protein in solution and the membrane surface prevent unspecific adsorption and pore-blocking, which cause deterioration in membrane performance in the form of flux losses and decrease in selectivity. For example, SUMs with a net negative surface charge showed no or negligible flux losses after filtration of solutions of ferritin, bovine serum albumin, or ovalbumin, which had a net negative surface charge under the applied experimental conditions.[3,189–193]

As in S-layer lattices the physicochemical properties are determined by those of the single constituent (glyco)protein subunit, SUMs are ideal model systems for studying the effects of chemical modifications on the rejection and adsorption properties of ultrafiltration membranes. For example, after the cross-linking, carboxyl groups from the S-layer lattices were activated with 1-ethyl-3(3-dimethylaminopropyl) carbodiimide (EDC) and allowed to react with the free amino groups from nucleophiles of different molecular sizes, structures, hydrophobicity, and charge.

Contact angle measurements clearly demonstrated that covalent attachment of low molecular weight nucleophiles to S-layer lattices led to SUMs with more hydrophilic or hydrophobic surface properties.

Covalent attachment of low molecular weight nucleophile SUMs not only led to alterations of the surface properties and antifouling characteristics but were also responsible for an accurately controlled shift of the rejection curves to the lower molecular weight range.[19] Moreover, a correlation was observed between the molecular size of attached nucleophiles and the shift of the rejection curve to the lower molecular weight range.[189,194]

In conclusion, up to now, SUMs are the only ultrafiltration membranes that enable most precisely controlled modifications of the physicochemical and molecular sieving properties. This broad spectrum of potential modifications allows the properties of SUMs to be adapted to very specific requirements.[19,187,195]

Moreover, it has to be remembered that native S-layers reveal remarkable antifouling properties. This is considered an essential requirement to prevent plugging of pores in the protein meshwork and maintain free exchange of molecules up to a defined molecular weight between the cell and the environment.

V. S-Layer as Matrix for the Immobilization of Functional Molecules and Nanoparticles

Because S-layers are periodic structures, they exhibit repetitive physicochemical and morphological properties down to the subnanometer scale and possess pores of identical size and morphology. Most importantly, S-layer recrystallization can be induced on flat surfaces and highly porous structures such as MFMs or porous beads. Owing to the high density of functional groups on the surface and their accessibility for chemical modifications, S-layers are well-defined matrices for controlled immobilization of functional molecules such as enzymes, antibodies, antigens, and ligands as required for affinity and enzyme membranes in the development of solid-phase immunoassays or in biosensors.

Chemical modification and labeling experiments revealed that S-layer lattices possess a high density of functional groups on the outermost surface. For covalent attachments of foreign (macro)molecules such as protein A, monoclonal antibodies, streptavidin, or various enzymes, the free carboxylic acid groups originating from either aspartic acid or glutamic acid in the S-layer protein were activated with carbodiimide and subsequently reacted with free amino groups of functional macromolecules leading to stable peptide bonds between the S-layer matrix and the immobilized macromolecule.[168,193,196–199] From the amount, molecular mass, and size of the foreign proteins bound to the S-layer lattice, as well as from the molecular size of the S-layer subunits and the area occupied by one morphological unit, it was derived that most macromolecules formed a monomolecular layer on the surface of the S-layer lattice. Immobilization via spacer molecules such as 6-amino capronic acid was advantageous when the molecules were small enough to be entrapped inside the pores of the S-layer lattice, which, in the case of enzymes, was linked to a significant activity loss.[168] In general, the activity of enzymes immobilized to S-layer lattices was well preserved.[19,191,193]

The enzymes were either coupled to the hexagonally ordered S-layer lattices from *Thermoanaerobacter thermohydrosulfuricus* L111-69[200] or from *G. stearothermophilus* PV72.[201] The covalently bound carbohydrate chains of the S-layer glycoprotein from *T. thermohydrosulfuricus* L111-69[202,203] were also exploited for enzyme immobilization.[168,191,198,204] Independent of the type of S-layer protein used from different *Bacillaceae*, the large enzymes invertase ($M_r = 270{,}000$), glucose oxidase (GOD) ($M_r = 150{,}000$), glucuronidase ($M_r = 280{,}000$), and β-galactosidase ($M_r = 116{,}000$) formed a dense monolayer on the outer face of the S-layer lattice.[29] After direct coupling of the enzymes invertase, GOD, naringinase ($M_r = 96{,}000$), and β-glucosidase ($M_r = 66{,}000$) to the EDC-activated carboxylic acid groups of the S-layer protein from

T. thermohydrosulfuricus L111-69, the retained enzymatic activities were in the range of 70%, 35%, 60%, and 16%, respectively. By immobilization via spacer molecules, a significant increase in enzymatic activity could be achieved for GOD and naringinase of 60% and 80%, respectively. The most striking increase was observed for β-glucosidase, for which immobilization via spacers led to a 10-fold increase in activity to 160%. The significant increase in enzymatic activity indicated that immobilization via spacers most probably increased the distance between the enzyme molecules and the crystalline S-layer matrix.[205]

The S-layer immobilization matrix can be used with planar and curved supports. Affinity microparticles (AMPs) represent 1-μm large cup-shaped structures. They are produced from S-layer carrying cell wall fragments, in which the S-layer protein is cross-linked with glutaraldehyde and Schiff bases are reduced with sodium borohydride. Because of the applied preparation procedure, AMPs possess a complete outer and inner S-layer, which can be exploited for immobilization of foreign macromolecules. Protein A as an Fc-binding ligand was linked to the carbodiimide-activated carboxylic acid groups of the S-layer protein of *T. thermohydrosulfuricus* L111-69.[199,206] The Fc-binding ligand formed a monolayer on the exposed outer face of the S-layer lattice. AMPs based on S-layer-carrying cell wall fragments revealed excellent stability properties under cross-flow conditions. AMPs were used as escort particles in affinity cross-flow filtration and as novel immunoadsorbent particles in blood purification.[199,206] For both applications, the advantage of AMPs can be seen in the cup-shaped structure, leading to a high surface-to-volume ratio, as well as in the dense monolayer of protein A molecules on the outermost surface of the S-layer lattices.

SUMs were not only used as ultrafiltration membranes but also exploited as novel matrices for the development of dipstick-style solid-phase immunoassays and for the development of an amperometric glucose sensor (Fig. 10). Depending on the test system, the respective monoclonal antibody was covalently bound to the carbodiimide-activated carboxylic acid groups of the S-layer lattice. After immobilization of the monoclonal antibodies, disks of 3-mm diameter were punched out and sandwiched between Teflon foils, leaving the SUM exposed for further binding reactions. By immobilizing monolayers of either protein A or streptavidin onto SUMs, a universal biospecific matrix for immunoassays and dipsticks could be generated.[207] Matrices based on protein A as an immunoglobulin G (IgG)-specific ligand were obtained by immobilizing dense monolayers of this ligand to carbodiimide-activated carboxylic acid groups from the S-layer protein of SUMs.[199,207] Because of the high affinity of human IgG and rabbit IgG to protein A, the protein A-SUM was shown to be particularly suitable for generating dense monolayers of correctly aligned antibodies on the SUM surface. However, mouse IgG with lower affinity to protein

A than human IgG or rabbit IgG was either first biotinylated and subsequently bound to a streptavidin-coated SUM, or it was directly linked to carbodiimide-activated carboxylic acid groups exposed on the surface of the S-layer lattice. Proof of principle was demonstrated for different types of SUM-based dipsticks: for example, for diagnosis of type I allergies (determination of IgE against the major birch pollen allergen Bet v1 in whole blood or serum); for quantification of tissue type plasminogen activator (t-PA) in patients whole blood or plasma for monitoring t-PA levels in the course of thrombolytic therapies after myocardial infarcts; or for determination of interleukin 8 in supernatants of human umbilical vein endothelial cells (HUVEC) induced with lipopolysaccharides.[208–210] Further, a dipstick assay was developed for prion diagnosis based on a sandwich enzyme-linked immunosorbent assay (ELISA) specific for prion protein, exploiting S-layer lattices as an immobilization matrix. The sensitivity of the prion dipsticks were similar to that published for time-resolved fluorescence ELISA methods, which are among the most sensitive detection methods for prions.[211]

In addition, the feasibility of SUMs as a new type of immobilization matrix was already demonstrated many years ago by the development of an amperometric glucose sensor using GOD as the biologically active component.[204,212] Subsequently, a layer-by-layer technique was established allowing the fabrication of a multienzyme biosensor for sucrose.[213] Based on the demonstrated suitability of the S-layer protein self-assembly system for covalent enzyme immobilization, genetic approaches were pursued to construct fusion proteins between S-layer proteins of *Bacillaceae* and enzymes from extremophiles for the development of novel biocatalysts (see Section VI).[214,215]

The ultimately high requirements in positional control at the nanometer scale, the synthesis of molecular functional units (memory cells or switches), and their internal (nano-to-nano) and external (nano-to-micro) interconnection can only be met when novel concepts based on bottom-up approaches are developed. In this context, the broad base of knowledge about the S-layer-mediated binding of biological molecules has paved the way for investigating the potential of S-layer proteins and their self-assembly products as catalysts, templates, and scaffolds for the generation of ordered nanoparticle arrays for nonlife-science applications (e.g., nonlinear optics, nanoelectronics). In particular, the *in situ* precipitation and the controlled binding of metallic or semiconducting nanoparticles on S-layers laid the foundation for novel concepts in the field of molecular electronics and optics (Fig.11).

The first approach in using S-layers as lithographic templates in the formation of perfectly ordered nanoparticle arrays was based essentially on the deposition of a metal vapor onto S-layer fragments of *Sulfolobus acidocaldarius*. In a three-step parallel process, a 1-nm thick tantalum/tungsten film with holes (15 nm in diameter) periodically arranged according to the

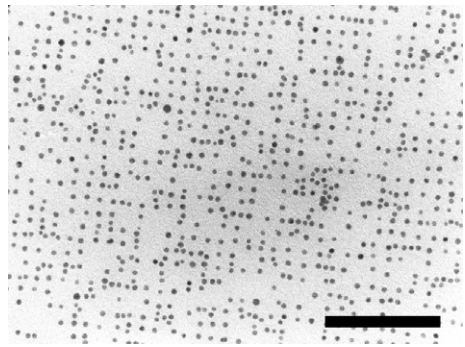

FIG. 11. TEM image of gold nanoparticles (mean diamter 5 nm) bound in a regular order on an S-layer exhibiting square lattice symmetry and a center-to-center spacing of 13.1 nm (bar, 100 nm).

center-to-center spacing (22 nm) of the hexagonal S-layer lattice was fabricated.[216] Although it has been demonstrated that nanoparticle arrays may be fabricated in this way, the real breakthrough was achieved by using S-layer lattices in the direct precipitation of metals from solution or by binding preformed nanoparticles. In the wet chemical approach, which was derived from mineral formation on bacterial surfaces,[217] self-assembled S-layer structures were exposed to metal salt solutions, such as tetrachloroauric (III) acid ($HAuCl_4$) solution, followed by slow reaction with a reducing agent such as hydrogen sulfide (H_2S) or by electron irradiation in an electron microscope.[218–223] As the precipitation of the metals was confined to the pores of the S-layer, nanoparticle arrays with prescribed symmetries and lattice geometries could be obtained. Although the wet chemical methods resulted in crystalline arrays of nanoparticles with spacings in register with the underlying S-layer lattice, they do not allow controlling of the particle size or composition, such as in core–shell nanoparticles. Thus, the binding of preformed standardized nanoparticles into regular arrays on S-layers has significant advantages in the development of biomolecule-driven assemblies of nanoscale electronic devices compared to vapor deposition or wet chemical methods.

Several studies have already demonstrated the outstanding performance of S-layer lattices as patterning elements.[165,218,224] The pattern of bound molecules and nanoparticles frequently reflects the lattice symmetry, the size of the morphological units, and the physicochemical properties of the array. For example, the distribution of net negatively charged domains on S-layers could be visualized by electron microscopic methods after labeling with positively charged topographical markers, such as polycationic ferritin (diameter, 12 nm).[19,151] Metal (Au) or semiconductor (CdSe) nanoparticles were either

electrostatically or covalently bound onto solid-supported S-layer monolayers and self-assembly products of SbpA, the S-layer protein of *Ly. sphaericus* CCM 2177.[165] Upon activation of carboxyl groups in the S-layer lattice, a close-packed monolayer of 4-nm sized, amino-functionalized CdSe nanoparticles could be covalently established on the outer face of the solid-supported S-layer lattices. However, owing to electrostatic interactions, anionic citrate-stabilized 5-nm gold nanoparticles formed a superlattice at those sites where the inner face of the S-layer lattice was exposed.[165]

Further, S-layer protein lattices isolated from the Gram-positive bacterium *D. radiodurans* and the acidothermophilic archaeon *S. acidocaldarius* were investigated and compared for their ability to biotemplate the formation of self-assembled, ordered arrays of inorganic nanoparticles.[225,226] The authors demonstrated the possibility to exploit the physicochemical/structural diversity of prokaryotic S-layer scaffolds to vary the morphological patterning of nanoscale metallic and semiconductor NP arrays.[225]

More recently, genetic approaches were used for the construction of chimeric S-layer fusion proteins whereby precipitation of metal ions or binding of metal nanoparticles is confined to specific and precisely localized positions in the S-layer lattice (see Section VI).[98,227]

VI. S-Layer Fusion Proteins—Construction Principles and Applications

During the past 10 years, genetic approaches have been focused on the construction of chimeric S-layer fusion proteins aiming at a very controlled and specific way of making highly ordered functional arrays. The genetically engineered S-layer fusion proteins comprised (i) an accessible N-terminal cell wall anchoring domain, which can be exploited for oriented binding on supports precoated with SCWP; (ii) the self-assembly domain; and (iii) a functional sequence.[8,15,228] The most relevant advantages of the genetically engineered self-assembly system based on S-layers over less nanostructured approaches are (i) the alignment of functional domains at predefined distance in the nanometer range on the outermost surface of the S-layer lattice and, thus, availability for further binding reaction (e.g., substrate binding, antibody binding, enzymatic reactions); (ii) the requirement of only a simple, one-step incubation process for site-directed immobilization without preceding surface activation of the support; (iii) the general applicability of the "S-layer tag" to any fusion partner; (iv) the high flexibility for variation of the functional groups within a single S-layer array by cocrystallization of different S-layer fusion proteins to construct multifunctional arrays; and (v) the provision of a cushion

for the functional group through the S-layer moiety preventing denaturation, and, consequently, loss of reactivity upon immobilization. Since these advantages opened up a broad spectrum of applications for S-layer fusion proteins particularly in the fields of biotechnology, molecular nanotechnology, and biomimetics (Fig.12),[3,5,7,15,228] a great variety of functional S-layer fusion proteins were cloned and heterologously expressed in *Escherichia coli* or used for surface display after homologous expression (overview given in Table III).

The S-layer protein SbpA of the mesophilic *Ly. sphaericus* CCM 2177 consists of total of 1268 amino acids, including a 30-amino-acid long signal peptide.[77] By producing various C-terminally truncated forms and performing surface accessibility screens, it became apparent that amino-acid position 1068 is located on the outer surface of the square lattice. The derivative $rSbpA_{31-1068}$ fully retaining its ability to self-assemble into a square S-layer lattice with a center-to-center spacing of the morphological units of 13.1 nm.[77] Therefore,

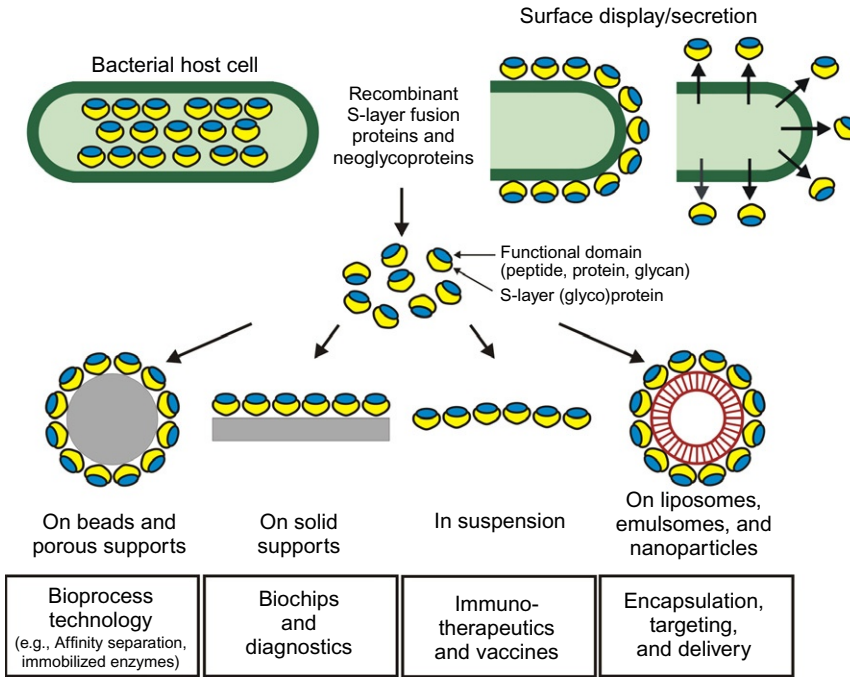

FIG. 12. Schematic drawing of technologies based on recombinant S-layer fusion proteins and their applications.

TABLE III
FUNCTIONAL RECOMBINANT S-LAYER FUSION PROTEINS AND THEIR APPLICATIONS

Recombinant S-layer protein	Functionality	Length of function	Application	References
SbpA, SbsB	Core streptavidin	118 aa	Binding of biotinylated ligands (DNA, protein), Biochip development	98,229
SbpA, SbsC	Major birch pollen allergen (Bet v1)	116 aa	Vaccine development, treatment of type 1 allergy	77,230
SbpA	*Strep*-tag II, affinity tag for streptavidin	9 aa	Biochip development	77
SbpA	ZZ, IgG-binding domain of Protein A	116 aa	Extracorporeal blood purification	231
SbpA	Enhanced green fluorescent protein (EGFP)	238 aa	Coating of liposomes, development of drug targeting and delivery systems	232
SbpA	cAb, heavy chain camel antibody	117 aa	Diagnostic systems and sensing layer for label-free detection systems	233
SbpA	Hyperthermophilic enzyme laminarinase (LamA)	263 aa	Immobilized biocatalysts	215
SbpA	Cysteine mutants	3 aa	Building of nanoparticle arrays	227
SbpA, SbsB	Mimotope of an Epstein–Barr virus (EBV) epitope (F1)	20 aa	Vaccine development	234
SbpA, SbsB	*M. tuberculosis* antigen (mpt64)	204 aa	Vaccine development	Tschiggerl H.*
SbpA	IgG-Binding domain of Protein G	110 aa	Downstream processing	Nano-S*
SgsE	Glucose-1-phosphate thymidylyltransferase (RmlA)	299 aa	Immobilized biocatalysts	214
SgsE	Enhanced cyan fluorescent protein (ECFP) Enhanced green fluorescent protein (EGFP) Yellow fluorescent protein (YFP) Monomeric red fluorescent protein (RFP1)	240 aa 240 aa 240 aa 225 aa	pH biosensors *in vivo* or *in vitro*, fluorescent markers for drug delivery systems	235,236
SbsA	*H. influenzae* antigen, (*Omp*26)	200 aa	Vaccine development	237
SlpA	Antigenic poliovirus epitope (VP1) Human c-myc proto-oncogene	11 aa 10 aa	Development of mucosal vaccines	127
SLH-EA1, SLH-Sap	Levansucrase of *B. subtilis*	473 aa	Vaccine development	238

SLH-EA1	Tetanus toxin fragment C of *C. tetani* (ToxC)	451 aa	Development of live veterinary vaccines	239
RsaA	*P. aeruginosa* strain K pilin	12 aa	Vaccine development	240
RsaA	IHNV glycoprotein	184 aa	Development of vaccines against hematopoietic virus infection	241
RsaA	Beta-1,4-glycanase (Cex)	485 aa	Immobilized biocatalysts	242
RsaA	IgG-binding domain of Protein G	$GB1_{xs}$	Development of immunoactive reagent	243
RsaA	Domain 1 of HIV receptor CD4 MIP1α ligand for HIV coreceptor CCR5	81 aa 70 aa	Anti-HIV microbicide development	244
RsaA	His-tag, affinity tag	6 aa	Bioremediation of heavy metals (Cd) from aqueous systems, bioreactor	245

S-layer proteins: SbsB of *Geobacillus stearothermophilus* PV72/*p2*, SbpA of *Lysinibacillus sphaericus* CCM 2177, SbsC of *Geobacillus stearothermophilus* ATCC 12980, SgsE of *Geobacillus stearothermophilus* NRS 2004/3a, SbsA of *Geobacillus stearothermophilus* PV72/*p6*, SlpA of *Lactobacillus brevis* ATCC 8287, SLH (S-layer homology domain of EA1 or Sap) of *Bacillus anthracis*, RsaA of *Caulobacter crescentus* CB15A.

°personal communication.

this C-terminally truncated form was used as base form for the construction of various S-layer fusion proteins. For SbpA, the recrystallization process is dependent on the presence of calcium ions, thus allowing control over lattice formation,[155] which is of advantage for nanobiotechnological applications of the SbpA system.

Another S-layer protein that adopts C-terminal fusions without affecting self-assembly into lattices is SbsB of thermophilic *G. stearothermophilus* PV72/*p2*. SbsB consists of a total of 920 amino acids, including a 31-amino-acid long signal peptide.[98] As the removal of fewer than 15 C-terminal amino acids led to water-soluble rSbsB forms, the C-terminal part can be considered extremely sensitive to deletions. When the C-terminal end of full-length SbsB was exploited for linking a foreign functional sequence, water-soluble S-layer fusion proteins were obtained,[98] which recrystallized into the oblique (*p1*) lattice on solid supports precoated with SCWP of *G. stearothermophilus* PV72/*p2*. Alternatively, functional groups were fused toward the N-terminus of SbsB to construct self-assembling S-layer fusion proteins, which attached with their outer surface to, for example, liposomes and silicon wafers, so that the N-terminal region with the fused functional sequence remained exposed to the environment.[98]

The protein precursor of the S-layer protein SbsC from *G. stearothermophilus* ATCC 12980 includes a 30-amino-acid long signal peptide and consists of 1099 amino acids.[100] The investigation of the self-assembly properties of several truncated SbsC forms revealed that on the C-terminal part, 179 amino acids could be deleted without interfering with the self-assembling properties of the S-layer protein.[78] Thus, $SbsC_{31–920}$, which is the shortest C-terminal truncation still capable of forming self-assembly products, was used as base form for the construction of functional SbsC fusion proteins.[230]

To generate a universal affinity matrix for binding of any kind of biotinylated molecules, S-layer streptavidin fusion proteins have been constructed.[98,229,246] For that purpose, core streptavidin was either fused to N-terminal positions of the S-layer protein SbsB or to the C-terminal end of the truncated form $SbpA_{31–1068}$.[98,229,246] As biologically active streptavidin occurs as tetramer, heterotetramers consisting of one chain fusion protein and three chains of core streptavidin were prepared by applying a special refolding procedure (Fig. 13). A biotin binding capacity of about 75% could be determined for soluble heterotetramers, indicating that three of four biotin binding sites were active.[98] In addition, the use of S-layer–streptavidin fusion proteins allowed specific binding of biotinylated ferritin molecules into regular arrays.[98] The lattice formed by the fusion protein displayed streptavidin in defined repetitive spacing, capable of binding D-biotin and biotinylated proteins, in particular ferritin.[98]

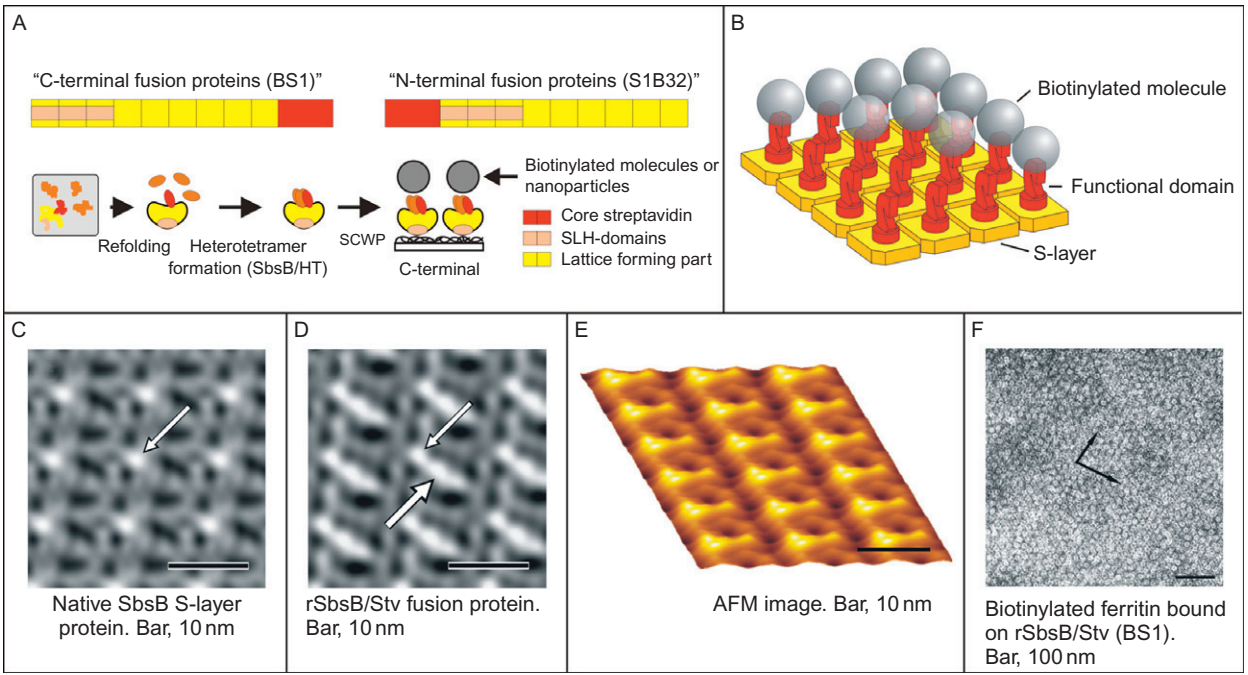

FIG. 13. S-layer/streptavidin fusion proteins as template for nanopatterned molecular arrays. (A) Refolding of heterotetrameric S-layer/streptavidin fusion protein. Core streptavidin and fusion protein were produced in *E. coli* and isolated independently, mixed in the molar ratio of 1:3, and refolded to heterotetramers by applying the rapid dilution protocol. (B) Cartoon illustrating self-assembled S-layer fusion protein carrying functional domains (e.g., streptavidin) in defined position and orientation with bound biotinylated molecules. (C and D) Digital image reconstruction by Fourier processing of electron micrographs showing self-assembly products of wild-type SbsB or rSbsB/Stv fusion protein, respectively. (C) The region of the highest protein mass in the SbsB lattice is the SLH domain. (D) In the lattice of the fusion protein, streptavidin showed up as additional protein mass. (E) Side-on view of the AFM image data of an rSbsB/Stv monolayer. (F) Electron micrograph of cell wall fragments carrying recrystallized S-layer/streptavidin fusion protein which was capable of binding biotinylated ferritin. Bound ferritin reflected the underlying oblique lattice symmetry.

Hybridization experiments with biotinylated and fluorescently labeled oligonucleotides evaluated by surface plasmon-field-enhanced fluorescence spectroscopy indicated that a functional sensor surface could be generated by recrystallization of heterotetramers on gold chips.[229] Such promising structures could be exploited for the development of DNA or protein chips as required for many nanobiotechnological applications.

The Z-domain is a synthetic analog of the B-domain of protein A from *Staphylococcus aureus*, capable of binding the Fc part of IgG. For production of an antibody-binding matrix, the S-layer fusion protein rSbpA$_{31–1068}$/ZZ carrying two copies of the 58-amino-acid long Fc-binding Z-domain on the C-terminal end was recrystallized on gold chips precoated with thiolated SCWP.[231] The binding capacity of the native or cross-linked rSbpA$_{31–1068}$/ZZ monolayer for human IgG was determined by SPR measurements. On average, ~66% of the theoretical saturation capacity of a planar surface was covered by IgG aligned in upright position.[231] By recrystallization of this chimeric protein on microbeads, a biocompatible matrix for the microsphere-based detoxification system used for extracorporeal blood purification of patients suffering from autoimmune disease has been generated. To increase the IgG-binding variety for further immunoaffinity applications, current approaches focus on the construction of an S-layer fusion protein carrying the SPG1 domain of protein G from *Streptococcus* (NanoS, personal communication).

For the development of a sensing layer for label-free detection systems such as SPR, surface acoustic wave, or quartz crystal microbalance with dissipation monitoring (QCM-D), the S-layer fusion protein rSbpA$_{31–1068}$/cAb-PSA carrying the camel antibody sequence recognizing the prostate-specific antigen (PSA) was recrystallized on gold chips precoated with thiolated SCWP.[233] For determining the binding capacity, PSA-containing sera were conducted over the sensor surface. The fused ligands on the S-layer lattice showed a well-defined spatial distribution down to the subnanometer scale, which might reduce diffusion-limited reactions.[233,247]

Owing to their immunomodulating capacity, chimeric S-layer proteins comprising allergens are generally considered as a novel approach to specific immunotherapy (SIT) of allergic diseases.[77,230,248] For that purpose, two chimeric S-layer proteins, rSbpA$_{31–1068}$/Bet v1 and rSbsC$_{31–920}$/Bet v1, carrying the major birch pollen allergen Bet v1 at the C-terminus have been constructed.[77,230] In cells of birch pollen-allergic individuals, the histamine-releasing capacity induced by the S-layer fusion proteins was significantly reduced compared to stimulation with free Bet v1 and no Th2-like immune response was observed.[248,249] These data clearly supported the concept that genetic fusion of allergens to S-layer proteins is a promising approach to improve vaccines for specific treatment of atopic allergy.

A further promising application potential can be seen in the development of drug and delivery systems based on liposome–DNA complexes coated with functional S-layer fusion protein for transfection of eukaryotic cell lines. In this context, the S-layer fusion protein rSbpA$_{31–1068}$/enhanced green fluorescent protein (EGFP) incorporating the sequence of EGFP was recrystallized as a monolayer on the surface of positively charged liposomes. Because of its ability to fluoresce, liposomes coated with rSbpA$_{31–1068}$/EGFP represent a useful tool to visualize the uptake of S-layer-coated liposomes into eukaryotic cells.[232]

Another field of research deals with the production of S-layer fusion proteins between the S-layer proteins of *Ly. sphaericus* CCM 2177 or *G. stearothermophilus* PV72/*p2* and peptide mimotopes such as F1 that mimics an immunodominant epitope of the Epstein–Barr virus (EBV). Diagnostic studies have been performed by screening 83 individual EBV IgM-positive, EBV-negative, and potential cross-reactive sera, which resulted in 98.2% specificity and 89.3% sensitivity as well as no cross-reactivity with related viral diseases. This result demonstrates the potential of these S-layer fusion proteins to act as a matrix for site-directed immobilization of small ligands in solid-phase immunoassays.[234]

In a recent study, C-terminally functionalization of the S-layer protein SbpA by introduction of cysteine residues combined with targeted chemical modification was used to identify amino acids that are located at the surface of the S-layer lattice.[227] Crystalline monolayers of these S-layer cysteine mutants offered free sulfhydryl groups for the activation with various heterobifunctional cross-linkers and covalent attachment of differently sized (macro)molecules. Finally, functionalized 2D S-layer lattices formed by rSbpA cysteine mutants exhibiting highly accessible cysteine residues in a well-defined arrangement on the surface were utilized for the template-assisted patterning of gold nanoparticles.[227]

On the basis of the remarkable intrinsic feature of S-layer proteins to self-assemble and the possibility for genetic modifications, S-layer proteins were exploited as component for the development of novel immobilized biocatalysts based on fusion proteins comprising S-layer proteins of Bacillaceae and enzymes from extremophilic organisms (extremozymes). By exploiting the self-assembly property of the S-layer protein moiety, the chimeric protein was used for spatial control over display of enzyme activity on planar and porous supports. As proof of principle, the enzyme β-1,3-endoglucanase LamA from the extremophilic *P. furiosus* was C-terminally fused to the S-layer protein SbpA$_{31–1068}$ of *Ly. sphaericus* CCM 2177.[215] The results obtained clearly demonstrate that S-layer-based bottom-up self-assembly systems for functionalizing solid supports with a catalytic function could have significant advantages over processes based on random immobilization of sole enzymes. In general, clear advantages for enzyme immobilization offered by

the S-layer self-assembly system include the high flexibility for variation of enzymatic groups within a single S-layer array by cocrystallization of different enzyme/S-layer fusion proteins to construct multifunctional, nanopatterned biocatalysts, as well as the possibility for deposition of the biocatalysts on different supports with the additional option of cross-linking of individual monomers to improve robustness.[215] It is remarkable to note that the measured enzyme activities of the recrystallized S-layer/enzyme fusion proteins reach up to 100% compared to the native enzyme. The S-layer protein portion of the biocatalysts confers significantly improved shelf-life to the fused enzyme without loss of activity over more than 3 months, and also enables biocatalyst recycling.

In addition, recent research activities are focused on the production of immobilized biocatalysts based on fusion proteins comprising self-assembling S-layer proteins and multimeric enzymes of extremophiles (e.g., xylose isomerase of *Thermoanaerobacterium strain* JW/SL-YS 489) (Fig. 14).[250]

SgsE, the S-layer glycoprotein of the thermophilic Gram-positive bacterium *G. stearothermophilus* NRS 2004/3a, has a molecular weight of 93,684 Da and a *p*I of 6.1.[214] SgsE has the ability to form 2D crystalline arrays with oblique symmetry exhibiting nanometer-scale periodicity. Studies on the structure–function relationship of SgsE revealed that the N-terminal region is involved in anchoring the protein to the cell wall and the C-terminal region encodes the self-assembly information.[214] Concerning the biotechnological application of S-layer fusion proteins aiming at controllable display of biocatalytic epitopes, storage stability, and reuse, S-layer/enzyme fusion proteins comprising the glucose-1-phosphate thymidylyltransferase RmlA from *G. stearothermophilus*

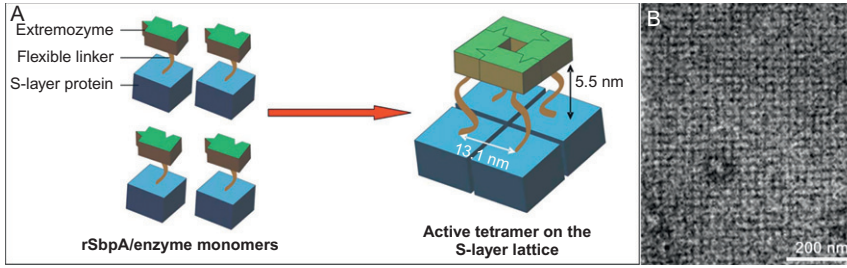

FIG. 14. Novel approach for site-directed immobilization of multimeric enzymes of extremophilic organisms via the S-layer self-assembly technique, allowing oriented and dense surface display of the extremozyme in its native confirmation and ensuring accessibility for the substrate. (A) Schematic drawing of an immobilized biocatalyst based on S-layer fusion proteins carrying a multimeric extremozyme. (B) Transmission electron micrograph of a negatively stained preparation of an S-layer/xylose isomerase fusion protein self-assembled in solution into a monomolecular array.

NRS 2004/3a as well as the SgsE derivatives $SgsE_{31–773}$ or $SgsE_{31–573}$ from *G. stearothermophilus* NRS 2004/3a, respectively, were cloned and expressed in *E. coli*.[214]

To build up novel functional fluorescent architectures, the 903-amino-acid containing S-layer protein SgsE from *G. stearothermophilus* NRS 2004/3a was used for the production of four S-layer fusion proteins carrying different colored GFP mutants.[235,236] For this purpose, the nucleotide sequence encoding the EGFP, the enhanced cyan fluorescent protein, the yellow-shifted YFP 10C variant, as well as the yellow-shifted red fluorescent protein mRFP1 were fused to the C-terminus of the N-terminally truncated form $SgsE_{131–903}$. Results derived from investigation of the recrystallization properties, absorptions spectra, steady-state, and lifetime fluorescence measurements in different pH environments revealed that the assembling and fluorescence properties of the fusion proteins can be used for building up nanopatterned bifunctional surfaces that can be exploited as pH biosensors *in vivo* and *in vitro* or as fluorescent markers for drug delivery systems.[235,236]

The molecular masses of *Lactobacillus* S-layer proteins are among the smallest (43–46 kDa) known S-layer proteins and show sequence similarity at the C-terminus, which is responsible for binding of the S-layer subunits to the cell wall layer.[107,127] In *L. brevis* ATCC 8287, the C-terminal part of the 48-kDa S-layer protein SlpA is heterogeneous and lacks a cell wall anchoring domain whereas this strain strongly adheres to several human epithelial cell types, pig intestinal epithelial cells, and fibronectin via a receptor-binding site that is located at the N-terminus of SlpA.[127] In terms of immunological studies, an inducible *L. brevis* expression system for the production, secretion, and surface display of antigenic epitopes inserted at distinct sites of the S-layer protein SlpA was developed.[127] So, for surface display of foreign antigenic epitopes, *L. brevis* strains displaying a VP1 poliovirus epitope of 10 amino acids and the 11-amino-acid c-Myc epitopes from the human *c-myc* proto-oncogene as part inserted into the outermost proteinaceous S-layer of the cell were constructed.[127] For this purpose, the epitope insertion site allowing the best surface expression was used for construction of an integration vector, and a gene replacement system for the replacement of the wild-type *slpA* gene with the *slpA-c-myc* construct was developed. Electron microscopy investigation revealed that the S-layer lattice structure was not affected by the presence of the c-Myc epitope expressed in every SlpA subunit.[127]

G. stearothermophilus strain PV72/*p6* contains the S-layer protein SbsA with a size of 1228 amino acids, which shows a hexagonal lattice symmetry.[251] In 2003, the antigen Omp26 was introduced at different positions of SbsA and the fusion protein was expressed in empty bacterial cell envelopes (ghosts) to deliver candidate antigens for the development of vaccines against nontypeable

Haemophilus influenzae (NTHi) infections.[237] The bacterial ghost system inducing Omp26-specific antibody response in mice is a novel vaccine delivery system endowed with intrinsic adjuvant properties.[237]

B. anthracis synthesizes two abundant surface proteins, EA1 and Sap, which form an S-layer.[252] Both proteins have the same modular organization, an N-terminal cell targeting domain consisting of three SLH motifs followed by a putative self-assembly domain.[93] Chimeric genes encoding the sequence of the SLH domains of Sap or EA1 as well as the levansucrase of *Bacillus subtilis* or the C-fragment of the tetanus toxoid of *Clostridium tetani* were cloned and expressed in *B. anthracis*.[238,239] The fusion proteins were secreted and could attach to the bacterial cell surface of *B. anthracis* and one resulting recombinant strain carrying the RPL-toxin fragment C (ToxC), was used for veterinary vaccinal purposes.[239]

C. crescentus is a Gram-negative, nonpathogenic bacterium that is covered by a hexagonal S-layer lattice composed of a single 98-kDa protein species termed RsaA.[253,254] A calcium binding domain that is located near the C-terminus likely mediates the calcium-dependent assembly process as well as surface attachment of RsaA.[253,255,256] The feasibility of the commercially available PurePro TM Caulobacter expression and secretion system (Invitrogen) for the surface display of functional epitopes (e.g., *Pseudomonas aeruginosa* strain K pilin peptide,[240] a 184-amino-acid segment of the infectious hematopoietic necrosis virus (IHNV),[241] the beta-1,4-glycanase from *Cellulomonas fimi*,[242] the IgG-binding domain of Streptococcal Protein G,[243] or Domain 1 of the HIV receptor CD4 and MIP1α ligand for HIV coreceptor CCR5[244]) could be demonstrated. In a recent study, the genetically engineered RsaA was employed as a delivery system for displaying hexahistidine peptides on the *Caulobacter* cell surface and to construct a recombinant bioremediation agent to remove heavy metals from aqueous solutions.[245]

In a biological context, protein glycosylation is often the key to protein function as well as for regulating and influencing many cellular processes.[257,258] Because of this, the development of tailor-made, bioactive glycoproteins (referred to as *neo*glycoproteins) by genetic engineering will drastically change the capabilities of influencing and controlling complex biological systems. Two different strategies are envisaged. The first one is the *in vivo* display of functional glycans on the surface of bacteria enabled by means of recombinant DNA technology with various applications in microbiology, nanobiotechnology, and vaccinology.[259,260] A second approach can be seen in the *in vitro* line of development that utilizes the recrystallization ability of the S-layer portion on a broad spectrum of supports. For both strategies, the S-layer "anchor" provides a crystalline, regular matrix for the display of functional glycosylation motifs.[27,68]

VII. S-Layers for Vaccine Development

Owing to their intrinsic adjuvant ability as well as their capability to surface display proteins and epitopes, S-layers are excellent candidates to be used as antigen carriers, either as self-assembly products coated on liposomes, or displayed on bacteria (overview given in Table IV).

B. anthracis causes lethal infections in mammals after cutaneous inoculation, inhalation, or ingestion.[273] As reported in Ref. 261, the gene *bslA* encoding the S-layer protein BslA of *B. anthracis* is located on the pXO1 pathogenicity island and the expressed S-layer protein is necessary and sufficient for adhesion of the anthrax vaccine strain, *B. anthracis* Sterne, to host cells.[261,262] Surface localization and abundant expression of BslA make this polypeptide a candidate antigen for purified subunit vaccines against *B. anthracis*.[261] In an earlier study, the S-layer protein genes of *B. anthracis* were used to develop a cell surface display system for vaccination studies. For this purpose, a recombinant *B. anthracis* strain was constructed by integrating a translational fusion harboring DNA fragments encoding the cell wall targeting domain of the S-layer protein EA1 and tetanus ToxC into the chromosome. The humoral immune response was sufficient to protect mice against tetanus toxin challenge. Therefore, the expression system will be tested for the development of new live veterinary vaccines.[239]

A further important field of S-layer-based vaccine development is the investigation of the immunomodulating capacity as well as the adjuvant activity of the S-layer proteins of *C. difficile*.[274,275] This pathogenic organism is the major cause of antibiotic-associated diarrhea as well as pseudomembraneous colitis in hospitalized patients.[276] For active immunization, the surface-layer protein of *C. difficile* R13537 was tested as a vaccine component in a series of immunization and challenge experiments with Golden Syrian hamsters, combined with different systemic and mucosal adjuvants.[263]

For the development of fish vaccines to fight *Aeromonas* infections which can cause furunculosis in fish in freshwater and marine environments, the crystalline cell surface protein of the fish-pathogenic bacteria itself is essential for virulence and was considered a good vaccine candidate.[264] Although numerous attempts have been made to vaccinate salmon, trout, and catfish using outer membrane protein,[277] extracellular products, lipopolysaccharide preparations,[278] biofilms,[279] or whole cells of *A. hydrophila*,[280,281] there is still no commercial vaccine available.[265] A possible reason can be seen in the inability of these vaccines to cross-protect against different isolates of *A. hydrophila*, which is a biochemically as well as serologically heterogeneous bacterium.[265] To overcome this problem, a common antigen among different isolates of *A. hydrophila* that could serve as a vaccine candidate is required.

TABLE IV
IMMUNOGENIC S-LAYER (FUSION) PROTEINS

Antigen/Hapten	Conjugation	S-layer source (S-layer protein)	References
	Sole S-layer	*B. anthracis* Sterne	261,262
	Sole S-layer	*C. difficile* R13537	263
	Sole S-layer	*A. salmonicida* A449, *A. hydrophila* TF7	264,265
S. pneumoniae serotype 8 poly- and oligosaccharides	Chemically coupled hapten	*B. alvei* CCM 2051	266
Tumor marker T-disaccharide	Chemically coupled hapten	*T. thermohydrosulfuricus* L111-69, *G. stearothermophilus* NRS2004/3A, *B. alvei* CCM 2051	64
Tumor-associated Lewis Y (Le^y) tetrasaccharides	Chemically coupled hapten	*G. stearothermophilus* PV72	267
Birch pollen allergen, Bet v1	Chemically coupled antigen	*Ly. sphaericus* CCM 2177, *T. thermohydrosulfuricus* L111-69, *T. thermohydrosulfuricus* L110-69	268–270
Tetanus toxin fragment, ToxC	S-layer fusion protein[a]	*B. anthracis* RPL686	239
H. influenzae antigen, *Omp*26	S-layer fusion protein[b]	*G. stearothermophilus* PV72/*p6*	237
Hematopoietic necrosis virus glycoprotein segment	S-layer fusion protein[a]	*C. crescentus* JS 4011	241
Birch pollen allergen, Bet v1	S-layer fusion protein[b]	*Ly. sphaericus* CCM 2177, *G. stearothermophilus* ATCC 12980	77,230,248,249,271
M. tuberculosis protein, mpt64	S-layer fusion protein[b]	*Ly. sphaericus* CCM 2177, *G. stearothermophilus* PV72/*p2*	Tschiggerl H., unpublished
Adhesintope of the *P. aeruginosa* pilin	S-layer fusion protein[a]	*C. crescentus* JS 4011	272
Human *c-myc* proto-oncogene	S-layer fusion protein[a]	*L. brevis* ATCC 8287 (GRL1)	127

[a]Surface display of S-layer fusion proteins.
[b]*In vitro* formation of immunogenic S-layers.

In this context, in a recent study, the S-layer protein of *A. hydrophila* was produced recombinantly in *E. coli* and its ability to protect common carp *Cyrinus carpio* L. against six virulent isolates of *A. hydrophila* could be demonstrated.[265]

IHNV causes a hemorrhagic disease in young salmonid fish and is another severe threat for fish farming. A recombinant subunit model vaccine was developed by fusing a 184-amino-acid segment of IHNV glycoprotein to the C-terminal portion of the S-layer protein of *C. crescentus*.[241] The fusion protein was expressed by the *C. crescentus* S-layer secretion system and laboratory trials revealed a relative survival of 26–34% in rainbow trout fry.[241]

Another application of S-layers is their use as carrier for immunogenic antigens and haptens.[62,266,282,283] As common carriers for peptide epitopes are used as monomers in solution (e.g., tetanus or diphtheria toxoids) or as dispersions of unstructured aggregates on aluminum salts, a reproducible immobilization of ligands to the carrier protein cannot be achieved.[284,285] Consequently, the use of regularly structured S-layer self-assembly products as immobilization matrices represents a completely new approach. Investigations focused on the development of several model conjugate vaccines with S-layer (glyco) proteins of thermophilic bacilli and clostridia and weekly immunogenic carbohydrate antigens, for example, Streptococcus pneumoniae serotype 8 poly- and oligosaccharides, haptens or recombinant birch pollen allergen showed promising results in vaccination trials.[64,266–268,286–288]

A further approach was the use of recombinant S-layer fusion proteins and empty bacterial cell envelopes (ghosts) to deliver candidate antigens (Omp26) for a vaccine against the nontypeable *H. influenzae* (NTHi) infection. Immunization studies with the resulting SbsA/Omp26 in bacterial ghosts induced an Omp26-specific antibody response in BALB/c mice.[237]

S-layer self-assembly products and S-layer-coated liposomes[168,169] can be considered as particulate adjuvants with dimensions comparable to those of bacteria or viruses that the immune system evolved to combat. The mechanical and thermal stability of S-layer-coated liposomes[169,289,290] and the possibility for immobilization or entrapping biologically active molecules[168,170,291] introduced a broad application potential, particularly as carrier and/or drug delivery and drug targeting systems or in gene therapy, for example, as artificial viruses.[20]

Further, there is an urgent need for new vaccines that allow mucosal administration instead of intramuscular injections for the achievement of specific desired effects, such as adjuvant targeting, site-specific delivery, and controlled immune responses. S-layer–hapten conjugates induced significant vaccination responses even after oral/nasal administration.[267] One project was directed toward immunotherapy of cancer, where conjugates of S-layer with small, tumor-associated oligosaccharides were found to elicit hapten-specific DTH responses.[267]

Immunization experiments in mice have indicated that S-layers served not only as carriers but also as adjuvants.[267–269] Allergen–S-layer conjugates and S-layer/allergen fusion proteins have been prepared with the intention of suppressing the Th2-directed, IgE-mediated allergic responses to Bet v1, the major allergen of birch pollen.[77,230,269,270] These studies showed that the S-layer protein conjugate induced IFN-γ production, thus activating the phagocytotic cells and confirming that Th1-enhancing properties were clearly attributable to the S-layer protein. Further, the recombinant S-layer/Bet v1 fusion proteins altered an established Th2-dominated phenotype as well as the *de novo* cytokine secretion profile toward a more balanced Th1/Th0-like phenotype.[248,249,271] These data clearly confirm the immunomodulating properties of the S-layer moiety in S-layer fusion proteins and support the concept that recombinant fusion of allergens and S-layer proteins is a promising approach to improve vaccines for SIT of atopic allergy.

Current studies using immunogenic self-assembly products of S-layer fusion proteins comprising the antigen mpt64, a *Mycobacterium tuberculosis* protein, investigate the ability of S-layer proteins to serve as a carrier and adjuvant for the vaccination against tuberculosis (Tschiggerl, unpublished).

A number of vaccine approaches involve the development of vaccination vehicles, serving to potentiate the immune response to an antigen. For using S-layers to display foreign peptides on the *C. crecentus* cell surface in the dense, highly ordered S-layer structure was explored,[240,272] and the *C. crescentus* RsaA secretion apparatus was used to produce a fusion protein comprising RsaA and the adhesintope of the *P. aeruginosa* pilin. This presentation system could have many potential applications, such as the development of whole-cell vaccines, tumor suppressors, cellular adsorbents, and peptide display libraries.[292–294] Further, the 11-amino-acid long epitope *c-myc* from the human c-*myc* proto-oncogene was successfully expressed in every S-layer subunit of the *L. brevis* S-layer (SlpA) while maintaining the S-layer lattice structure.[127] Delivery of antigens to mucosal surfaces by lactic acid bacteria was considered to offer a safe alternative to live attenuated pathogens because of their food grade status.

VIII. S-Layers as Supporting Structure for Functional Lipid Membranes

One major topic in nanobiotechnology nowadays is the design, synthesis, and fabrication of supramolecular interfacial architectures comprising biomolecules (lipids, (membrane)-proteins, glycans, nucleic acids, and combinations thereof) and inorganic or organic materials of technological importance.[295,296]

Biological systems are prime candidates for controlled "bottom-up" production of defined nanostructures.[2,297,298] Although self-assembly of molecules is a ubiquitous strategy of morphogenesis in nature, research in the area of molecular nanotechnology, nanobiotechnology, and biomimetics are only beginning to exploit its potential for the functionalization of surfaces and interfaces as well as for the production of biomimetic membranes and encapsulation systems.

Biomimetic model membranes (free-standing, tethered, and supported lipid mono- or bilayers with associated or integral peptides or proteins) have attracted lively interest in recent years, as the advances in genome mapping revealed that approximately one-third of all the genes of an organism encode for membrane proteins such as pores, ion channels, receptors, and membrane-anchored enzymes.[299–302] These proteins are key factors in the cell's metabolism, for example, in cell–cell interaction, signal transduction, and transport of ions and nutrients, and, thus, in health and disease.[303] Owing to this important function, membrane proteins are a preferred target for pharmaceuticals (at present more than 60% of consumed drugs)[304] and have received widespread recognition for their application in drug discovery, protein–ligand screening, and biosensors.

The present section intends to give a survey on particular biomimetic planar and spherical lipid membranes, which consist, besides the lipid matrix, of a closely associated proteinaceous S-layer lattice. The concept of exploiting this supramolecular building principle for stabilizing planar or vesicular membrane systems[11,13,16,20] evolved from the observation that most archaea are exclusively composed of a cytoplasmic membrane and a closely associated or even integrated monomolecular crystalline S-layer (Fig. 15A). Moreover, these organisms dwell under extreme environmental conditions such as temperatures up to 120 °C, pH down to zero, high hydrostatic pressure, or high salt concentrations.[305–307] As suitable methods for disintegration of archaeal S-layer protein lattices and their reassembly into monomolecular arrays on lipid films are not yet available, S-layer proteins from Gram-positive bacteria were used for copying the archaeal building principle for the generation of S-layer-stabilized lipid membranes. S-layer proteins can be utilized as biofunctional surfaces[308] and constitute also a fascinating base structure for hosting functionalized planar lipid membranes.[12,13,16,20] The lipid membranes either consists of an artificial phospholipid bilayer (Fig. 15B) or a tetraetherlipid monolayer replaces the cytoplasmic membrane, and isolated bacterial S-layer proteins may be attached on one or even on both sides of the lipid membrane (Fig. 15E and F).

Further, S-layer lattices as the outermost envelope component covering spherical supramolecular structures such as liposomes or emulsomes constitute biomimetic "artificial virus-like particles" enabling both stabilization of, for example, liposomes and presenting addressor molecules in a well-defined

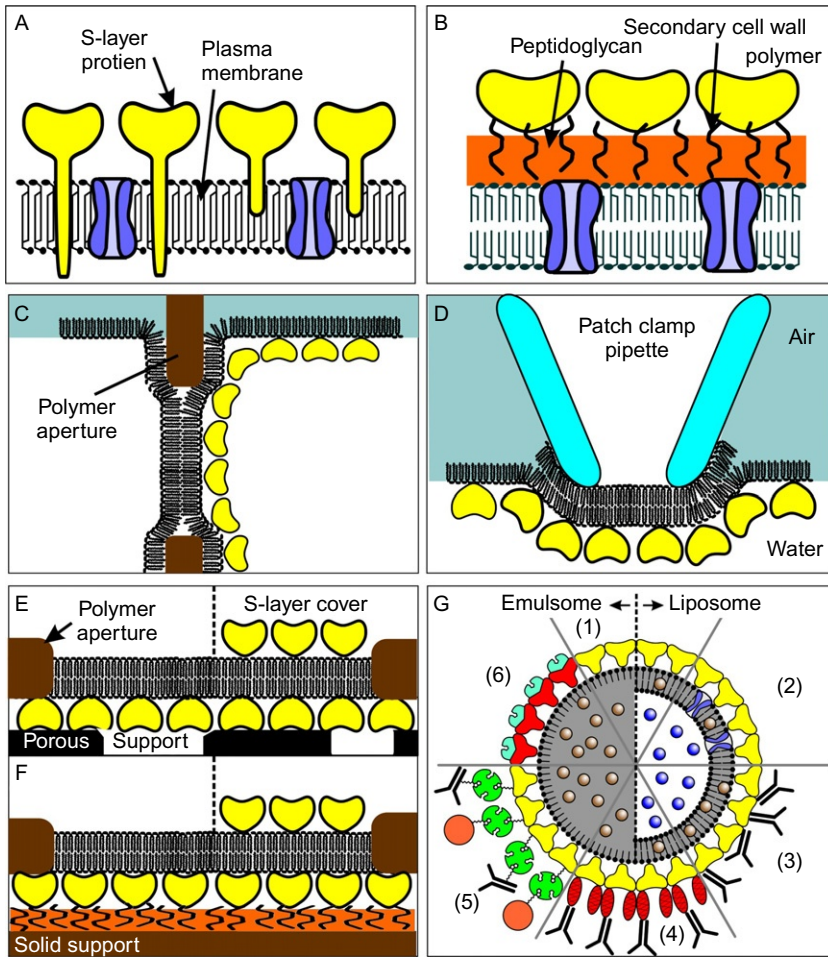

FIG. 15. Supramolecular structure of an archaeal (A) and Gram-positive bacterial cell envelope (B). Schematic illustrations of various S-layer-supported lipid membranes. In (C), a folded or painted membrane spanning a Teflon aperture is shown. A closed S-layer lattice can be self-assembled on either one or both (not shown) sides of the lipid membranes. (D) A bilayer lipid membrane is generated across an orifice of a patch clamp pipette by the tip-dip method. Subsequently, a closely attached S-layer lattice is formed on one side of the lipid membrane. (E) Schematic drawing of a lipid membrane generated on an S-layer ultrafiltration membrane (SUM). Optionally, an S-layer lattice can be attached on the external side of the SUM-supported lipid membrane (right part). (F) Schematic drawing of a solid support covered by a layer of modified secondary cell wall polymer (SCWP). Subsequently, a closed S-layer lattice is assembled and bound via the specific interaction between S-layer protein and SCWP. On this biomimetic structure, a lipid membranes is generated. As shown in (E), a closed S-layer lattice can be recrystallized on the external side of the solid-supported lipid membrane (right part). (G) Schematic drawing of (1) an S-layer-coated emulsome (left part) and S-liposome (right part) with

orientation and spatial distribution (Fig. 15G). The prerequisite for creating such supramolecular structures is given by the unique noncovalent interaction of S-layer proteins with lipid head groups within planar and spherical lipid mono- and bilayers.[11,13,166,167,309]

A. Planar Lipid Membranes

A broad range of techniques including TEM and AFM, Fourier transform infrared spectroscopy, dual-label fluorescence microscopy, and X-ray and neutron reflectivity measurements have been applied to characterize S-layer-supported lipid membranes[154,160,310–314] Formation of S-layer lattices covering the entire area of lipid films has been observed on zwitterionic phospholipids such as phosphatidyl ethanolamines and phosphatidyl cholines.[315] The addition of a small portion of positively charged surfactants[168,316] or lipid derivatives[317] facilitated the crystallization process, in particular, on phosphatidyl cholines. A systematic study has provided evidence that electrostatic interactions exist between exposed carboxyl groups on the S-layer lattice and zwitterionic lipid head groups. At least two to three contact points between the lipid film and the attached S-layer protein have been identified.[315] Hence, less than 5% of the lipid molecules of the adjacent monolayer are anchored to these contact points on the S-layer protein, whereas the remaining $\geq 95\%$ lipid molecules diffuse freely in the membrane between the pillars consisting of anchored lipid molecules.[318,319] This calculation is based on the S-layer lattice of SbpA from *Ly. sphaericus* CCM 2177 having a square unit cell with a spacing of 13.1 nm[153,171] and an area per lipid molecule of 0.65 nm.[320] These nanopatterned lipid membranes are also referred to as "semifluid membranes"[154] because of its widely retained fluid behavior.[317,321] Most importantly, although peptide side groups of the S-layer protein interpenetrate the phospholipid head group regions almost in its entire depth, no impact on the hydrophobic lipid alkyl chains has been observed.[312–314,322,323] Further, the S-layer lattice neither constitutes a significant barrier for the porcine pancreatic phospholipase A_2 (PLA_2; $M_r = 13.8$ kDa) nor induces lipid packing defects that would result in shorter enzymatic lag periods.[324] The alterations of the molecular-level organization of the lipid monolayer upon S-layer protein binding and

entrapped water-soluble (gray) or lipid-soluble (black) functional molecules and (2) functionalized by reconstituted integral membrane proteins. S-layer-coated emulsomes and S-liposomes can be used as immobilization matrix for functional molecules (e.g., IgG) either by direct binding (3), by immobilization via the Fc-specific ligand protein A (4), or biotinylated ligands can be bound to S-layer-coated emulsome and S-liposome via the biotin–streptavidin system (5). Alternatively, emulsomes and liposomes can be coated with S-layer fusion proteins incorporating functional domains (6). Modified after, Ref. 20 Copyright (2002) and, Ref. 16 Copyright (2004), with permission from Wiley–VCH.

recrystallization observed by various biophysical methods do not cause serious inhibition of the PLA_2. Hence, there is much evidence that the recrystallized S-layer lattice did not modulate a large proportion of the head group region of the phospholipid monolayer to an extent that could dramatically impede the recognition of the phospholipids by the biological interplay with the PLA_2.[324]

In addition, a second S-layer acting as protective molecular sieve and further stabilizing scaffolding can be recrystallized on the top of S-layer-supported lipid membranes. With two recrystallized S-layers, nanopatterned fluidity determined by S-layer–lipid head group interactions from both sides are introduced. This is particularly the case whenever S-layer lattices differing in lattice constants and symmetry are used. Therefore, S-layer lattices constitute unique supporting scaffolding, resulting in lipid membranes with nanopatterned fluidity and considerably extended longevity.[11,166,167,309,325,326]

Schematic illustrations of S-layer-supported lipid membranes spanning the orifice of a bilayer lipid membrane (BLM) chamber and on the tip of a micropipette are shown in Fig. 15C and D, respectively. Whereas the impact of an attached S-layer lattice on the membrane capacitance, membrane resistance, and the boundary potential on free-standing BLMs is negligible, the mechanical properties of S-layer-supported lipid membranes are considerably altered. Hydrostatic pressure applied across painted BLMs caused them to bulge, resulting in an increase of the membrane capacitance due to area expansion. A significantly higher area expansion was observed for plain BLMs compared to S-layer-supported lipid membranes forced from the S-layer-facing side, demonstrating a protecting effect of the S-layer lattice against hydrostatic pressure.[327] Relaxation experiments revealed a considerably longer delay time between the applied voltage pulse and the appearance of an initial defect at S-layer-supported lipid membranes.[316] The membrane tension of BLMs upon the attachment of S-layer proteins has been determined by dynamic light scattering.[317] For BLMs, the collective motions of the lipid molecules are dominated by membrane tension rather than by membrane curvature energy. S-layer lattices on both sides of the BLM resulted in a considerable reduction of the membrane tension by a factor of approximately five. However, the membrane bending energy increased by three orders of magnitude.[317] Hence, the attached S-layer lattice facilitates the transverse shear motions of the lipid molecules. In accordance with voltage pulse experiments,[316] a significant increase of the previously negligible surface viscosity of the membrane has been observed during the S-layer protein attachment.[317]

The most challenging property of model lipid membranes is the feasibility to incorporate membrane-active peptides and, more important, (complex) integral membrane proteins in a functional state. Reconstitution of the staphylococcal pore-forming protein α-hemolysin (αHL),[328,329] the M2 segment that forms the ion-conducting channel of the nicotinic acetylcholine receptor,[330]

and the ion carrier valinomycin into plain and S-layer supported lipid membranes has been successfully performed. S-layer-supported tetraetherlipid monolayers functionalized with valinomycin revealed a 10-fold higher life time compared to a membrane without an attached S-layer lattice.[323] Although no reconstitution of αHL could be achieved with tetraetherlipid membranes, lytic pores were formed in a membrane mainly composed of the branched phospholipid 1,2-diphytanosyl-*sn*-glycero-3-phosphocholine (DPhPC) by adding αHL to the lipid-exposed side of the S-layer-supported lipid membrane. No pore formation was detected upon addition of αHL monomers to the S-layer face of the S-layer-supported lipid membrane. Therefore, one can conclude that the intrinsic molecular sieving properties of the S-layer lattice do not allow passage of αHL monomers through the S-layer pores to the lipid surface.[322] In addition, these data represent a quality control for the existence of a closed S-layer lattice without any defects and a tight attachment to the BLM. Compared to plain BLMs, S-layer-supported lipid membranes have a decreased tendency to rupture in the presence of αHL, again indicating an enhanced stability due to the attached S-layer lattice.[322] Nevertheless, even single pore recordings have been performed with αHL reconstituted in free-standing S-layer-supported lipid membranes.[331]

S-layer-stabilized lipid membranes formed by the tip-dip methodology were functionalized with M2 ion channels.[332] The M2 ion channel characteristics were compared for BLMs of the same lipid composition with and without S-layers, and the attached S-layer lattices were found to be nonintrusive to the channel functionality and characteristics. The ability of S-layer proteins to stabilize BLMs and their nonintrusive character on ion channel activity make them attractive for biosensor applications, especially those that enhance the stability of BLMs beyond the use of tethers or polymer supports.[332]

However, although free-standing S-layer-supported lipid membranes revealed a higher mechanical stability (e.g., against hydrostatic pressure) and longevity in particular with reconstituted peptides or proteins, these membranes are up to now not stable enough for many practical applications.[13,167,318] Hence, a sophisticated long-term strategy is to attach BLMs to porous or solid supports to enhance their practical applicability.[333–338] Lipid membranes generated on a porous support combine the advantage of possessing an essentially unlimited ionic reservoir on each side of the BLM, individual excess to both membrane surfaces, and easy manual handling (Fig. 15E). This is seen as basic requirement of experiments copying the *in vivo* situation (e.g., plasmatic/exoplasmatic side). However, the surface properties of porous supports, such as roughness or great differences in pore size, have significantly impaired the stability of attached BLMs. Hence, the strategy to use SUMs with the S-layer as the stabilizing and smoothening biomimetic layer between the lipid membrane and the porous support is a straightforward approach.[325,339,340]

Composite SUM-supported DPhPC bilayers are structures that maintain its membrane resistance in the gigaohm range during their whole life time of up to 17 h.[325,339,340] In contrast, lipid membranes on plain MFMs revealed only a life time of approximately 3 h.[340] Interestingly, an additional monomolecular S-layer protein lattice recrystallized on the lipid-faced side, forming an S-layer–lipid membrane–S-layer sandwich-like structure, increased the life time significantly to about 1 day.[325,339] Stable membranes comprising tetraetherlipids, phospholipids, and their mixtures have also been generated on SUMs.[340] The capacitance of these electrically tight SUM-supported membranes increased continuously with increasing tetraetherlipid-to-phospholipid ratio. This result nicely demonstrated that the pure DPhPC membrane was thicker than membranes with a certain amount of tetraetherlipid and finally, the pure tetraetherlipid monolayer constituted the thinnest membrane.[340]

Incorporation of the membrane-active peptide gramicidin D resulted in high-resolution conductance measurements on single gramicidin D pores in all the above-mentioned S-layer-supported lipid membranes.[340] Functional reconstitution of αHL could be achieved with SUM-supported DPhPC bilayers, but no pore formation was observed with BLMs generated on pure MFMs.[339] However, even single pore recordings have been performed with αHL reconstituted in BLMs resting on an SUM.[339]

Solid-supported lipid membranes have been fabricated by several methods. A common feature of the S-layer lattice is not only to provide a stabilizing and defined tethering layer to decouple the BLM from the (inorganic) support but also to generate an ionic reservoir if desired. First, S-layer proteins have been self-assembled on glass and modified silicon surfaces before generating a BLM by the LB technique.[311,321] This composite structure has been compared with silane- and dextran-supported phospholipid bilayers.[321] Most probably due to the repetitive local interactions of the S-layer lattice with the lipid head groups, the nanopatterned fluidity of lipids was highest in the S-layer-supported lipid membranes compared to hybrid silane alkyl-phospholipid membranes or dextran-supported phospholipid bilayers, as determined by the fluorescence recovery after photobleaching. Phospholipid bilayers and tetraetherlipid monolayers have also been generated on S-layer-covered gold electrodes (Fig. 15F). The tetraetherlipid monolayer in between the S-layer covering the gold electrode and a second S-layer on the top revealed an exceptional long-term robustness of approximately 1 week.[13,167,318] If desired, a layer of thiolated SCWP may be chemisorbed on the gold surface prior recrystallization of the S-layer protein to enhance the long-range order and the smoothness of the S-layer lattice.[9,308,309] Hence, the nanopatterned anchoring of the membrane is a promising strategy for generating stable *and* fluid lipid membranes.

The functionality of these biomimetic membranes resting on solid supports has been investigated by the incorporation of the membrane-active peptides valinomycin, alamethicin, and gramicidin D.[325] S-layer-supported lipid membranes with incorporated valinomycin, a potassium-selective ion carrier, revealed a remarkable high resistance when bathed in a sodium buffer. In contrast, because of the valinomycin-mediated ion transport, a pronounced decrease in resistance by a factor of 500 was observed for the same membrane bathed in a potassium buffer.[325] Further, alamethicin channels could not only be incorporated in S-layer-supported lipid membranes on solid supports, but the conductive alamethicin channels could even be blocked as increasing amounts of inhibitor gave rise to a significantly increased membrane resistance.[325] Thus, proof of principle for the applicability of these composite structures for biosensing and screening purposes has been demonstrated. In future, the ability to reconstitute integral membrane proteins in defined structures on, for example, sensor surfaces is one of the most important concerns in designing biomimetic sensing devices.

B. S-Layer-Coated Liposomes and Emulsomes

Unilamellar liposomes are artificially prepared vesicles comprising of a phospholipid bilayer shell and an aqueous core.[341–343] The core can be filled with hydrophilic drugs, whereas the lipidic shell can be loaded with hydrophobic drugs. Emulsomes, however, are lipoidal vesicular systems with an internal solid fat core surrounded by a phospholipid mono- or bilayer.[344,345] Hence, emulsomes can be loaded with a much higher amount of lipidic drugs. Both spherical structures can be used for targeted drug delivery for cancer and other diseases.[345,346]

Isolated S-layer subunits were recrystallized on positively charged, unilamellar liposomes (Fig. 15G) composed of 1,2-dipalmitoyl-*sn*-glycero-3-phosphocholine (DPPC), cholesterol, and hexadecylamine in a molar ratio of 10:5:4.[168–170] The subunits attached to positively charged liposomes by their inner face (bearing a net negative charge) in an orientation identical to the lattice on intact cells. The S-layer protein, once recrystallized on liposomes, can be cross-linked with glutaraldehyde or bis(sulfosuccinimidyl)suberate to achieve stabilization of the whole supramolecular structure and can be utilized for covalent attachment of macromolecules.

Coating of the positively charged liposomes with the S-layer protein of *G. stearothermophilus* PV72/*p2* resulted in inversion of the ζ-potential from $+29.1$ to -27.1 mV.[169] A similar behavior was also observed for liposomes coated with S-layer proteins from lactobacilli.[347] To study the influence of an S-layer lattice on the stability of liposomes, the hydrophilic marker carboxyfluorescein (CF) was encapsulated and its release was determined for plain and

S-layer-coated liposomes in the course of mechanical and thermal challenges. In comparison to plain liposomes, S-layer-coated liposomes released only half the amount of enclosed CF upon exposure to shear forces or ultrasonication as mechanical stress factors. Further, temperature shifts from 25 to 55 °C and vice versa induced considerably less CF release from S-layer-coated than from plain liposomes. A similar stabilizing effect of the S-layer lattice was observed after glutaraldehyde treatment of plain and S-layer-coated liposomes, although there was increased CF release in all glutaraldehyde-treated liposomes.[169] As chemical analysis revealed that almost all amino groups (> 95%) from hexadecylamine in the liposomal membrane were involved in the cross-linking reaction, phase separation phenomena might be responsible for this observed behavior.[169,290]

The thermotropic phase behavior of S-layer-coated and uncoated liposomes was characterized by differential scanning microcalorimetry, indicating, for both preparations, a broad phase transition around 50 °C due to the chain-melting from a liquid-ordered gel-like to a liquid-ordered fluid phase as described for DPPC/cholesterol mixtures. The slightly higher phase transition temperature for the S-layer-coated liposomes was explained by increased intermolecular order. Covalent cross-linking of the S-layer subunits to hexadecylamine with glutaraldehyde induced phase separation within the liposomes. Based on deconvolution of the normalized excess heat capacity functions, it was proposed that the different lipid domains arise from phospholipids representing different degrees of mobility.[290] This is also in accordance with data of the CF release experiments.[169]

Sound velocity and density measurements have been used to study further physical properties of plain and S-layer-coated unilamellar liposomes.[289] It turned out that the adiabatic compressibility of S-layer-coated liposomes at $T < 20$ °C was higher and at $T > 20$ °C lower in comparison with that of plain liposomes. This provided evidence of an interesting phenomenon of softening and condensing effects of S-layer proteins on the liposomal lipid bilayer depending on the temperature.[289]

S-layer-coated liposomes have been investigated for their ability to act as a versatile system for entrapping and binding target molecules (Fig. 15G). A first study provided evidence that S-layer-coated liposomes constitute a proper matrix for the covalent attachment of macromolecules like ferritin.[168] The latter was used as a model system for demonstrating the suitability of S-layers attached to liposomes as immobilization matrices because ferritin does not penetrate into S-layer pores[184] and can be easily detected by electron microscopy procedures. Further, a targeted immobilization of immunoglobulins by bacterial S-layer proteins recrystallized on liposomes was exploited as immobilization matrix for antibody (Ab)-human IgG. The interaction of rabbit or swine anti-human IgG as antigens (Ag) was studied by measuring changes of the

ultrasound velocity.[291] The ultrasound velocity decreased linearly with increase in Ag concentration. The decrease of ultrasound velocity was presumably caused by changes of hydration of the membrane due to the binding process. Finally, no substantial differences in the behavior of ultrasound velocity were observed for interactions of human IgG with rabbit or swine anti-human IgG.[291]

Another approach was the biotinylation of S-layer-coated liposomes. This was achieved by coupling *p*-diazobenzoyl biocytin, which preferably reacts with the phenolic residue of tyrosine or with the imidazole ring of histidine. By applying this method, two biotin residues accessible for subsequent avidin binding were introduced per S-layer subunit.[170] As visualized by labeling with biotinylated ferritin, an ordered monomolecular layer of streptavidin was formed on the surface of the S-layer-coated liposomes. As a second model system, biotinylated anti-human IgG was attached via the streptavidin bridge to the biotinylated S-layer-coated liposomes. The biological activity of the bound anti-human IgG was confirmed by ELISA.[170] Further, S-layer/streptavidin fusion proteins have been constructed, and hence biotinylated binding partners can be bound in a much better defined orientation and position. By applying this method, three biotin residues accessible for subsequent avidin binding were introduced per S-layer subunit.[98]

Another approach is to recrystallize functional chimeric S-layer fusion proteins carrying the sequence of EGFP on liposomes.[232] Because of the intrinsic EGFP fluorescence, the uptake of S-layer/EGFP fusion protein-coated liposomes into eukaryotic cells such as, for example, HeLa cells could nicely be visualized by confocal laser scanning microscopy. For instance, in HeLa cells the major part of the coated liposomes was internalized within 2 h of incubation by endocytosis.[232] With regard to further experiments, the most interesting advantage of these fusion proteins can be seen in recrystallization of this S-layer/EGFP fusion protein in combination with other S-layer fusion proteins such as the S-layer/streptavidin fusion proteins[98] on the same liposome surface. The uptake of these specially coated liposomes by target cells and the functionality of transported drugs could be investigated simultaneously without using any additional labeling.

Up to now, only preliminary studies have been performed with S-layer-coated emulsomes. Cationic emulsomes could be entirely covered with a crystalline S-layer lattice as demonstrated by transmission electron microscopical studies (Ücisik, M., unpublished data). Further, the coating of emulsomes with the S-layer proteins resulted in inversion of the ζ-potential from a positive value to a negative one. This shift in ζ-potential was in the same dimension as observed with liposomes (Ücisik, M., unpublished data).

To summarize, S-layer-protein-coated liposomes (Fig. 15G) are biomimetic structures with remarkably high mechanical and thermal stability.[169] Further, the possibility for entrapping and, most importantly, for immobilizing

biologically active molecules[168,170] makes S-layer-coated liposomes and S-layer-coated emulsomes attractive for nanobiotechnological applications, particularly as carrier and/or drug delivery systems, as artificial virus envelopes in, for example, medicinal applications and in gene therapy.[13,170,319,348,349] These biomimetic approaches are exciting examples for synthetic biology mimicking structural and functional aspects of many bacterial and archaeal cell envelopes having S-layer lattices as the outermost component.[34]

IX. S-Layers as Matrix for Biomineralization

Currently, there is much interest in the synthesis of inorganic materials using biomimetic approaches. Unlike physical methods such as electron beam microlithography, there are relatively few reports of self-assembled organic templates being employed in the direct chemical synthesis of patterned arrays of inorganic nanoparticles.[220–223,350,351] Such materials are required as patterning and functional elements in molecular electronics and optics. But more than a decade ago and based on the investigation of mineral formation by bacteria in natural environments, S-layer lattices had already been used to generate periodic templates for the *in situ* nucleation of ordered arrays of uniform 5-nm sized cadmium sulfide (CdS) and gold (Au) nanoparticles.[222] Inorganic superlattices with either oblique or square lattice symmetry of approximately 10 nm repeat distance and particle sizes of 4–5 nm have been fabricated by exposing self-assembled S-layers to the respective metal salt solutions (e.g., Cd (II)) followed by either slow reaction with a reducing agent such as H_2S or by exposing the precipitated inorganic layer (attached to the S-layer) to the electron beam in a transmission electron microscope.[222,350] The latter approach is particularly interesting since nanoparticles were only formed at the exposed regions, allowing to gain spatial control over the array formation. Based on this approach, a broad range of further inorganic (mostly metallic) materials was used to fabricate nanoparticle arrays: palladium (Pd; salt: $PdCl_2$), nickel (Ni; $NiSO_4$), platinum (Pt; salt: $KPtCl_6$), lead (Pb; salt: $Pb(NO_3)_2$), and iron (Fe; salt: $(KFe(CN)_6)$).[220–223,350,351] As a general rule, the nanoparticles were mostly microcrystalline but not crystallographically aligned along the lattice lines of their superlattice. Further, the lattice spacing of the nanoparticles arrays resembled the lattice parameters of the underlying S-layer lattice (lattice symmetry and lattice spacings). As the precipitation of the metals was confined to the pores of the S-layer, the nanoparticles also resembled the morphology of the pores. Recently, small-spot X-ray photoelectron spectroscopy (XPS) was used to characterize the elemental composition of the nanoclusters.[219] XPS demonstrated that they consisted primarily of elemental gold. In addition to the precipitation of nanoparticles for applications in molecular

electronics and optics, it must be noted here that recent investigations of the electronic structure of an S-layer protein revealed a semiconductor-like behavior with an energy gap value of ~3.0 eV and the Fermi energy close to the bottom of the lowest unoccupied molecular orbital.[352–354]

In a different work, S-layer protein lattices were used as scaffolds in the precipitation of biogenic silica and titania.[355] The current understanding of the key proteins (silicateins and sillafins), genes, and molecular mechanisms involved in the bioinspired formation of silica structures laid the foundation for investigating the biocatalytic activity of S-layer proteins and their self-assembly products as catalysts, templates, and scaffolds for the directed growth of silica and titania into novel nano- to micrometer sized structures. Based on established and published protocols for silica and titania synthesis, *in vitro* investigations were focused on native S-layer proteins and on genetically engineered S-layer fusion proteins involving silica and titania precipitating peptides as exposed surface functionalities.

Precipitation of tetramethoxysilane led to the formation of silica layers and of titanium(IV) bis(ammonium lactato)dihydroxide to titania layers on S-layer lattices (Göbel, C., personal communication). It was shown that the silicification of S-layer lattices led to a downsizing of the diameters of the S-layer pores (comparable to closing an iris diaphragm). This result is important for the development of nanoporous materials as, for example, used in fuel cells. Further, genetically engineered S-layer–rSilC (recombinant sillafin C (rSilC)) fusion protein lattices were coated with silica and titania.[356] In particular, due to its high refractive index, rutile titania would be a highly desirable material for applications in nano-optics.

X. Conclusion and Perspectives

The study of biological self-assembly systems is a new and rapidly growing scientific and engineering field that crosses the boundaries of different disciplines. Although self-assembly processes are common in biosystems, there are only a few examples where proteins possess the intrinsic capability to aggregate into monomolecular crystalline arrays.

S-layers composed of a single protein or glycoprotein species represent the simplest self-assembling membrane developed during biological evolution. Moreover, S-layers are now recognized as one of the most common cell surface component of prokaryotic organisms and consequently one of the most abundant biopolymers on earth. S-layers reveal different lattice types (*p1*, *p2*, *p3*, *p4*, *p6*), lattice constants (~5–30 nm), and a great diversity regarding their constituent (glyco)protein subunits. Moreover, S-layers that share almost identical lattice parameters can have dissimilar molecular sequences.[20,27] Those that

possess similar physicochemical characteristics or functions might not be related at all to one another. This raises the question: are they an example of parallel evolution or a common structural theme, or an example of extreme divergence from a single ancient structure?[34]

Currently, most nanobiotechnological applications based on S-layers depend on the *in vitro* self-assembling capabilities of isolated S-layer subunits in suspension and on surfaces of solids, lipid films, liposomes, emulsomes, and nanoparticles. Most important, S-layer proteins also assemble as coherent layers on highly corrugated and porous structures.

The wealth of information accumulated on the structure, chemistry, morphogenesis, function, and genetics of S-layers has led to a broad spectrum of applications in areas of both life- and materials sciences. Presently, the most important area of development for S-layer technologies concerns changes of the natural properties of S-layer proteins or glycoproteins by genetic manipulation. Most important, S-layer proteins incorporating specific single- or multifunctional domains of proteins (e.g., antibodies, antigens, ligands, enzymes, fluorescent proteins, and peptide mimotopes) maintain the capability to assemble into coherent lattices on a great variety of solid supports. Such S-layer fusion proteins have already revealed a broad application potential for the production of affinity matrices, diagnostics, vaccines, biocompatible and antifouling surfaces, microcarriers, and matrices for biomineralization. It is expected that many other potentials for nanobiotechnological and biomimetic applications will emerge. A major advantage in using S-layer fusion proteins for functionalizing solids relates to the observation that functional domains associated with S-layers are more resistant to denaturation and thus exhibit a prolonged life time. Moreover, S-layer (fusion)proteins can be considerably strengthened by introducing intermolecular and/or intramolecular bonds. Up to now, fusion proteins have been produced with S-layers from organisms dwelling at moderate environmental conditions but even higher stability of fusion proteins may be achieved if S-layers of archaea are used that grow in extreme habitats (e.g., up to 120 °C, pH 0). An important line of development concerns strategies for copying the supramolecular principle of cell envelopes of archaea that possess S-layers as exclusive wall component and inhabit thermophilic and acidophilic environments. This biomimetic approach is expected to lead to new technologies for stabilizing functional lipid membranes and their use at the mesoscopic and macroscopic scale.[13] Such composite structures have the potential for generating very stable, long-lasting plane and vesicular membrane systems incorporating functional proteins as required for biosensors, photovoltaics, and high-throughput screening. Moreover, preliminary studies have clearly demonstrated that S-layer technologies have a great potential for nanopatterning of surfaces, biological templating, and functionalizing microfluidic devices. S-layer lattices may also enable the defined

generation and deposition of metal or semiconductor nanoparticles across macroscopic surface areas as required for nonlife-science applications (e.g., nanoelectronics, nonlinear optics, or catalytic substrates).[6] Another area of future development of S-layers concerns their utilization as cell surface display system of rationally designed glycosylation motifs. Controlled S-layer glycosylation may add a new and very valuable component to an S-layer-based molecular construction kit as required for receptor mimics, vaccine design, and drug delivery involving carbohydrate recognition.[14,67]

Finally, a most challenging question remains unanswered: Could S-layer-like membranes fulfill barrier and supporting functions as required for self-reproducing systems at the beginning of life?[34,147]

Acknowledgments

Financial support from the Austrian Science Fund (FWF, projects P18510-B12 and P20256-B11), the EU project MemS (Grant Agreement No. 244967), the Erwin-Schrödinger Society for Nanosciences, the Austrian NanoInitiative under the project SLAYSENS within the project cluster ISOTEC, and the Air Force Office of Scientific Research, USA (AFOSR, projects FA9550-06-1-0208, FA9550-07-1-0313, FA9550-09-1-0342, and FA9550-10-1-0223) is gratefully acknowledged.

References

1. Papapostolou D, Howorka S. Engineering and exploiting protein assemblies in synthetic biology. *Mol Biosyst* 2009;**5**:723–32.
2. Sleytr UB, Sára M, Pum D, Schuster B. Crystalline bacterial cell surface layers (S-layers): a versatile self-assembly system. In: Ciferri A, editor. *Supramolecular polymers*. 2nd ed. Boca Raton: CRC Press LLC; 2005. pp. 583–612.
3. Egelseer EM, Ilk N, Pum D, Messner P, Schäffer C, Schuster B, Sleytr UB. S-layers, microbial, biotechnological applications. In: Flickinger MC, editor. *The encyclopedia of industrial biotechnology: bioprocess, bioseparation, and cell technology*,Vol. 7. Hoboken, USA: John Wiley & Sons, Inc.; 2010. pp. 4424–48.
4. Egelseer EM, Sára M, Pum D, Schuster B, Sleytr UB. Genetically engineered S-layer proteins and S-layer-specific heteropolysaccharides as components of a versatile molecular construction kit for applications in nanobiotechnology. In: Shoseyov O, Levy I, editors. *NanoBioTechnology*. Totowa, New Jersey: Humana Press; 2008. pp. 55–86.
5. Ilk N, Egelseer EM, Ferner-Ortner J, Küpcü S, Pum D, Schuster B, Sleytr UB. Surfaces functionalized with self-assembling S-layer fusion proteins for nanobiotechnological applications. *Colloids Surf A Physicochem Eng Aspects* 2008;**321**:163–7.
6. Pum D, Sleytr UB. Protein-based nanobioelectronics. In: Offenhäusser A, Rinaldi R, editors. *Nanobioelectronics for electronics, biology, and medicine*. Berlin, Germany: Springer; 2009. pp. 167–80.
7. Sára M, Egelseer EM, Huber C, Ilk N, Pleschberger M, Pum D, Sleytr UB. S-layer proteins: potential application in nano(bio)technology. In: Rehm B, editor. *Microbial bionanotechnology: biological self-assembly systems and biopolymer-based nanostructures*. New Zealand: Bernd Rehm Massey University, PN; 2006. pp. 307–38.

8. Sára M, Pum D, Schuster B, Sleytr UB. S-layers as patterning elements for application in nanobiotechnology. *J Nanosci Nanotechnol* 2005;**5**:1939–53.
9. Schuster B, Györvary E, Pum D, Sleytr UB. Nanotechnology with S-layer proteins. *Methods Mol Biol* 2005;**300**:101–23.
10. Schuster, B. & Sletyr, U. B. (in press). Nanotechnology with S-layer proteins. In *Protein nanotechnology: protocols, instrumentation and applications* (Gerrard, J., ed.). Humana Press, Heidelberg.
11. Schuster B, Sleytr UB. Biomimetic S-layer supported lipid membranes. *Curr Nanosci* 2006;**2**:143–52.
12. Schuster B, Sleytr UB. Fabrication and characterization of functionalized S-layer supported lipid membranes. In: Bernstein EM, editor. *Bioelectrochemistry research developments*. Hauppauge, NY: Nova Science Publishers Inc.; 2008. pp. 105–24.
13. Schuster B, Sleytr UB. Composite S-layer lipid structures. *J Struct Biol* 2009;**168**:207–16.
14. Sleytr UB, Egelseer EM, Ilk N, Messner P, Schäffer C, Pum D, Schuster B. Nanobiotechnological applications of S-layers. In: König H, Claus H, Varma A, editors. *Prokaryotic cell wall compounds—structure and biochemistry.* Heidelberg, Germany: Springer; 2010. pp. 459–81.
15. Sleytr UB, Egelseer EM, Ilk N, Pum D, Schuster B. S-layers as a basic building block in a molecular construction kit. *FEBS J* 2007;**274**:323–34.
16. Sleytr UB, Egelseer EM, Pum D, Schuster B. S-layers. In: Niemeyer CM, Mirkin CA, editors. *Nanobiotechnology: concepts, methods and perspectives.* Vol. 7. Weinheim, Germany: Wiley-VCH; 2004. pp. 77–92.
17. Sleytr UB, Messner P, Pum D, Sára M. Crystalline bacterial cell surface layers (S-layers): from supramolecular cell structure to biomimetics and nanotechnology. *Angew. Chem. Int. Ed.* 1999;**38**:1034–54.
18. Sleytr, U. B., Pum, D., Egelseer, E., Ilk, N. & Schuster, B. (in press). S-layer proteins. In *Handbook of biofunctional surfaces* (Knoll, W., ed.). Pan Stanford Publishing.
19. Sleytr UB, Sára M, Pum D, Schuster B. Molecular nanotechnology and nanobiotechnology with two-dimensional protein crystals (S-layers). In: Rosoff M, editor. *Nano-surface chemistry.* New York, Basel: Marcel Dekker, Inc.; 2001. pp. 333–89.
20. Sleytr UB, Sára M, Pum D, Schuster B, Messner P, Schäffer C. Self-assembly protein systems: microbial S-layers. In: Steinbüchel A, Fahnestock SR, editors. *Biopolymers*. 1st Ed. *Polyamides and complex proteinaceous materials I* Vol. 7. Weinheim: Wiley-VCH; 2002. pp. 285–338.
21. Houwink AL, Le Poole JB. Eine Struktur in der Zellwand einer Bakterie. *Physikalische Verhandlung* 1952;**98**.
22. Sleytr UB, Adam H, Klaushofer H. Die elektronenmikroskopische Feinstruktur von Zellwand, Cytoplasmamembran und Geißeln von *Bacillus stearothermophilus*, dargestellt mit Hilfe der Gefrierätztechnik. *Mikroskopie* 1967;**22**:233–42.
23. Sleytr UB, Adam H, Klaushofer H. Die Feinstruktur der Zellwandoberfläche von zwei thermophilen Clostridienarten, dargestellt mit Hilfe der Gefrierätztechnik. *Mikroskopie* 1968;**23**:1–10.
24. Sleytr UB. Regular arrays of macromolecules on bacterial cell walls: structure, chemistry, assembly, and function. *Int Rev Cytol* 1978;**53**:1–62.
25. Sleytr UB, Messner P, Pum D, Sára M, editors. *Crystalline bacterial cell surface layers*. Berlin: Springer; 1988.
26. Claus H, Akca E, Debaerdemaeker T, Evrard C, Declercq JP, Harris JR, Schlott B, König H. Molecular organization of selected prokaryotic S-layer proteins. *Can J Microbiol* 2005;**51**:731–43.

27. Messner P, Schäffer C, Egelseer EM, Sleytr UB. Occurence, structure, chemistry, genetics, morphogenesis, and function of S-layers. In: König H, Claus H, Varma A, editors. *Prokaryotic cell wall compounds-structure and biochemistry.* Berlin: Springer-Verlag; 2010. pp. 53–109.
28. Sleytr UB, Messner P, Pum D, Sára M. *Crystalline bacterial cell surface proteins*. *Molecular biology intelligence unit*. Austin: R.G. Landes Comp., and San Diego: Academic Press; 1996.
29. Sleytr UB, Messner P, Pum D, Sára M. Crystalline surface layers on eubacteria and archaeobacteria. In: Sleytr UB, Messner P, Pum D, Sára M, editors. *Crystalline bacterial cell surface proteins*. Austin, Texas, USA: R.G. Landes Company and Academic Press Inc.; 1996. pp. 211–25.
30. Baumeister W, Lembcke G. Structural features of archaebacterial cell envelopes. *J Bioenerg Biomembr* 1992;**24**:567–75.
31. Baumeister W, Wildhaber I, Phipps BM. Principles of organization in eubacterial and archaebacterial surface proteins. *Can J Microbiol* 1989;**35**:215–27.
32. Hovmöller S, Sjogren A, Wang DN. The structure of crystalline bacterial surface layers. *Prog Biophys Mol Biol* 1988;**51**:131–63.
33. Sleytr UB. Heterologous reattachment of regular arrays of glycoproteins on bacterial surfaces. *Nature* 1975;**257**:400–2.
34. Sleytr UB, Beveridge TJ. Bacterial S-layers. *Trends Microbiol* 1999;**7**:253–60.
35. Sleytr UB, Glauert AM. Bacterial cell walls and membranes. In: Harris JR, editor. *Electron microscopy of proteins*Vol. 3. London: Academic Press Inc.; 1982. pp. 41–76.
36. Sleytr UB, Messner P. Crystalline surface layers on bacteria. *Annu Rev Microbiol* 1983;**37**:311–39.
37. Sleytr UB, Messner P. Self-assembly of crystalline bacterial cell surface layers (S-layers). In: Plattner H, editor. *Electron microscopy of subcellular dynamics*. Boca Raton, Florida: CRC Press; 1989. pp. 13–31.
38. Sleytr UB, Messner P, Pum D. Analysis of crystalline bacterial surface layers by freeze-teching, metal shadowing, negative staining and ultrathin sectioning. *Methods Microbiol* 1988;**20**:29–60.
39. Sleytr UB, Glauert AM. Analysis of regular arrays of subunits on bacterial surfaces: evidence for a dynamic process of assembly. *J Ultrastruct Res* 1975;**50**:103–16.
40. Beveridge TJ. Bacterial S-layers. *Curr Opin Struct Biol* 1994;**4**:204–12.
41. Hovmöller S. Crystallographic image processing applications for S-layers. In: Beveridge TJ, Koval S, editors. *Advances in paracrystalline bacterial surface layers*. *NATO ASI series, Series A: life sciences*, Vol. 252. New York: Plenum Press; 1993. pp. 13–21.
42. Müller DJ, Baumeister W, Engel A. Conformational change of the hexagonally packed intermediate layer of *Deinococcus radiodurans* monitored by atomic force microscopy. *J Bacteriol* 1996;**178**:3025–30.
43. Pum D, Tang J, Hinterdorfer P, Tocca Herrera JL, Sletyr UB. S-layer protein lattices studied by scanning force microscopy. In: Kumar CSSR, editor. *Biomimetic and bioinspired nanomaterials*. Weinheim, Germany: Wiley-VCH Verlag; 2010. pp. 459–510.
44. Engelhardt H. Are S-layers exoskeletons? The basic function of protein surface layers revisited. *J Struct Biol* 2007;**160**:115–24.
45. Veith A, Klingl A, Zolghadr B, Lauber K, Mentele R, Lottspeich F, Rachel R, Albers SV, Kletzin A. *Acidianus*, *Sulfolobus* and *Metallosphaera* surface layers: structure, composition and gene expression. *Mol Microbiol* 2009;**73**:58–72.
46. Bergey DH, Holt JG, Krieg NR, Sneath PHA. *Bergey's manual of determinative bacteriology.* Baltimore: Lippincott Williams & Wilkins; 1994.
47. Gram HC. Über die isolierte Färbung der *Schizomyceten* in Schnitt- und Trockenpräparaten. *Fortschr Med* 1884;**2**:185–9.
48. Beveridge TJ. Use of the gram stain in microbiology. *Biotech Histochem* 2001;**76**:111–8.

49. Sára M, Sleytr UB. S-layer proteins. *J Bacteriol* 2000;**182**:859–68.
50. Sleytr U, Messner P. Crystalline bacterial cell surface layers (S-layers). In: Lederberg J, editor. *Encyclopedia of microbiology*, Vol. 2. San Diego: Academic Press Inc.; 2000. pp. 899–906.
51. Sleytr UB, Sára M, Pum D, Schuster B. Characterization and use of crystalline bacterial cell surface layers. *Prog Surf Sci* 2001;**68**:231–78.
52. Engelhardt H. Mechanism of osmoprotection by archaeal S-layers: a theoretical study. *J Struct Biol* 2007;**160**:190–9.
53. Lortal S, van Heijenoort J, Gruber K, Sleytr UB. S-layer of *Lactobacillus helveticus* ATCC 12046: isolation, chemical characterization and re-formation after extraction with lithium chloride. *J Gen Microbiol* 1992;**138**:611–8.
54. Thompson SA, Shedd OL, Ray KC, Beins MH, Jorgensen JP, Blaser MJ. *Campylobacter fetus* surface layer proteins are transported by a type I secretion system. *J Bacteriol* 1998;**180**:6450–8.
55. Messner P, Sleytr UB. Separation and purification of S-layers from gram-positive and gram-negative bacteria. In: Hancock IC, Poxton IR, editors. *Bacterial cell surface techniques*. Chichester: John Wiley & Sons; 1988. pp. 97–104.
56. Sleytr UB, Glauert AM. Ultrastructure of the cell walls of two closely related clostridia that possess different regular arrays of surface subunits. *J Bacteriol* 1976;**126**:869–82.
57. Bröckl G, Behr M, Fabry S, Hensel R, Kaudewitz H, Biendl E, Konig H. Analysis and nucleotide sequence of the genes encoding the surface-layer glycoproteins of the hyperthermophilic methanogens *Methanothermus fervidus* and *Methanothermus sociabilis*. *Eur J Biochem* 1991;**199**:147–52.
58. Kosma P, Wugeditsch T, Christian R, Zayni S, Messner P. Glycan structure of a heptose-containing S-layer glycoprotein of *Bacillus thermoaerophilus*. *Glycobiology* 1995;**5**:791–6.
59. Pei Z, Ellison 3rd RT, Lewis RV, Blaser MJ. Purification and characterization of a family of high molecular weight surface-array proteins from *Campylobacter fetus*. *J Biol Chem* 1988;**263**:6416–20.
60. Lechner J, Sumper M. The primary structure of a procaryotic glycoprotein. Cloning and sequencing of the cell surface glycoprotein gene of halobacteria. *J Biol Chem* 1987;**262**:9724–9.
61. Trachtenberg S, Pinnick B, Kessel M. The cell surface glycoprotein layer of the extreme halophile *Halobacterium salinarum* and its relation to *Haloferax volcanii*: cryo-electron tomography of freeze-substituted cells and projection studies of negatively stained envelopes. *J Struct Biol* 2000;**130**:10–26.
62. Sleytr UB, Messner P, Pum D, Sara M. Crystalline bacterial cell surface layers. *Mol Microbiol* 1993;**10**:911–6.
63. Sumper M, Wieland FT. Bacterial glycoproteins. In: Montreuil J, Vliegenthart JFG, Schachter H, editors. *Glycoproteins*. Amsterdam: Elsevier; 1995. pp. 455–73.
64. Messner P, Sleytr UB. Crystalline bacterial cell-surface layers. In: Rose AH, editor. *Advances in microbial physiology*Vol. 33. London: Academic Press Inc.; 1992. pp. 213–75.
65. Sára M, Sleytr UB. Crystalline bacterial cell surface layers (S-layers): from cell structure to biomimetics. *Prog Biophys Mol Biol* 1996;**65**:83–111.
66. Kuen B, Lubitz W, Sleytr UB, Messner P, Pum D, Sára M. Analysis of S-layer proteins and genes. In: Sleytr U, Messner P, Pum D, Sára M, editors. *Crystalline bacterial cell surface layer proteins*. Austin, TX: R.G. Landes Comp./Academic Press Inc.; 1996. pp. 77–102.
67. Messner P, Egelseer EM, Sleytr UB, Schäffer C. Bacterial surface layer glycoproteins and "non-classical" secondary cell wall polymers. In: Moran A, Holst O, Brennan PJ, von Itzstein M, editors. *Microbial glycobiology: structures, relevance and applications*. San Diego: Elsevier; 2009. pp. 109–28.

68. Messner P, Steiner K, Zarschler K, Schäffer C. S-layer nanoglycobiology of bacteria. *Carbohydr Res* 2008;**343**:1934–51.
69. Akca E, Claus H, Schultz N, Karbach G, Schlott B, Debaerdemaeker T, Declercq JP, König H. Genes and derived amino acid sequences of S-layer proteins from mesophilic, thermophilic, and extremely thermophilic methanococci. *Extremophiles* 2002;**6**:351–8.
70. Avall-Jääskeläinen S, Palva A. *Lactobacillus* surface layers and their applications. *FEMS Microbiol Rev* 2005;**29**:511–29.
71. Eidhin DN, Ryan AW, Doyle RM, Walsh JB, Kelleher D. Sequence and phylogenetic analysis of the gene for surface layer protein, *slpA*, from 14 PCR ribotypes of *Clostridium difficile*. *J Med Microbiol* 2006;**55**:69–83.
72. Kato H, Yokoyama T, Arakawa Y. Typing by sequencing the *slpA* gene of *Clostridium difficile* strains causing multiple outbreaks in Japan. *J Med Microbiol* 2005;**54**:167–71.
73. Poilane I, Humeniuk-Ainouz C, Durand I, Janoir C, Cruaud P, Delmee M, Popoff MR, Collignon A. Molecular characterization of *Clostridium difficile* clinical isolates in a geriatric hospital. *J Med Microbiol* 2007;**56**:386–90.
74. Radnedge L, Agron PG, Hill KK, Jackson PJ, Ticknor LO, Keim P, Andersen GL. Genome differences that distinguish *Bacillus anthracis* from *Bacillus cereus* and *Bacillus thuringiensis*. *Appl Environ Microbiol* 2003;**69**:2755–64.
75. Tu ZC, Zeitlin G, Gagner JP, Keo T, Hanna BA, Blaser MJ. *Campylobacter fetus* of reptile origin as a human pathogen. *J Clin Microbiol* 2004;**42**:4405–7.
76. Huber C, Ilk N, Rünzler D, Egelseer EM, Weigert S, Sleytr UB, Sára M. The three S-layer-like homology motifs of the S-layer protein SbpA of *Bacillus sphaericus* CCM 2177 are not sufficient for binding to the pyruvylated secondary cell wall polymer. *Mol Microbiol* 2005;**55**:197–205.
77. Ilk N, Völlenkle C, Egelseer EM, Breitwieser A, Sleytr UB, Sára M. Molecular characterization of the S-layer gene, *sbpA*, of *Bacillus sphaericus* CCM 2177 and production of a functional S-layer fusion protein with the ability to recrystallize in a defined orientation while presenting the fused allergen. *Appl Environ Microbiol* 2002;**68**:3251–60.
78. Jarosch M, Egelseer EM, Huber C, Moll D, Mattanovich D, Sleytr UB, Sára M. Analysis of the structure-function relationship of the S-layer protein SbsC of *Bacillus stearothermophilus* ATCC 12980 by producing truncated forms. *Microbiology* 2001;**147**:1353–63.
79. Kroutil M, Pavkov T, Birner-Gruenberger R, Tesarz M, Sleytr UB, Egelseer EM, Keller W. Towards the structure of the C-terminal part of the S-layer protein SbsC. *Acta Crystallogr Sect F Struct Biol Cryst Commun* 2009;**65**:1042–7.
80. Pavkov T, Egelseer EM, Tesarz M, Svergun DI, Sleytr UB, Keller W. The structure and binding behavior of the bacterial cell surface layer protein SbsC. *Structure* 2008;**16**:1226–37.
81. Horejs C, Pum D, Sleytr UB, Tscheliessnig R. Structure prediction of an S-layer protein by the mean force method. *J Chem Phys* 2008;**128**:1–11 065106.
82. Kinns H, Badelt-Lichtblau H, Egelseer EM, Sleytr UB, Howorka S. Identifying assembly-inhibiting and assembly-tolerant sites in the SbsB S-layer protein from *Geobacillus stearothermophilus*. *J Mol Biol* 2010;**395**:742–53.
83. Howorka S, Sára M, Wang Y, Kuen B, Sleytr UB, Lubitz W, Bayley H. Surface-accessible residues in the monomeric and assembled forms of a bacterial surface layer protein. *J Biol Chem* 2000;**275**:37876–86.
84. Kinns H, Howorka S. The surface location of individual residues in a bacterial S-layer protein. *J Mol Biol* 2008;**377**:589–604.
85. Vilen H, Hynonen U, Badelt-Lichtblau H, Ilk N, Jaaskelainen P, Torkkeli M, Palva A. Surface location of individual residues of SlpA provides insight into the *Lactobacillus brevis* S-layer. *J Bacteriol* 2009;**191**:3339–49.

86. Lupas A, Engelhardt H, Peters J, Santarius U, Volker S, Baumeister W. Domain structure of the *Acetogenium kivui* surface layer revealed by electron crystallography and sequence analysis. *J Bacteriol* 1994;**176**:1224–33.
87. Cava F, de Pedro MA, Schwarz H, Henne A, Berenguer J. Binding to pyruvylated compounds as an ancestral mechanism to anchor the outer envelope in primitive bacteria. *Mol Microbiol* 2004;**52**:677–90.
88. Chauvaux S, Matuschek M, Beguin P. Distinct affinity of binding sites for S-layer homologous domains in *Clostridium thermocellum* and *Bacillus anthracis* cell envelopes. *J Bacteriol* 1999;**181**:2455–8.
89. Ilk N, Kosma P, Puchberger M, Egelseer EM, Mayer HF, Sleytr UB, Sára M. Structural and functional analyses of the secondary cell wall polymer of *Bacillus sphaericus* CCM 2177 that serves as an S-layer-specific anchor. *J Bacteriol* 1999;**181**:7643–6.
90. Lemaire M, Miras I, Gounon P, Beguin P. Identification of a region responsible for binding to the cell wall within the S-layer protein of *Clostridium thermocellum*. *Microbiology* 1998;**144**:211–7.
91. Mader C, Huber C, Moll D, Sleytr UB, Sára M. Interaction of the crystalline bacterial cell surface layer protein SbsB and the secondary cell wall polymer of *Geobacillus stearothermophilus* PV72 assessed by real-time surface plasmon resonance biosensor technology. *J Bacteriol* 2004;**186**:1758–68.
92. Mesnage S, Fontaine T, Mignot T, Delepierre M, Mock M, Fouet A. Bacterial SLH domain proteins are non-covalently anchored to the cell surface via a conserved mechanism involving wall polysaccharide pyruvylation. *EMBO J* 2000;**19**:4473–84.
93. Mesnage S, Tosi-Couture E, Mock M, Fouet A. The S-layer homology domain as a means for anchoring heterologous proteins on the cell surface of *Bacillus anthracis*. *J Appl Microbiol* 1999;**87**:256–60.
94. Ries W, Hotzy C, Schocher I, Sleytr UB, Sára M. Evidence that the N-terminal part of the S-layer protein from *Bacillus stearothermophilus* PV72/p2 recognizes a secondary cell wall polymer. *J Bacteriol* 1997;**179**:3892–8.
95. Rünzler D, Huber C, Moll D, Kohler G, Sára M. Biophysical characterization of the entire bacterial surface layer protein SbsB and its two distinct functional domains. *J Biol Chem* 2004;**279**:5207–15.
96. May A, Pusztahelyi T, Hoffmann N, Fischer RJ, Bahl H. Mutagenesis of conserved charged amino acids in SLH domains of *Thermoanaerobacterium thermosulfurigenes* EM1 affects attachment to cell wall sacculi. *Arch Microbiol* 2006;**185**:263–9.
97. Petersen BO, Sára M, Mader C, Mayer HF, Sleytr UB, Pabst M, Puchberger M, Krause E, Hofinger A, Duus JO, Kosma P. Structural characterization of the acid-degraded secondary cell wall polymer of *Geobacillus stearothermophilus* PV72/p2. *Carbohydr Res* 2008;**343**:1346–58.
98. Moll D, Huber C, Schlegel B, Pum D, Sleytr UB, Sára M. S-layer-streptavidin fusion proteins as template for nanopatterned molecular arrays. *Proc Natl Acad Sci USA* 2002;**99**:14646–51.
99. Egelseer EM, Leitner K, Jarosch M, Hotzy C, Zayni S, Sleytr UB, Sára M. The S-layer proteins of two *Bacillus stearothermophilus* wild-type strains are bound via their N-terminal region to a secondary cell wall polymer of identical chemical composition. *J Bacteriol* 1998;**180**:1488–95.
100. Jarosch M, Egelseer EM, Mattanovich D, Sleytr UB, Sára M. S-layer gene *sbsC* of *Bacillus stearothermophilus* ATCC 12980: molecular characterization and heterologous expression in *Escherichia coli*. *Microbiology* 2000;**146**(Pt. 2):273–81.
101. Schäffer C, Kählig H, Christian R, Schulz G, Zayni S, Messner P. The diacetamidodideoxyuronic-acid-containing glycan chain of *Bacillus stearothermophilus* NRS 2004/3a represents

the secondary cell-wall polymer of wild-type *B. stearothermophilus* strains. *Microbiology* 1999;**145**:1575–83.

102. Schäffer C, Wugeditsch T, Kählig H, Scheberl A, Zayni S, Messner P. The surface layer (S-layer) glycoprotein of *Geobacillus stearothermophilus* NRS 2004/3a. Analysis of its glycosylation. *J Biol Chem* 2002;**277**:6230–9.
103. Egelseer EM, Danhorn T, Pleschberger M, Hotzy C, Sleytr UB, Sára M. Characterization of an S-layer glycoprotein produced in the course of S-layer variation of *Bacillus stearothermophilus* ATCC 12980 and sequencing and cloning of the sbsD gene encoding the protein moiety. *Arch Microbiol* 2001;**177**:70–80.
104. Weis WI. Cell-surface carbohydrate recognition by animal and viral lectins. *Curr Opin Struct Biol* 1997;**7**:624–30.
105. Ferner-Ortner J, Mader C, Ilk N, Sleytr UB, Egelseer EM. High-affinity interaction between the S-layer protein SbsC and the secondary cell wall polymer of *Geobacillus stearothermophilus* ATCC 12980 determined by surface plasmon resonance technology. *J Bacteriol* 2007;**189**:7154–8.
106. Antikainen J, Anton L, Sillanpaa J, Korhonen TK. Domains in the S-layer protein CbsA of *Lactobacillus crispatus* involved in adherence to collagens, laminin and lipoteichoic acids and in self-assembly. *Mol Microbiol* 2002;**46**:381–94.
107. Smit E, Oling F, Demel R, Martinez B, Pouwels PH. The S-layer protein of *Lactobacillus acidophilus* ATCC 4356: identification and characterisation of domains responsible for S-protein assembly and cell wall binding. *J Mol Biol* 2001;**305**:245–57.
108. Masuda K, Kawata T. Reassembly of the regularly arranged subunits in the cell wall os *Lactobacillus brevis* and their reattachment to cell walls. *Microbiol Immunol* 1980;**24**:299–308.
109. Masuda K, Kawata T. Reassembly of a regularly arranged protein in the cell wall of *Lactobacillus buchneri* and its reattachment to cell walls: chemical modification studies. *Microbiol Immunol* 1985;**29**:927–38.
110. Doig P, McCubbin WD, Kay CM, Trust TJ. Distribution of surface-exposed and non-accessible amino acid sequences among the two major structural domains of the S-layer protein of *Aeromonas salmonicida*. *J Mol Biol* 1993;**233**:753–65.
111. Dworkin J, Tummuru MK, Blaser MJ. A lipopolysaccharide-binding domain of the *Campylobacter fetus* S-layer protein resides within the conserved N terminus of a family of silent and divergent homologs. *J Bacteriol* 1995;**177**:1734–41.
112. Yang LY, Pei ZH, Fujimoto S, Blaser MJ. Reattachment of surface array proteins to *Campylobacter fetus* cells. *J Bacteriol* 1992;**174**:1258–67.
113. Bingle WH, Nomellini JF, Smit J. Linker mutagenesis of the *Caulobacter crescentus* S-layer protein: toward a definition of an N-terminal anchoring region and a C-terminal secretion signal and the potential for heterologous protein secretion. *J Bacteriol* 1997;**179**:601–11.
114. Bingle WH, Nomellini JF, Smit J. Secretion of the *Caulobacter crescentus* S-layer protein: further localization of the C-terminal secretion signal and its use for secretion of recombinant proteins. *J Bacteriol* 2000;**182**:3298–301.
115. Ford MJ, Nomellini JF, Smit J. S-layer anchoring and localization of an S-layer-associated protease in *Caulobacter crescentus*. *J Bacteriol* 2007;**189**:2226–37.
116. Boot HJ, Kolen CP, Pouwels PH. Identification, cloning, and nucleotide sequence of a silent S-layer protein gene of *Lactobacillus acidophilus* ATCC 4356 which has extensive similarity with the S-layer protein gene of this species. *J Bacteriol* 1995;**177**:7222–30.
117. Boot HJ, Kolen CP, Pouwels PH. Interchange of the active and silent S-layer protein genes of *Lactobacillus acidophilus* by inversion of the chromosomal *slp* segment. *Mol Microbiol* 1996;**21**:799–809.

118. Calabi E, Ward S, Wren B, Paxton T, Panico M, Morris H, Dell A, Dougan G, Fairweather N. Molecular characterization of the surface layer proteins from *Clostridium difficile*. *Mol Microbiol* 2001;**40**:1187–99.
119. Cerquetti M, Molinari A, Sebastianelli A, Diociaiuti M, Petruzzelli R, Capo C, Mastrantonio P. Characterization of surface layer proteins from different *Clostridium difficile* clinical isolates. *Microb Pathog* 2000;**28**:363–72.
120. Dworkin J, Blaser MJ. Molecular mechanisms of *Campylobacter fetus* surface layer protein expression. *Mol Microbiol* 1997;**26**:433–40.
121. Jakava-Viljanen M, Avall-Jääskeläinen S, Messner P, Sleytr UB, Palva A. Isolation of three new surface layer protein genes (*slp*) from *Lactobacillus brevis* ATCC 14869 and characterization of the change in their expression under aerated and anaerobic conditions. *J Bacteriol* 2002;**184**:6786–95.
122. Karjalainen T, Waligora-Dupriet AJ, Cerquetti M, Spigaglia P, Maggioni A, Mauri P, Mastrantonio P. Molecular and genomic analysis of genes encoding surface-anchored proteins from *Clostridium difficile*. *Infect Immun* 2001;**69**:3442–6.
123. Mignot T, Mesnage S, Couture-Tosi E, Mock M, Fouet A. Developmental switch of S-layer protein synthesis in *Bacillus anthracis*. *Mol Microbiol* 2002;**43**:1615–27.
124. Sára M, Kuen B, Mayer HF, Mandl F, Schuster KC, Sleytr UB. Dynamics in oxygen-induced changes in S-layer protein synthesis from *Bacillus stearothermophilus* PV72 and the S-layer-deficient variant T5 in continuous culture and studies of the cell wall composition. *J Bacteriol* 1996;**178**:2108–17.
125. Sára M, Sleytr UB. Comparative studies of S-layer proteins from *Bacillus stearothermophilus* strains expressed during growth in continuous culture under oxygen-limited and non-oxygen-limited conditions. *J Bacteriol* 1994;**176**:7182–9.
126. Thompson SA, Blaser MJ. Pathogenesis of *Campylobacter fetus* infections. In: Nachamkin I, Blaser MJ, editors. *Campylobacter*. 2nd ed. Washington, DC: ASM Press; 2000. pp. 321–47.
127. Avall-Jääskeläinen S, Kylä-Nikkilä K, Kahala M, Miikkulainen-Lahti T, Palva A. Surface display of foreign epitopes on the *Lactobacillus brevis* S-layer. *Appl Environ Microbiol* 2002;**68**:5943–51.
128. Scholz HC, Riedmann E, Witte A, Lubitz W, Kuen B. S-layer variation in *Bacillus stearothermophilus* PV72 is based on DNA rearrangements between the chromosome and the naturally occurring megaplasmids. *J Bacteriol* 2001;**183**:1672–9.
129. Egelseer EM, Idris R, Jarosch M, Danhorn T, Sleytr UB, Sara M. ISBst12, a novel type of insertion-sequence element causing loss of S-layer-gene expression in *Bacillus stearothermophilus* ATCC 12980. *Microbiology* 2000;**146**(Pt. 9):2175–83.
130. Gustafson CE, Chu S, Trust TJ. Mutagenesis of the paracrystalline surface protein array of *Aeromonas salmonicida* by endogenous insertion elements. *J Mol Biol* 1994;**237**:452–63.
131. Sleytr UB. Basic and applied S layer research: an overview. *FEMS Microbiol Rev* 1997;**20**:5–12.
132. Luckevich MD, Beveridge TJ. Characterization of a dynamic S layer on Bacillus thuringiensis. *J Bacteriol* 1989;**171**:6656–67.
133. Tsukagoshi N, Tabata R, Takemura T, Yamagata H, Udaka S. Molecular cloning of a major cell wall protein gene from protein-producing *Bacillus brevis* 47 and its expression in *Escherichia coli* and *Bacillus subtilis*. *J Bacteriol* 1984;**158**:1054–60.
134. Breitwieser A, Gruber K, Sleytr UB. Evidence for an S-layer protein pool in the peptidoglycan of *Bacillus stearothermophilus*. *J Bacteriol* 1992;**174**:8008–15.
135. Boot HJ, Kolen CP, Andreadaki FJ, Leer RJ, Pouwels PH. The *Lactobacillus acidophilus* S-layer protein gene expression site comprises two consensus promoter sequences, one of which directs transcription of stable mRNA. *J Bacteriol* 1996;**178**:5388–94.

136. Chu S, Gustafson CE, Feutrier J, Cavaignac S, Trust TJ. Transcriptional analysis of the *Aeromonas salmonicida* S-layer protein gene *vapA*. *J Bacteriol* 1993;**175**:7968–75.
137. Fisher JA, Smit J, Agabian N. Transcriptional analysis of the major surface array gene of *Caulobacter crescentus*. *J Bacteriol* 1988;**170**:4706–13.
138. Boot HJ, Pouwels PH. Expression, secretion and antigenic variation of bacterial S-layer proteins. *Mol Microbiol* 1996;**21**:1117–23.
139. Peters J, Peters M, Lottspeich F, Schafer W, Baumeister W. Nucleotide sequence analysis of the gene encoding the *Deinococcus radiodurans* surface protein, derived amino acid sequence, and complementary protein chemical studies. *J Bacteriol* 1987;**169**:5216–23.
140. Faraldo MM, de Pedro MA, Berenguer J. Sequence of the S-layer gene of *Thermus thermophilus* HB8 and functionality of its promoter in *Escherichia coli*. *J Bacteriol* 1992;**174**:7458–62.
141. Carl M, Dobson ME, Ching WM, Dasch GA. Characterization of the gene encoding the protective paracrystalline-surface-layer protein of *Rickettsia prowazekii*: presence of a truncated identical homolog in *Rickettsia typhi*. *Proc Natl Acad Sci USA* 1990;**87**:8237–41.
142. Noonan B, Trust TJ. Molecular analysis of an A-protein secretion mutant of *Aeromonas salmonicida* reveals a surface layer-specific protein secretion pathway. *J Mol Biol* 1995;**248**:316–27.
143. Awram P, Smit J. The *Caulobacter crescentus* paracrystalline S-layer protein is secreted by an ABC transporter (type I) secretion apparatus. *J Bacteriol* 1998;**180**:3062–9.
144. Kawai E, Akatsuka H, Idei A, Shibatani T, Omori K. *Serratia marcescens* S-layer protein is secreted extracellularly via an ATP-binding cassette exporter, the Lip system. *Mol Microbiol* 1998;**27**:941–52.
145. Blight MA, Holland IB. Heterologous protein secretion and the versatile *Escherichia coli* haemolysin translocator. *Trends Biotechnol* 1994;**12**:450–5.
146. Wandersman C. Secretion across the bacterial outer membrane. *Trends Genet* 1992;**8**:317–22.
147. Sleytr UB, Plohberger R. The dynamic process of assembly of two-dimensional arrays of macromolecules on bacterial cell walls. In: Baumeister W, Vogell W, editors. *Electron microscopy at molecular dimensions*. Berlin, Heidelberg, New York: Springer-Verlag; 1980. pp. 36–47.
148. Gruber K, Sleytr UB. Localized insertion of new S-layer during growth of *Bacillus stearothermophilus* strains. *Arch Microbiol* 1988;**149**:485–91.
149. Smit J, Agabian N. Cell surface patterning and morphogenesis: biogenesis of a periodic surface array during *Caulobacter* development. *J Cell Biol* 1982;**95**:41–9.
150. Harris WF, Scriven LE. Function of dislocations in cell walls and membranes. *Nature* 1970;**228**:827–9.
151. Messner P, Pum D, Sára M, Stetter KO, Sleytr UB. Ultrastructure of the cell envelope of the archaebacteria *Thermoproteus tenax* and *Thermoproteus neutrophilus*. *J Bacteriol* 1986;**166**:1046–54.
152. Pum D, Messner P, Sleytr UB. Role of the S layer in morphogenesis and cell division of the archaebacterium *Methanocorpusculum sinense*. *J Bacteriol* 1991;**173**:6865–73.
153. Györvary ES, Stein O, Pum D, Sleytr UB. Self-assembly and recrystallization of bacterial S-layer proteins at silicon supports imaged in real time by atomic force microscopy. *J Microsc* 2003;**212**:300–6.
154. Pum D, Sleytr UB. Large-scale reconstruction of crystalline bacterial surface layer proteins at the air-water interface and on lipids. *Thin Solid Films* 1994;**244**:882–6.
155. Pum D, Sleytr UB. Anisotropic crystal growth of the S-layer of *Bacillus sphaericus* CCM 2177 at the air/water interface. *Colloids Surf A Physicochem Eng Aspects* 1995;**102**:99–104.
156. Pum D, Sleytr UB. Monomolecular reassembly of a crystalline bacterial cell surface layer (S layer) on untreated and modified silicon surfaces. *Supramol Sci* 1995;**2**:193–7.

157. Messner P, Pum D, Sleytr UB. Characterization of the ultrastructure and the self-assembly of the surface layer of *Bacillus stearothermophilus strain* NRS 2004/3a. *J Ultrastruct Mol Struct Res* 1986;**97**:73–88.
158. Sleytr UB. Self-assembly of the hexagonally and tetragonally arranged subunits of bacterial surface layers and their reattachment to cell walls. *J Ultrastruct Res* 1976;**55**:360–77.
159. Jaenicke R, Welsch R, Sára M, Sleytr UB. Stability and self-assembly of the S-layer protein of the cell wall of *Bacillus stearothermophilus*. *Biol Chem Hoppe Seyler* 1985;**366**:663–70.
160. Pum D, Weinhandl M, Hödl C, Sleytr UB. Large-scale recrystallization of the S-layer of *Bacillus coagulans* E38-66 at the air/water interface and on lipid films. *J Bacteriol* 1993;**175**:2762–6.
161. Györvary E, O´Riordan A, Quinn A, Redmond G, Pum D, Sleytr UB. Biomimetic nanostructure fabrication: non-lithographic lateral patterning and self-assembly of functional bacterial S-layers at silicon supports. *Nano Lett* 2003;**3**:315–9.
162. Lopez AE, Moreno-Flores S, Pum D, Sleytr UB, Toca-Herrera JL. Surface dependence of protein nanocrystal formation. *Small* 2009;**6**:396–403.
163. Moreno-Flores S, Kasry A, Butt HJ, Vavilala C, Schmittel M, Pum D, Sleytr UB, Toca-Herrera JL. From native to non-native two-dimensional protein lattices through underlying hydrophilic/hydrophobic nanoprotrusions. *Angew Chem Int Ed Engl* 2008;**47**:4707–10.
164. Ulman A. Formation and structure of self-assembled monolayers. *Chem Rev* 1996;**96**:1533–54.
165. Györvary E, Schroedter A, Talapin DV, Weller H, Pum D, Sleytr UB. Formation of nanoparticle arrays on S-layer protein lattices. *J Nanosci Nanotechnol* 2004;**4**:115–20.
166. Schuster B, Sleytr UB. S-layer-supported lipid membranes. *J Biotechnol* 2000;**74**:233–54.
167. Schuster B, Sleytr UB. 2D-protein crystals (S-layers) as support for lipid membranes. In: Tien TH, Ottova A, editors. *Advances in planar lipid bilayers and liposomes*, Vol. 1. Amsterdam, The Netherlands: Elsevier Science; 2005. pp. 247–93.
168. Küpcü S, Sára M, Sleytr UB. Liposomes coated with crystalline bacterial cells surface protein (S-layer) as immobilization structures for macromolecules. *Biochim Biophys Acta* 1995;**1235**:263–9.
169. Mader C, Küpcü S, Sára M, Sleytr UB. Stabilizing effect of an S-layer on liposomes towards thermal or mechanical stress. *Biochim Biophys Acta* 1999;**1418**:106–16.
170. Mader C, Küpcü S, Sleytr UB, Sára M. S-layer-coated liposomes as a versatile system for entrapping and binding target molecules. *Biochim Biophys Acta* 2000;**1463**:142–50.
171. Toca-Herrera JL, Krastev R, Bosio V, Küpcü S, Pum D, Fery A, Sára M, Sleytr UB. Recrystallization of bacterial S-layers on flat polyelectrolyte surfaces and hollow polyelectrolyte capsules. *Small* 2005;**1**:339–48.
172. Pum D, Stangl G, Sponer C, Fallmann W, Sleytr UB. Deep UV patterning of monolayers of crystalline S layer protein on silicon surfaces. *Colloids Surf B* 1997;**8**:157–62.
173. Chung S, Shin SH, Bertozzi CR, De Yoreo JJ. Self-catalyzed growth of S layers via an amorphous-to-crystalline transition limited by folding kinetics. *Proc Natl Acad Sci USA* 2010;**107**:16536–41.
174. Fagan RP, Albesa-Jove D, Qazi O, Svergun DI, Brown KA, Fairweather NF. Structural insights into the molecular organization of the S-layer from *Clostridium difficile*. *Mol Microbiol* 2009;**71**:1308–22.
175. Norville JE, Kelly DF, Knight Jr. TF, Belcher AM, Walz T. 7A projection map of the S-layer protein sbpA obtained with trehalose-embedded monolayer crystals. *J Struct Biol* 2007;**160**:313–23.
176. Pavkov T, Oberer M, Egelseer EM, Sara M, Sleytr UB, Keller W. Crystallization and preliminary structure determination of the C-terminal truncated domain of the S-layer protein SbsC. *Acta Crystallogr D Biol Crystallogr* 2003;**59**:1466–8.

177. Whitelam S. Control of pathways and yields of protein crystallization through the interplay of nonspecific and specific attractions. *Phys Rev Lett* 2010;**105**: 088102.
178. Horejs C, Pum D, Sleytr UB, Peterlik H, Jungbauer A, Tscheliessnig R. Surface layer protein characterization by small angle x-ray scattering and a fractal mean force concept: from protein structure to nanodisk assemblies. *J Chem Phys* 2010;**133**: 175102.
179. Horejs C, Gollner H, Pum D, Sleytr UB, Peterlik H, Jungbauer A, Tscheliessnig R. Atomistic structure of monomolecular surface layer self-assemblies: towards functionalized nanostructures. *ACS Nano* 2011;**5**:2288–97.
180. Horejs C, Mitra MK, Pum D, Sleytr UB, Muthukumar M. Monte Carlo study of the molecular mechanisms of S-layer self-assembly. *J Chem Phys* 2011;**134**:125103.
181. Baumeister W, Engelhardt H. Three-dimensional structure of bacterial surface layers. In: Harris JR, Horne RW, editors. *Electron microscopy of proteins*, Vol. 6. London: Academic Press; 1987. pp. 109–54.
182. Sára M, Sleytr UB. Molecular sieving through S layers of *Bacillus stearothermophilus* strains. *J Bacteriol* 1987;**169**:4092–8.
183. Scherrer R, Gerhardt P. Molecular sieving by the *Bacillus megaterium* cell wall and protoplast. *J Bacteriol* 1971;**107**:718–35.
184. Sára M, Pum D, Sleytr UB. Permeability and charge-dependent adsorption properties of the S-layer lattice from *Bacillus coagulans* E38-66. *J Bacteriol* 1992;**174**:3487–93.
185. Sára M, Manigley C, Wolf G, Sleytr UB. Isoporous ultrafiltration membranes from bacterial cell envelope layers. *J Membr Sci* 1988;**36**:179–86.
186. Sára M, Sleytr UB. Membrane biotechnology: two-dimensional protein crystals for ultrafiltration purposes. In: Rehm HJ, editor. *Biotechnology*. Weinheim: VCH; 1988. pp. 615–36.
187. Sára M, Sleytr UB. Production and characteristics of ultrafiltration membranes with uniform pores from two-dimensional arrays of proteins. *J Membr Sci* 1987;**33**:27–49.
188. Sleytr UB, Sára M. *Structure with membrane having continuous pores.* U.S. Pat. 4,752,395.
189. Küpcü S, Sára M, Sleytr UB. Chemical modification of crystalline ultrafiltration membranes and immobilization of macromolecules. *J Membr Sci* 1991;**61**:167–75.
190. Sára M, Küpcü S, Sleytr UB. Crystalline bacterial cell surface layers used as ultrafiltration membranes and immobilization matrix. *Genet Eng Biotechnol* 1990;**10**:10–3.
191. Sára M, Küpcü S, Weiner C, Weigert S, Sleytr UB. Crystalline protein layers as isoporous molecular sieves and immobilisation and affinity matrices. In: Sleytr UB, Messner P, Pum D, Sára M, editors. *Immobilised macromolecules: application potentials*. London, UK: Springer-Verlag; 1993. pp. 71–86.
192. Sára M, Küpcü S, Weiner C, Weigert S, Sleytr UB. S-layers as immobilization and affinity matrices. In: Beveridge TJ, Koval SF, editors. *Advances in bacterial paracrystalline surface layers*. New York & London: Plenum Press; 1993.
193. Sleytr UB, Messner P, Pum D, Sára M. *Immobilised macromolecules: application potentials.* London, UK: Springer-Verlag; 1993.
194. Küpcü S, Sára M, Sleytr UB. Influence of covalent attachment of low molecular weight substances on the rejection and adsorption properties of crystalline proteinaceous ultra filtration membranes. *Desalination* 1993;**90**:65–76.
195. Weigert S, Sára M. Ultrafiltration membranes prepared from crystalline bacterial cell surface layers as model systems for studying the influence of surface properties on protein adsorption. *J Membr Sci* 1996;**121**:185–96.
196. Breitwieser A, Küpcü S, Howorka S, Weigert S, Langer C, Hoffmann-Sommergruber K, Scheiner O, Sleytr UB, Sára M. 2-D protein crystals as an immobilization matrix for producing reaction zones in dipstick-style immunoassays. *Biotechniques* 1996;**21**:918–25.

197. Küpcü S, Sleytr UB, Sara M. Two-dimensional paracrystalline glycoprotein S-layers as a novel matrix for the immobilization of human IgG and their use as microparticles in immunoassays. *J Immunol Methods* 1996;**196**:73–84.
198. Sára M, Sleytr UB. Use of regularly structured bacterial cell envelope layers as matrix for the immobilization of macromolecules. *Appl Microbiol Biotechnol* 1989;**30**:184–9.
199. Weiner C, Sára M, Sleytr UB. Novel protein A affinity matrix prepared from two-dimensional protein crystals. *Biotechnol Bioeng* 1994;**43**:321–30.
200. Crowther RA, Sleytr UB. An analysis of the fine structure of the surface layers from two strains of *Clostridia*, including correction for distorted images. *J Ultrastruct Res* 1977;**58**:41–9.
201. Sleytr UB, Sára M, Küpcü Z, Messner P. Structural and chemical characterization of S-layers of selected strains of *Bacillus stearothermophilus* and *Desulfotomaculum nigrificans*. *Arch Microbiol* 1986;**146**:19–24.
202. Bock K, Schuster-Kolbe J, Altman E, Allmaier G, Stahl B, Christian R, Sleytr UB, Messner P. Primary structure of the O-glycosidically linked glycan chain of the crystalline surface layer glycoprotein of *Thermoanaerobacter thermohydrosulfuricus* L111-69. Galactosyl tyrosine as a novel linkage unit. *J Biol Chem* 1994;**269**:7137–44.
203. Christian R, Messner P, Weiner C, Sleytr UB, Schulz G. Structure of a glycan from the surface-layer glycoprotein of *Clostridium thermohydrosulfuricum* strain L111-69. *Carbohydr Res* 1988;**176**:160–3.
204. Pum D, Sára M, Sleyt UB. Two-dimensional (glyco)protein crystals as patterning elements and immobilisation matrices for the development of biosensors. In: Sleytr UB, Messner P, Pum D, Sára M, editors. *Immobilised macromolecules: application potentials*. London, UK: Springer-Verlag; 1993. pp. 141–60.
205. Küpcü S, Mader C, Sára M. The crystalline cell surface layer of *Thermoanaerobacter thermohydrosulfuricus* L111-69 as an immobilization matrix: influence of the morphological properties and the pore size of the matrix on activity loss of covalently bound enzymes. *Biotechnol Appl Biochem* 1995;**21**:275–86.
206. Weber V, Weigert S, Sára M, Sleytr UB, Falkenhagen D. Development of affinity microparticles for extracorporeal blood purification based on crystalline bacterial cell surface proteins. *Ther Apher* 2001;**5**:433–8.
207. Sára M, Küpcü S, Sleytr UB. Biotechnological applications of S-layers. In: Sleytr UB, Messner P, Pum D, Sára M, editors. *Crystalline bacterial cell surface proteins*. Austin, Texas, USA: R.G. Landes Company and Academic Press Inc.; 1996. pp. 133–59.
208. Breitwieser A, Mader C, Schocher I, Hoffmann-Sommergruber K, Aberer W, Scheiner O, Sleytr UB, Sára M. A novel dipstick developed for rapid Bet v 1-specific IgE detection: recombinant allergen immobilized via a monoclonal antibody to crystalline bacterial cell-surface layers. *Allergy* 1998;**53**:786–93.
209. Sleytr UB, Pum D, Sára M, Schuster B. Molecular nanotechnology and nanobiotechnology with 2-D protein crystals. In: Nalwa HS, editor. *Encylopedia of nanoscience and nanotechnology*Vol. 5. San Diego: Academic Press; 2004. pp. 693–702.
210. Sleytr UB, Sára M. Bacterial and archaeal S-layer proteins: structure-function relationships and their biotechnological applications. *Trends Biotechnol* 1997;**15**:20–6.
211. Völkel D, Zimmermann K, Breitwieser A, Pable S, Glatzel M, Scheiflinger F, Schwarz HP, Sára M, Sleytr UB, Dorner F. Immunochemical detection of prion protein on dipsticks prepared with crystalline bacterial cell-surface layers. *Transfusion* 2003;**43**:1677–82.
212. Neubauer A, Pum D, Sleytr UB. An amperometric glucose sensor based on isoporous crystalline protein membranes as immobilization matrix. *Anal Lett* 1993;**26**:1347–60.
213. Neubauer A, Hödl C, Pum D, Sleytr UB. A multistep enzyme sensor for sucrose based on S-layer microparticles as immobilization matrix. *Anal Lett* 1994;**27**:849–65.

214. Schäffer C, Novotny R, Kupcu S, Zayni S, Scheberl A, Friedmann J, Sleytr UB, Messner P. Novel biocatalysts based on S-layer self-assembly of *Geobacillus stearothermophilus* NRS 2004/3a: a nanobiotechnological approach. *Small* 2007;**3**:1549–59.
215. Tschiggerl H, Breitwieser A, de Roo G, Verwoerd T, Schäffer C, Sleytr UB. Exploitation of the S-layer self-assembly system for site directed immobilization of enzymes demonstrated for an extremophilic laminarinase from *Pyrococcus furiosus*. *J Biotechnol* 2008;**133**:403–11.
216. Douglas K, Clark NA, Rothschild KJ. Nanometer molecular lithography. *Appl Phys Lett* 1986;**48**:676–8.
217. Douglas S, Beveridge TJ. Mineral formation by bacteria in natural microbial communities. *FEMS Microbiol Ecol* 1998;**26**:79–88.
218. Bergkvist M, Mark SS, Yang X, Angert ER, Batt CA. Bionanofabrication of ordered nanoparticle arrays: effect of particle properties and adsorption conditions. *J Phys Chem B* 2004;**108**:8241–8.
219. Dieluweit S, Pum D, Sleytr UB, Kautek W. Monodisperse gold nanoparticles formed on bacterial crystalline surface layers (S-layers) by electroless deposition. *Mater Sci Eng C* 2005;**25**:727–32.
220. Mertig M, Kirsch R, Pompe W, Engelhardt H. Fabrication of highly orineted nanocluster arrays by biomolecular templating. *Eur Phys J D* 1999;**9**:45–8.
221. Mertig M, Wahl R, Lehmann M, Simon P, Pompe W. Formation and manipulation of regular metallic nanoparticle arrays on bacterial surface layers: an advanced TEM study. *Eur Phys J D* 2001;**16**:317–20.
222. Shenton W, Pum D, Sleytr UB, Mann S. Biocrystal templating of CdS superlattices using self-assembled bacterial S-layers. *Nature* 1997;**389**:585–7.
223. Wahl R, Mertig M, Raff J, Selenska-Pobell S, Pompe W. Electron-beam induced formation of highly ordered palladium and platinum nanoparticle arrays on the S-layer of *Bacillus sphaericus* NCTC 9602. *Adv Mater Sci Technol* 2001;**13**:736–40.
224. Hall SR, Shenton W, Engelhardt H, Mann S. Site-specific organization of gold nanoparticles by biomolecular templating. *Chemphyschem* 2001;**3**:184–6.
225. Mark SS, Bergkvist M, Yang X, Angert ER, Batt CA. Self-assembly of dendrimer-encapsulated nanoparticle arrays using 2-D microbial S-layer protein biotemplates. *Biomacromolecules* 2006;**7**:1884–97.
226. Mark SS, Bergkvist M, Yang X, Teixeira LM, Bhatnagar P, Angert ER, Batt CA. Bionanofabrication of metallic and semiconductor nanoparticle arrays using S-layer protein lattices with different lateral spacings and geometries. *Langmuir* 2006;**22**:3763–74.
227. Badelt-Lichtblau H, Kainz B, Völlenkle C, Egelseer EM, Sleytr UB, Pum D, Ilk N. Genetic engineering of the S-layer protein SbpA of *Lysinibacillus sphaericus* CCM 2177 for the generation of functionalized nanoarrays. *Bioconjug Chem* 2009;**20**:895–903.
228. Sleytr UB, Huber C, Ilk N, Pum D, Schuster B, Egelseer E. S-Layers as a tool kit for nanobiotechnological applications. *FEMS Microbiol Lett* 2007;**267**:131–44.
229. Huber C, Liu J, Egelseer EM, Moll D, Knoll W, Sleytr UB, Sára M. Heterotetramers formed by an S-layer-streptavidin fusion protein and core-streptavidin as nanoarrayed template for biochip development. *Small* 2006;**2**:142–50.
230. Breitwieser A, Egelseer EM, Moll D, Ilk N, Hotzy C, Bohle B, Ebner C, Sleytr UB, Sára M. A recombinant bacterial cell surface (S-layer)-major birch pollen allergen-fusion protein (rSbsC/Bet v1) maintains the ability to self-assemble into regularly structured monomolecular lattices and the functionality of the allergen. *Protein Eng* 2002;**15**:243–9.
231. Völlenkle C, Weigert S, Ilk N, Egelseer E, Weber V, Loth F, Falkenhagen D, Sleytr UB, Sára M. Construction of a functional S-layer fusion protein comprising an immunoglobulin G-binding domain for development of specific adsorbents for extracorporeal blood

purification. *Appl Environ Microbiol,* 2004;**70**:1514–21, Highlight in Nature Rewiews Microbiology 2(5), 353.

232. Ilk N, Küpcü S, Moncayo G, Klimt S, Ecker RC, Hofer-Warbinek R, Egelseer EM, Sleytr UB, Sára M. A functional chimaeric S-layer-enhanced green fluorescent protein to follow the uptake of S-layer-coated liposomes into eukaryotic cells. *Biochem J* 2004;**379**:441–8.
233. Pleschberger M, Saerens D, Weigert S, Sleytr UB, Muyldermans S, Sára M, Egelseer EM. An S-layer heavy chain camel antibody fusion protein for generation of a nanopatterned sensing layer to detect the prostate-specific antigen by surface plasmon resonance technology. *Bioconjug Chem* 2004;**15**:664–71.
234. Tschiggerl H, Casey JL, Parisi K, Foley M, Sleytr UB. Display of a peptide mimotope on a crystalline bacterial cell surface layer (S-layer) lattice for diagnosis of Epstein-Barr virus infection. *Bioconjug Chem* 2008;**19**:860–5.
235. Kainz B, Steiner K, Möller M, Pum D, Schäffer C, Sleytr UB, Toca-Herrera JL. Absorption, steady-state fluorescence, fluorescence lifetime, and 2D self-assembly properties of engineered fluorescent S-layer fusion proteins of *Geobacillus stearothermophilus* NRS 2004/3a. *Biomacromolecules* 2010;**11**:207–14.
236. Kainz B, Steiner K, Sleytr UB, Pum D, Toca-Herrera JL. Fluorescence energy transfer in the bi-fluorescent S-layer tandem fusion protein ECFP-SgsE-YFP. *J Struct Biol* 2010;**172**:276–83.
237. Riedmann EM, Kyd JM, Smith AM, Gomez-Gallego S, Jalava K, Cripps AW, Lubitz W. Construction of recombinant S-layer proteins (rSbsA) and their expression in bacterial ghosts–a delivery system for the nontypeable Haemophilus influenzae antigen Omp26. *FEMS Immunol Med Microbiol* 2003;**37**:185–92.
238. Mesnage S, Tosi-Couture E, Fouet A. Production and cell surface anchoring of functional fusions between the SLH motifs of the *Bacillus anthracis* S-layer proteins and the *Bacillus subtilis* levansucrase. *Mol Microbiol* 1999;**31**:927–36.
239. Mesnage S, Weber-Levy M, Haustant M, Mock M, Fouet A. Cell surface-exposed tetanus toxin fragment C produced by recombinant *Bacillus anthracis* protects against tetanus toxin. *Infect Immun* 1999;**67**:4847–50.
240. Bingle WH, Nomellini JF, Smit J. Cell-surface display of a *Pseudomonas aeruginosa* strain K pilin peptide within the paracrystalline S-layer of *Caulobacter crescentus*. *Mol Microbiol* 1997;**26**:277–88.
241. Simon B, Nomellini JF, Chiou P, Binale W, Thornton J, Smit J, Leong JA. Recombinant vaccines against infectious hematopoietic necrosis virus: production line by the *Caulobacter crescentus* S-layer protein secretion system and evaluation in laboratory trials. *Dis Aquat Organ* 2001;**44**:400–2.
242. Duncan G, Tarling CA, Bingle WH, Nomellini JF, Yamage M, Dorocicz IR, Withers SG, Smit J. Evaluation of a new system for developing particulate enzymes based on the surface (S)-layer protein (RsaA) of *Caulobacter crescentus*: fusion with the beta-1,4-glycanase (Cex) from the cellulolytic bacterium *Cellulomonas fimi* yields a robust, catalytically active product. *Appl Biochem Biotechnol* 2005;**127**:95–110.
243. Nomellini JF, Duncan G, Dorocicz IR, Smit J. S-layer-mediated display of the immunoglobulin G-binding domain of streptococcal protein G on the surface of *Caulobacter crescentus*: development of an immunoactive reagent. *Appl Environ Microbiol* 2007;**73**:3245–53.
244. Nomellini JF, Li C, Lavallee D, Shanina I, Cavacini LA, Horwitz MS, Smit J. Development of an HIV-1 specific microbicide using *Caulobacter crescentus* S-layer mediated display of CD4 and MIP1alpha. *PLoS One* 2010;**5**:e10366.
245. Patel J, Zhang Q, McKay RM, Vincent R, Xu Z. Genetic engineering of *Caulobacter crescentus* for removal of cadmium from water. *Appl Biochem Biotechnol* 2010;**160**:232–43.

246. Huber C, Egelseer EM, Ilk N, Sleytr UB, Sára M. S-layer-streptavidin fusion proteins and S-layer-specific heteropolysaccharides as part of a biomolecular construction kit for application in nanobiotechnology. *Microelectron Eng* 2006;**83**:1589–93.
247. Pleschberger M, Neubauer A, Egelseer EM, Weigert S, Lindner B, Sleytr UB, Muyldermans S, Sára M. Generation of a functional monomolecular protein lattice consisting of an S-layer fusion protein comprising the variable domain of a camel heavy chain antibody. *Bioconjug Chem* 2003;**14**:440–8.
248. Bohle B, Breitwieser A, Zwölfer B, Jahn-Schmid B, Sára M, Sleytr UB, Ebner C. A novel approach to specific allergy treatment: the recombinant fusion protein of a bacterial cell surface (S-layer) protein and the major birch pollen allergen Bet v 1 (rSbsC-Bet v 1) combines reduced allergenicity with immunomodulating capacity. *J Immunol* 2004;**172**:6642–8.
249. Gerstmayr M, Ilk N, Schabussova I, Jahn-Schmid B, Egelseer EM, Sleytr UB, Ebner C, Bohle B. A novel approach to specific allergy treatment: the recombinant allergen-S-layer fusion protein rSbsC-Bet v 1 matures dendritic cells that prime Th0/Th1 and IL-10-producing regulatory T cells. *J Immunol* 2007;**179**:7270–5.
250. Ferner-Ortner-Beckmann, J., Tesarz, M., Egelseer, E. M., Sleytr, U. B. & Ilk, N. (submitted). S-layer-based biocatalysts carrying multimeric extremozymes. *Small*.
251. Kuen B, Sleytr UB, Lubitz W. Sequence analysis of the *sbsA* gene encoding the 130-kDa surface-layer protein of *Bacillus stearothermophilus* strain PV72. *Gene* 1994;**145**:115–20.
252. Fouet A, Mesnage S. *Bacillus anthracis* cell envelope components. *Curr Top Microbiol Immunol* 2002;**271**:87–113.
253. Smit J, Engelhardt H, Volker S, Smith SH, Baumeister W. The S-layer of *Caulobacter crescentus:* three-dimensional image reconstruction and structure analysis by electron microscopy. *J Bacteriol* 1992;**174**:6527–38.
254. Smit J, Grano DA, Glaeser RM, Agabian N. Periodic surface array in *Caulobacter crescentus*: fine structure and chemical analysis. *J Bacteriol* 1981;**146**:1135–50.
255. Gilchrist A, Fisher JA, Smit J. Nucleotide sequence analysis of the gene encoding the *Caulobacter crescentus* paracrystalline surface layer protein. *Can J Microbiol* 1992;**38**:193–202.
256. Walker SG, Smith SH, Smit J. Isolation and comparison of the paracrystalline surface layer proteins of freshwater caulobacters. *J Bacteriol* 1992;**174**:1783–92.
257. Apweiler R, Hermjakob H, Sharon N. On the frequency of protein glycosylation, as deduced from analysis of the SWISS-PROT database. *Biochim Biophys Acta* 1999;**1473**:4–8.
258. Spiro RG. Protein glycosylation: nature, distribution, enzymatic formation, and disease implications of glycopeptide bonds. *Glycobiology* 2002;**12**:43R–NaN.
259. Samuelson P, Gunneriusson E, Nygren PA, Stahl S. Display of proteins on bacteria. *J Biotechnol* 2002;**96**:129–54.
260. Zarschler K, Janesch B, Kainz B, Ristl R, Messner P, Schäffer C. Cell surface display of chimeric glycoproteins via the S-layer of *Paenibacillus alvei*. *Carbohydr Res* 2010;**345**:1422–31.
261. Kern JW, Schneewind O. BslA, a pXO1-encoded adhesin of *Bacillus anthracis*. *Mol Microbiol* 2008;**68**:504–15.
262. Kern J, Schneewind O. BslA, the S-layer adhesin of *B. anthracis*, is a virulence factor for anthrax pathogenesis. *Mol Microbiol* 2010;**75**:324–32.
263. Ní Eidhin DB, O´Brien JB, McCabe MS, Athié-Morales V, Kelleher DP. Active immunization of hamsters against *Clostridium difficile* infection using surface-layer protein. *FEMS Immunol Med Microbiol* 2008;**52**:207–18.
264. Ford LA, Thune RL. Immunization of channel catfish with crude, acid-extracted preparation of motile aeromonad S-layer protein. *Biomed Lett* 1992;**47**:355–62.

265. Poobalane S, Thompson KD, Ardo L, Verjan N, Han HJ, Jeney G, Hirono I, Aoki T, Adams A. Production and efficacy of an *Aeromonas hydrophila* recombinant S-layer protein vaccine for fish. *Vaccine* 2010;**28**:3540–7.
266. Malcolm AJ, Messner P, Sleytr UB, Smith RH, Unger FM. Crystalline bacterial cell surface layers (S-layers) as combined carrier/adjuvants for conjugated vaccines. In: Sleytr UB, Messner P, Pum D, Sára M, editors. *Immobilized macromolecules: application potentials*. London, UK: Springer-Verlag; 1993. pp. 195–207.
267. Smith RH, Messner P, Lamontagne LR, Sleytr UB, Unger FM. Induction of T-cell immunity to oligosaccharide antigens immobilized on crystalline bacterial surface layers (S-layers). *Vaccine* 1993;**11**:919–24.
268. Jahn-Schmid B, Siemann U, Zenker A, Bohle B, Messner P, Unger FM, Sleytr UB, Scheiner O, Kraft D, Ebner C. Bet v 1, the major birch pollen allergen, conjugated to crystalline bacterial cell surface proteins, expands allergen-specific T cells of the Th1/Th0 phenotype in vitro by induction of IL-12. *Int Immunol* 1997;**9**:1867–74.
269. Jahn-Schmid B, Graninger M, Glozik M, Küpcü S, Ebner C, Unger FM, Sleytr UB, Messner P. Immunoreactivity of allergen (Bet v 1) conjugated to crystalline bacterial cell surface layers (S-layers). *Immunotechnology* 1996;**2**:103–13.
270. Jahn-Schmid B, Messner P, Unger FM, Sleytr UB, Scheiner O, Kraft D. Toward selective elicitation of TH1-controlled vaccination responses: vaccine applications of bacterial surface layer proteins. *J Biotechnol* 1996;**44**:225–31.
271. Gerstmayr M, Ilk N, Jahn-Schmid B, Sleytr UB, Bohle B. Natural self-assembly of allergen-S-layer fusion proteins is no prerequisite for reduced allergenicity and T cell stimulatory capacity. *Int Arch Allergy Immunol* 2009;**149**:231–8.
272. Umelo-Njaka E, Nomellini JF, Bingle WH, Glasier LG, Irvin RT, Smit J. Expression and testing of *Pseudomonas aeruginosa* vaccine candidate proteins prepared with the *Caulobacter crescentus* S-layer protein expression system. *Vaccine* 2001;**19**:1406–15.
273. Mock M, Fouet A. Anthrax. *Annu Rev Microbiol* 2001;**55**:647–71.
274. Ausiello CM, Cerquetti M, Fedele G, Spensieri F, Palazzo R, Nasso M, Frezza S, Mastrantonio P. Surface layer proteins from *Clostridium difficile* induce inflammatory and regulatory cytokines in human monocytes and dendritic cells. *Microbes Infect* 2006;**8**:2640–6.
275. Brun P, Scarpa M, Grillo A, Palu G, Mengoli C, Zecconi A, Spigaglia P, Mastrantonio P, Castagliuolo I. *Clostridium difficile* TxAC314 and SLP-36kDa enhance the immune response toward a co-administered antigen. *J Med Microbiol* 2008;**57**:725–31.
276. O´Brien JB, McCabe MS, Athié-Morales V, McDonald GS, Ní Eidhin DB, Kelleher DP. Passive immunization of hamsters against *Clostridium difficile* infection using antibodies to surface layer proteins. *FEMS Microbiol Lett* 2005;**246**:199–205.
277. Rahman MH, Kawai K. Outer membrane proteins of *Aeromonas hydrophila* induce protective immunity in goldfish. *Fish Shellfish Immunol* 2000;**10**:379–82.
278. Baba T, Imamura J, Izawa K, Ikeda K. Immune protection in carp. *Cyprinus carpido* L. after immunization with Aeromonas hydrophila crude lipopolysaccaride. *J Fish Dis* 1988;**11**:237–44.
279. Azad IS, Shankar KM, Mohan CV, Kalita B. Uptake and processing of biofilm and free-cell vaccines of *Aeromonas hydrophila* in indian major carps and common carp following oral vaccination–antigen localization by a monoclonal antibody. *Dis Aquat Organ* 2000;**43**:103–8.
280. Lamers CHJ, De Haas MJH, Van Muiswinkel WB. The reaction of the immune system of fish vaccination: development of immunological memory in carp. *Cyprinus carpio* L., following direct immersion in *Aeromonas hydrophila* bacterin. *J Fish Dis* 1985;**8**:253–62.
281. Leung KY, Wong LS, Low KW, Sin YM. Mini-Tn5 induced growth- and protease- deficient mutants of *Aeromonas hydrophila* as live vaccines for blue gourami, *Trichogaster trichopterus* (Pallas). *Aquaculture* 1997;**158**:11–22.

282. Messner P, Unger FM, Sleytr U. Vaccine development based on S-layer technology. In: Sleytr UB, Messner P, Pum D, Sára M, editors. *Crystalline bacterial cell surface proteins*. Austin, Texas, USA: Landes Company and Academic Press Inc.; 1996. pp. 161–73.
283. Sleytr UB, Mundt W, Messner P. *Immunogenic composition containing ordered carriers.* US Patent Nr. 5,043,158.
284. Brown FGD, Hoey EM, Martin S, Rima BK, Trudgett A. Vaccine design. In: James K, Morris A, editors. *Molecular medical science series*. England, UK: John Wiley & Sons; 1993.
285. Powell MF, Newman MJ. Vaccine design: the subunit and adjuvant approach. In: Powell MF, Newman MJ, editors. *Pharmaceutical biotechnology.* New York, USA: Plenum Press; 1995.
286. Malcolm AJ, Best MW, Szarka RJ, Mosleh Z, Unger FM, Messner P, Sleytr UB. Surface layers of *Bacillus alvei* as a carrier for a *Streptococcus pneunoniae* conjugate vaccine. In: Beveridge J, Koval SF, editors. *Bacterial paracrystalline surface layers*. New York, USA: Plenum Press; 1993. pp. 219–33.
287. Messner P. Chemical composition and biosynthesis of S-layer. In: Sleytr UB, Messner P, Pum D, Sára M, editors. *Crystalline bacterial cell surface proteins*. Austin, Texas, USA: R.G. Landes Company and Academic Press Inc.; 1996. pp. 35–76.
288. Messner P, Unger FM, Sleytr UB. Vaccine development based on S-layer technology. In: Sleytr UB, Messner P, Pum D, Sara M, editors. *Crystalline bacterial cell surface proteins*. Austin, TX: R.G. Landes and Academic Press; 1996. pp. 161–73.
289. Hianik T, Küpcü S, Sleytr UB, Rybar P, Krivanek R, Kaatze U. Interaction of crystalline bacterial cell surface proteins with lipid bilayers in liposomes. *Colloids Surf A* 1999;**147**:331–9.
290. Küpcü S, Lohner K, Mader C, Sleytr UB. Microcalorimetric study on the phase behaviour of S-layer coated liposomes. *Mol Membr Biol* 1998;**15**:69–74.
291. Krivanek R, Rybar P, Küpcü S, Sleytr UB, Hianik T. Affinity interactions on a liposome surface detected by ultrasound velocimetry. *Bioelectrochemistry* 2002;**55**:57–9.
292. Bhatnagar PK, Awasthi A, Nomellini JF, Smit J, Suresh MR. Anti-tumor effects of the bacterium *Caulobacter crescentus* in murine tumor models. *Cancer Biol Ther* 2006;**5**:485–91.
293. Georgiou G, Stathopoulos C, Daugherty PS, Nayak AR, Iverson BL, Curtiss 3rd R. Display of heterologous proteins on the surface of microorganisms: from the screening of combinatorial libraries to live recombinant vaccines. *Nat Biotechnol* 1997;**15**:29–34.
294. Nomellini JF, Toporowski MC, Smit J. Secrtetion or presentation of recombinant proteins and peptides mediated by the S-layer of *Caulobacter crescentus*. In: Banex F, editor. *Expression technologies: current status and future trends*. Norfolk, UK: Horizon Scientific Press; 2004. pp. 477–524.
295. Ratner BD, Bryant SJ. Biomaterials: where we have been and where we are going. *Annu Rev Biomed Eng* 2004;Vol. 6. 41–75.
296. Zhang Z, Zhang M, Chen S, Horbett TA, Ratner BD, Jiang S. Blood compatibility of surfaces with superlow protein adsorption. *Biomaterials* 2008;**29**:4285–91.
297. Goodsell DS. *Bionanotechnology, Lessons from nature.* Hoboken, NJ: Wiley-Liss; 2004.
298. Whitesides GM, Mathias JP, Seto CT. Molecular selfassembly and nanochemistry: a chemical strategy for the synthesis of nanostructures. *Science* 1991;**254**:1312–9.
299. Galdiero S, Falanga A, Vitiello M, Raiola L, Russo L, Pedone C, Isernia C, Galdiero M. The presence of a single N-terminal histidine residue enhances the fusogenic properties of a membranotropic peptide derived from herpes simplex virus type 1 glycoprotein H. *J Biol Chem* 2010;**285**:17123–36.
300. Galdiero S, Galdiero M, Pedone C. Beta-barrel membrane bacterial proteins: structure, function, assembly and interaction with lipids. *Curr Protein Pept Sci* 2007;**8**:63–82.
301. Gerstein M, Hegyi H. Comparing genomes in terms of protein structure: surveys of a finite parts list. *FEMS Microbiol Rev* 1998;**22**:277–304.

302. Sleytr UB, Sára M, Pum D. Crystalline bacterial cell surface layers (S-layers): a versatile self-assembly system. In: Ciferri A, editor. *Supramolecular polymers*. New York, Basel: Marcel Dekker Inc.; 2000. pp. 177–213.
303. Viviani B, Gardoni F, Marinovich M. Cytokines and neuronal ion channels in health and disease. *Int Rev Neurobiol* 2007;**82**:247–63.
304. Ellis C, Smith A. Highlighting the pitfalls and possibilities of drug research. *Nat Rev Drug Discov* 2004;**3**:238–78.
305. De Rosa M. Archaeal lipids: structural features and supramolecular organization. *Thin Solid Films* 1996;**284–285**:13–7.
306. Hanford MJ, Peeples TL. Archaeal tetraether lipids. *Appl Biochem Biotechnol* 2002;**97**:45–62.
307. Stetter KO. Extremophiles and their adaptation to hot environments. *FEBS Lett* 1999;**452**:22–5.
308. Schuster B, Sleytr UB. Tailor-made crystalline structures of truncated S-layer proteins on heteropolysaccharides. *Soft Matter* 2009;**5**:334–41.
309. Schuster B, Pum D, Sleytr UB. S-layer stabilized lipid membranes (Review). *Biointerphases* 2008;**3**:FA3–FA11.
310. Diederich A, Sponer C, Pum D, Sleytr UB, Lösche M. Reciprocal influence between the protein and lipid components of a lipid-protein membrane model. *Colloids Surf B* 1996;**6**:335–46.
311. Wetzer B, Pum D, Sleytr UB. S-layer stabilized solid supported lipid bilayers. *J Struct Biol* 1997;**119**:123–8.
312. Weygand M, Kjaer K, Howes PB, Wetzer B, Pum D, Sleytr UB, Lösche M. Structural reorganization of phospholipid headgroups upon recrystallization of an S-layer lattice. *J Phys Chem B* 2002;**106**:5793–9.
313. Weygand M, Schalke M, Howes PB, Kjaer K, Friedmann J, Wetzer B, Pum D, Sleytr UB, Lösche M. Coupling of protein sheet crystals (S-layers) to phospholipid monolayers. *J Mater Chem* 2000;**10**:141–8.
314. Weygand M, Wetzer B, Pum D, Sleytr UB, Cuvillier N, Kjaer K, Howes PB, Losche M. Bacterial S-layer protein coupling to lipids: x-ray reflectivity and grazing incidence diffraction studies. *Biophys J* 1999;**76**:458–68.
315. Wetzer B, Pfandler A, Györvary E, Pum D, Lösche M, Sleytr UB. S-layer reconstitution at phospholipid monolayers. *Langmuir* 1998;**14**:6899–906.
316. Schuster B, Sleytr UB, Diederich A, Bahr G, Winterhalter M. Probing the stability of S-layer-supported planar lipid membranes. *Eur Biophys J* 1999;**28**:583–90.
317. Hirn R, Schuster B, Sleytr UB, Bayerl TM. The effect of S-layer protein adsorption and crystallization on the collective motion of a planar lipid bilayer studied by dynamic light scattering. *Biophys J* 1999;**77**:2066–74.
318. Schuster B. Biomimetic design of nanopatterned membranes. *NanoBiotechnology* 2005;**1**:153–64.
319. Schuster B, Pum D, Sára M, Sleytr UB. S-Layer proteins as key components of a versatile molecular construction kit for biomedical Nanotechnology. *Mini Rev Med Chem* 2006;**6**:909–20.
320. Lee BW, Faller R, Sum AK, Vattulainen I, Patra M, Karttunen M. Structural effects of small molecules on phospholipid bilayers investigated. *Fluid Phase Equilibria* 2004;**225**:63–8.
321. Györvary E, Wetzer B, Sleytr UB, Sinner A, Offenhäuser A, Knoll W. Lateral diffusion of lipids in silane-, dextrane- and S-layer protein-supported mono- and bilayers. *Langmuir* 1999;**15**:1337–47.
322. Schuster B, Pum D, Braha O, Bayley H, Sleytr UB. Self-assembled alpha-hemolysin pores in an S-layer-supported lipid bilayer. *Biochim Biophys Acta* 1998;**1370**:280–8.

323. Schuster B, Pum D, Sleytr UB. Voltage clamp studies on S-layer-supported tetraether lipid membranes. *Biochim Biophys Acta* 1998;**1369**:51–60.
324. Schuster B, Gufler PC, Pum D, Sleytr UB. Interplay of phospholipase A2 with S-layer-supported lipid monolayers. *Langmuir* 2003;**19**:3393–7.
325. Gufler PC, Pum D, Sleytr UB, Schuster B. Highly robust lipid membranes on crystalline S-layer supports investigated by electrochemical impedance spectroscopy. *Biochim Biophys Acta* 2004;**1661**:154–65.
326. Schuster B, Gufler PC, Pum D, Sleytr UB. S-layer proteins as supporting scaffoldings for functional lipid membranes. *IEEE Trans Nanobioscience* 2004;**3**:16–21.
327. Schuster B, Sleytr UB. The effect of hydrostatic pressure on S-layer-supported lipid membranes. *Biochim Biophys Acta* 2002;**1563**:29–34.
328. Bayley H, Cremer PS. Stochastic sensors inspired by biology. *Nature* 2001;**413**:226–30.
329. Bhakdi S, Tranum-Jensen J. Alpha-toxin of *Staphylococcus aureus*. *Microbiol Rev* 1991;**55**:733–51.
330. Revah F, Bertrand D, Galzi JL, Devillers-Thiery A, Mulle C, Hussy N, Bertrand S, Ballivet M, Changeux JP. Mutations in the channel domain alter desensitization of a neuronal nicotinic receptor. *Nature* 1991;**353**:846–9.
331. Schuster B, Sleytr UB. Single channel recordings of alpha-hemolysin reconstituted in S-layer-supported lipid bilayers. *Bioelectrochemistry* 2002;**55**:5–7.
332. Keizer HM, Andersson M, Chase C, Laratta WP, Proemsey JB, Tabb J, Long JR, Duran RS. Prolonged stochastic single ion channel recordings in S-layer protein stabilized lipid bilayer membranes. *Colloids Surf B Biointerfaces* 2008;**65**:178–85.
333. Castellana ET, Cremer PS. Solid supported lipid bilayers: from biophysical studies to sensor design. *Surf Sci Rep* 2006;**61**:429–44.
334. Chan YH, Boxer SG. Model membrane systems and their applications. *Curr Opin Chem Biol* 2007;**11**:581–7.
335. Katsaras J, Kucerka N, Nieh MP. Structure from substrate supported lipid bilayers. *Biointerphases* 2008;**3**:FB55–63.
336. Knoll W, Naumann R, Friedrich M, Robertson JWF, Lösche M, Heinrich F, McGillivray DJ, Schuster B, Gufler PC, Pum D, Sleytr UB. Solid supported lipid membranes: new concepts for the biomimetic functionalization of solid surfaces. *Biointerphases* 2008;**3**:FA125–35.
337. Reimhult E, Kumar K. Membrane biosensor platforms using nano- and microporous supports. *Trends Biotechnol* 2008;**26**:82–9.
338. Steinem C, Janshoff A. Multicomponent membranes on solid substrates: interfaces for protein binding. *Curr Opin Colloid Interface Sci* 2010;**15**:479–88.
339. Schuster B, Pum D, Sára M, Braha O, Bayley H, Sleytr UB. S-layer ultrafiltration membranes: a new support for stabilizing functionalized lipid membranes. *Langmuir* 2001;**17**:499–503.
340. Schuster B, Weigert S, Pum D, Sára M, Sleytr UB. New method for generating tetraether lipid membranes on porous supports. *Langmuir* 2003;**19**:2392–7.
341. Bangham AD, Standish MM, Watkins JC. Diffusion of univalent ions across the lamellae of swollen phospholipids. *J Mol Biol* 1965;**13**:238–52.
342. Cui HF, Ye JS, Leitmannova Lui A, Tien HT. Lipid microvesicles: on the four decades of liposome research. In: Leitmannova Lui A, Tien HT, editors. *Advances in planar lipid bilayers and liposomes*Vol. 4. Amsterdam: Elsevier; 2006. pp. 1–48.
343. Tien HT, Ottova-Leitmannova A. *Membrane biophysics: as viewed from experimental bilayer lipid membranes.* Elsevier, Amsterdam: Planar lipid bilayers and spherical liposomes; 2000.
344. Amselem AS, Yogev A, Zawoznik E, Friedman D. Emulsomes, a novel drug delivery technology. *Proc Int Symp Control Release Bioactive Mater* 1994;**21**:1369.
345. Vyas SP, Subhedar R, Jain S. Development and characterization of emulsomes for sustained and targeted delivery of an antiviral agent to liver. *J Pharm Pharmacol* 2006;**58**:321–6.

346. Andresen TL, Jensen SS, Jorgensen K. Advanced strategies in liposomal cancer therapy: problems and prospects of active and tumor specific drug release. *Prog Lipid Res* 2005;**44**:68–97.
347. Hollmann A, Delfederico L, Glikmann G, De Antoni G, Semorile L, Disalvo EA. Characterization of liposomes coated with S-layer proteins from *lactobacilli*. *Biochim Biophys Acta* 2007;**1768**:393–400.
348. Pum D, Sára M, Schuster B, Sleytr UB, Chen J, Jonoska N, Rozenberg G. Bacterial surface layer proteins: a simple but versatile biological self-assembly system in nature. In: Chen J, Jonoska N, Rosenberg G, editors. *Nanotechnology: science and computation*. Berlin: Springer; 2006. pp. 277–90.
349. Schuster B, Kepplinger C, Sleytr UB. Biomimetic S-layer stabilized lipid membranes. In: Toca-Herrera JL, editor. *Biomimetics in biophysics: model systems, experimental techniques and computation*. Kerala, India: Research Signpost; 2010. pp. 1–12.
350. Dieluweit S, Pum D, Sleytr UB. Formation of a gold superlattice on an S-layer with square lattice symmetry. *Supramol Sci* 1998;**5**:15–9.
351. Wahl R, Engelhardt H, Pompe W, Mertig M. Multivariate statistical analysis of two-dimensional metal cluster arrays grown in vitro on a bacterial surface layer. *Chem Mater* 2005;**17**:1887–94.
352. Maslyuk VV, Mertig I, Bredow T, Mertig M, Vyalikh DV, Molodtsov SL. Electronic structure of bacterial surface protein layers. *Phys Rev B* 2008;**77**:45419.
353. Vyalikh DV, Danzenbächer S, Mertig M, Kirchner A, Pompe W, Dedkov YS, Molodtsov SL. Electronic structure of regular bacterial surface layers. *Phys Rev Lett* 2004;**93**: 238103-1-238103-4.
354. Vyalikh DV, Kummer K, Kade A, Blüher A, Katzschner B, Mertig M, Molodtsov SL. Site-specific electronic structure of bacterial surface protein layers. *Appl Phys A* 2009;**94**:455–9.
355. Göbel C, Schuster B, Baurecht D, Sleytr UB, Pum D. S-layer templated bioinspired synthesis of silica. *Colloids Surf B Biointerfaces* 2009;**75**:565–72.
356. Kröger N, Lorenz S, Brunner E, Sumper M. Self-Assembly of highly phosphorylated silaffins and their function in biosilica morphoGenesis. *Science* 2002;**298**:584–6.